EXPLORING DUAL-TARGETING GROEL/ES & PTPB INHIBITORS AS A NEW ANTIBIOTIC STRATEGY FOR TUBERCULOSIS

J. Alex Washburn

Submitted to the faculty of the University Graduate School
in partial fulfillment of the requirements
for the degree
Master of Science
in the Department of Biochemistry and Molecular Biology
Indiana University

May 2019

Accepted by the Graduate Faculty of Indiana University, in partial fulfillment of the requirements for the degree of Master of Science

Master's Thesis Committee

_____
Steven M. Johnson, Ph.D., Chair

_____
Millie M. Georgiadis, Ph.D.

_____
Quyen Q. Hoang, Ph.D.

DEDICATION

To my parents, Jeff and Nancy, brother, Jack, and girlfriend, Annika, for helping and supporting me through everything along the way.

ACKNOWLEDGEMENT

Dr. Steven Johnson for compound synthesis, research training, and helping me with the project; Dr. Sanofar Abdeen for research training and assisting with protein purification and biochemical assays; Dr. Anne-Marie Ray for research training and assisting with cell culture and cell viability assays; Lab members Mckayla Stevens and Siddhi Chitre for helping with protein purification and running assays; and Arkaprabha Banerjee for helping with the *Mycobacterium smegmatis* proliferation assay. I would also like to thank Dr. Tanya Parish and Dr. Yulia Ovechkina at the Infectious Disease Research Institute (Seattle, WA) for evaluating compounds in their *Mycobacterium tuberculosis* proliferation assay. Research reported in this thesis was supported by the National Institute of General Medical Sciences (NIGMS) of the National Institutes of Health (NIH) under Award Number R01GM120350. The content is solely the responsibility of the authors and does not necessarily represent the official views of the NIH.

J. Alex Washburn

EXPLORING DUAL-TARGETING GROEL/ES & PTPB INHIBITORS AS A NEW ANTIBIOTIC STRATEGY FOR TUBERCULOSIS

Current *Mycobacterium tuberculosis (Mtb)* treatments suffer from an increase in antibiotic resistance strains and the lack of efficacy against latent state tuberculosis, thus novel approaches targeting different mechanisms of action are needed. One strategy to target *Mtb* is to target protein homeostasis pathways by inhibiting molecular chaperones, in particular, GroEL/ES (HSP60/10) chaperonin systems. *Mtb* has two homologs of GroEL, of which GroEL1 is not essential, but is important for cytokine-dependent granuloma formation, and GroEL2 is essential for survival and the likely canonical housekeeping chaperonin. Another strategy to target *Mtb* is to target the protein tyrosine phosphatase B (PtpB) virulence factor that *Mtb* secretes into host cells to help evade immune responses. Thus, we envisioned that this analog series might also be capable of inhibiting *Mtb* PtpB along with GroEL. By developing compound **1** inhibitors that could act on all of GroEL1, GroEL2, and PtpB, we could have an antibiotic candidate that targets all stages of tuberculosis: actively replicating bacteria, bacteria evading host cell immune response, and granuloma formation in latent disease.

In the Johnson lab, previous studies explored GroEL/ES inhibitors, with compound **1** being one of the most potent inhibitors, inhibiting both *Trypanosoma brucei* and *Staphylococcus aureus* proliferation. In the present study, we have screened previously developed compound **1** analogs, as well as a series of newly synthesized analogs that we term “half-molecules”. In this study, our results indicated two potential avenues to explore for future research. The first is a series of carboxyl-bearing compound **1** inhibitors, compounds **2m-*o***, **2m-*m***, and **2m-*p***, which act solely on *Mtb* PtpB phosphatase activity without inhibiting GroEL. The second is a series of compound **1** inhibitors (e.g. **20R** and **20L**) that are able to inhibit both the PtpB phosphatase and

GroEL/ES chaperonin system. Thus, this exploratory study showed the possibility of pursuing such a polypharmacological antibiotic strategy against *Mtb* infections and with further optimization, such dual-targeting GroEL/ES and PtpB inhibitors could be effective against all stages of tuberculosis.

Steven M. Johnson, Ph.D., Chair

TABLE OF CONTENTS

LIST OF TABLES

LIST OF FIGURES

LIST OF ABBREVIATIONS

ADP – Adenosine diphosphate
ATP – Adenosine triphosphate
BCG – Bacille Calmette-Guérin
CC_{50} – Cytotoxicity concentration for half-maximal signal in human cell viability assays
Da – Dalton
EC_{50} – Effective concentration for half-maximal signal in bacterial proliferation assays
ESKAPE – Enterococcus faecium, Staphylococcus aureus, Klebsiella pneumoniae, Acinetobacter baumanii, Pseudomonas aeruginosa, Enterobacter species
^{1}H-NMR – Proton nuclear magnetic resonance
HPLC – High-performance liquid chromatography
HSP – Heat shock protein
IC_{50} – Inhibitory concentration for half-maximal signal in biochemical assays
MDH – Malate dehydrogenase
MOA – Mechanism of action
MRSA – Methicillin-resistant *Staphylococcus aureus*
MS – Mass spectrometry
Mtb – *Mycobacterium tuberculosis*
NAD^{+} – Nicotinamide adenine dinucleotide (oxidized form)
NADH – Nicotinamide adenine dinucleotide (reduced form)
OD – Optical density
OMTS – (Oxalylamino-methylene)-thiophene sulfonamide
PBS – Phosphate buffered saline
pNPP – *para*-Nitrophenylphosphate
PTP – Protein tyrosine phosphatase
PtpB – Protein tyrosine phosphatase B
Rho – Rhodanese
SAR – Structure activity relationship
SDS PAGE – Sodium dodecyl sulfate polyacrylamide gel electrophoresis
TB – Tuberculosis
WT – Wild-type

INTRODUCTION

Mycobacterium tuberculosis stages and implications.

Tuberculosis is a serious bacterial infectious disease that has beset people over the course of human history. *Mycobacterium tuberculosis (Mtb)*, the causative agent of tuberculosis, has survived for over 70,000 years with the *Mycobacterium* genus originating more than 150 million years ago (Barberis 2017). Tuberculosis rates and deaths soared during the 19th century, prompting physicians and scientists to try to understand the etiology of the disease. It wasn't until the late 19th century, when Robert Koch isolated the tubercle bacillus and put forward his famous postulates about infectious etiology, that scientists could understand how tuberculosis is contracted (Daniel 2006). *Mtb* infects around 1 in 4 people, or about 2 billion people worldwide (CDC Features 2018). In 2016, over 10 million active cases of tuberculosis infection were reported with 1.7 million deaths attributed to the deadly disease. Countries with poorer access to healthcare and socioeconomic problems are affected more and hit harder with cases of tuberculosis, as outlined in Figure 1 (Tuberculosis 2018).

Mtb is a facultative intracellular bacterium that is neither Gram-positive nor Gram-negative, but instead is coated in a fatty, mycolic acid outer wall. *Mtb* is transmitted as an airborne particulate generated when people with active tuberculosis cough or sneeze (Jackson 2016). When inhaled, the infectious bacteria traverse the respiratory tract to the alveoli where they infect phagocytic cells, namely macrophages. *Mtb* has adapted to endure a diverse set of microenvironments in the host. Each unique microenvironment, along with host immune effectors, encourages *Mtb* to exist in either an active or latent state (Pai 2016, Lupoli 2018). *Mtb* are a slow replicating bacterium with doubling rates between 18-54 h (Gill 2009). Initially, infection with *Mtb* is believed to occur in alveolar macrophages (Flynn 2001). The bacteria replicate within macrophages and induce cytokines that initiate the inflammatory response in the lungs. Macrophages and

lymphocytes migrate to the site of infection and form a granuloma. Latent TB is essentially where there is equilibrium between the host and bacillus. During this state is where the host prevents the disease from becoming active while the bacterium avoids elimination (Flynn 2001). Latent TB in a granuloma state can persist for years without producing any symptoms (Figure 2). In around 90% of all TB infections, the immune response is sufficient to keep the disease in a latent state (Flynn 2001). However, a weakened immune system can lead to re-activation of dormant *Mtb* from the granulomas. Active TB spreads and proliferates to other macrophages in the body, having mild to severe symptoms depending on the severity of the disease (Figure 2). If left untreated, tuberculosis can affect other body organs and functions, which can ultimately become fatal (Smith 2003).

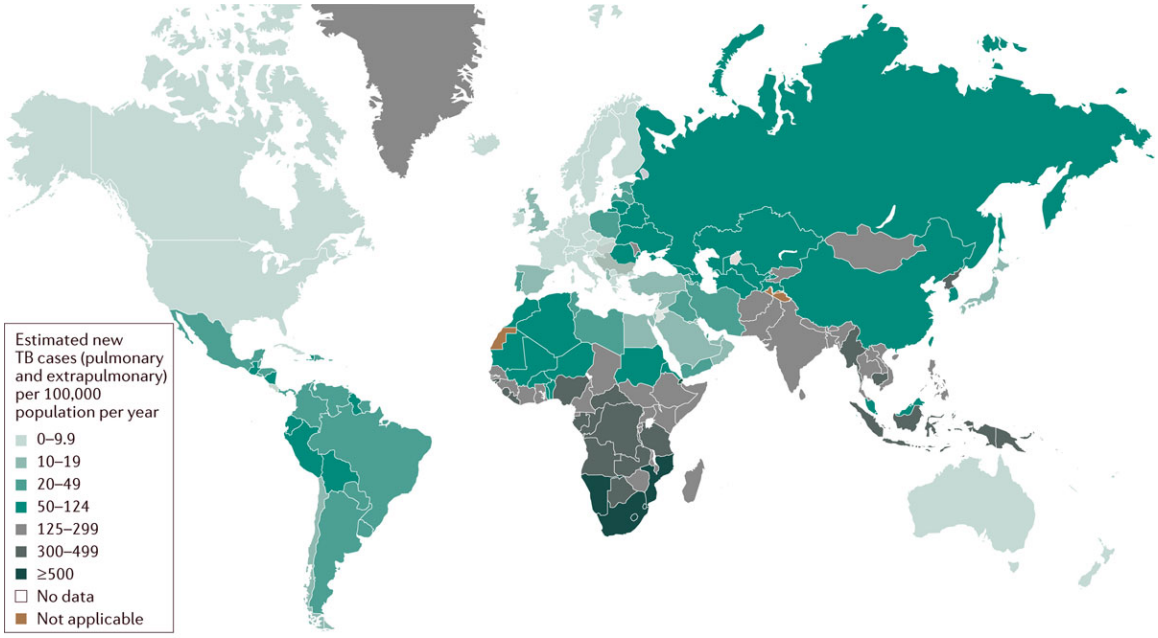

Figure 1 – Estimated global TB incidence per 100,000 people. Tuberculosis is proportional to access to healthcare and socioeconomic problems. Southeast Asia and southern Africa have the highest cases of tuberculosis per population. (Figure adapted from Pai 2016).

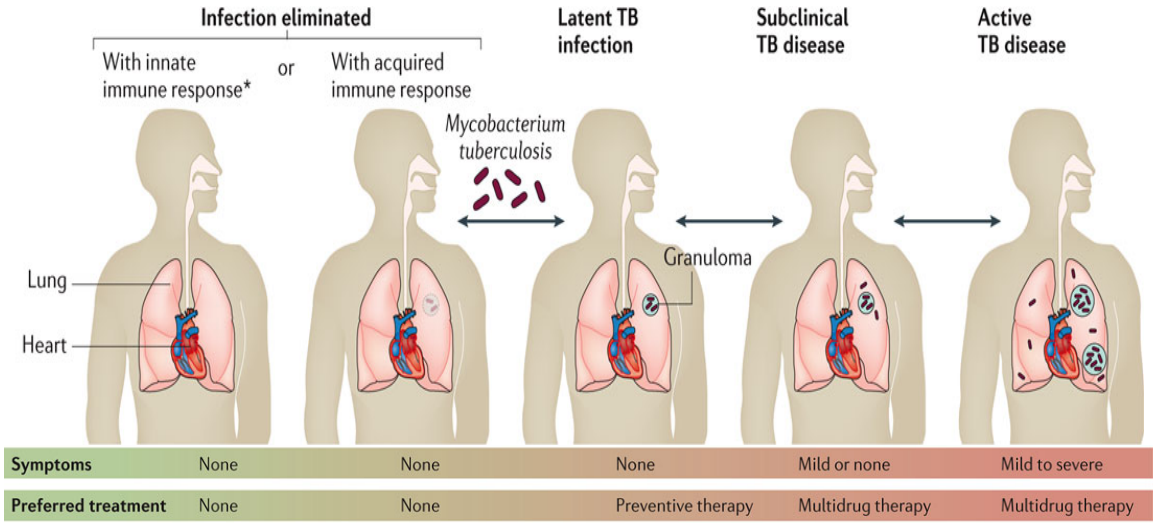

Figure 2 – Different stages of tuberculosis with symptoms and treatments. Bacterial infection can be eliminated but if not, can be present at multiple TB phases. Latent TB has bacteria evading host cell immune response by hiding in macrophages and forming a granuloma. Latent TB produce no symptoms, so diagnosis and treatment are difficult. Latent TB can become active which spread to and infect other cells. Active TB has actively replicating bacteria spreading to other cells in the body. Symptoms for active TB can be mild to severe with multidrug therapy required for treatment. (Figure from Pai 2016).

Current tuberculosis treatments.

Current efforts to abate tuberculosis include vaccinations for prevention and antibiotics for treatment. The only available vaccination for *Mtb* is Bacille Calmette-Guérin (BCG) and its efficacy varies for patients. The efficacy depends on the variability and virulence of the disease (Vaudry 2003). BCG is not administered in the United States and is generally only given to children in countries with a high TB prevalence. BCG does prevent some serious TB complications, such as meningitis, but fails to effectively protect children from TB-related pulmonary disease, to prevent latent infection from progressing to active disease, and to prevent the spread of the disease (Luca 2013). Furthermore, the vaccine is not used much in adults because of their lower risk of infection as well as the variable effectiveness of the vaccine against adult pulmonary TB (Luca 2013). Because of the inefficacy of TB vaccinations, antibiotic drugs have been

the primary method for countering *Mtb* infections. Typical first-line antibiotics include isoniazid, rifampin, ethambutol, and pyrazinamide (Table 1), which function by targeting cell wall synthesis as well as protein synthesis (Treatment of Tuberculosis 2010). Because of their mechanisms of action, compounds are primarily successful against actively replicating bacteria; however, since *Mtb* replicates so slowly, combination therapy is typically administered for at least six-to-nine months to completely eliminate the bacteria. This extensive treatment often leads to patient non-compliance (Tuberculosis 2018). When patients neglect to finish the full extent of their treatments, the mycobacteria colonies can become resistant to antibiotics and persist, leading to increasing resistance to first-line antibiotics. Multi-drug resistant tuberculosis requires more potent second-line antibiotics such as fluoroquinolones and injectable second-line drugs such as kanamycin in combination with first-line antibiotics (CDC Features 2018). Extensively-drug resistant *Mtb* are resistant to first-line drugs as well as second-line antibiotics used to treat multi-drug resistant tuberculosis. Antibiotics used to treat extensively-drug resistant tuberculosis include the recently approved drugs bedaquiline and delamanid, which target and block ATP synthase and mycolic acid biosynthesis in mycobacteria (D'Ambrosio 2017). Furthermore, *Mtb* colonies can persist in lung tissue in the latent phase, which often evades medical notice and makes proper diagnosis of the disease increasingly difficult. If diagnosed, first-line antibiotics such as rifampicin and isoniazid can be used to prevent the bacteria from becoming active, but many of the active tuberculosis antibiotics used are ineffective against latent-phase infection (Houston 2002). Accordingly, while vaccines and treatments are available, their efficacy is mixed, in particular because incidences of multi-drug and extensively-drug resistant strains are rising.

Table 1 – Information on current tuberculosis antibiotics on the market (Butler 2016).

Example	Therapy Use	Date Introduced	Mechanism of Action
Isoniazid 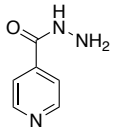	First-line	1952	Inhibits synthesis of mycolic acids
Rifampicin 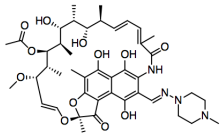	First-line	1966	Inhibits RNA polymerase
Ethambutol 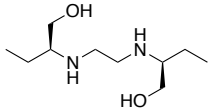	First-line	1961	Inhibits arabinosyl transferase, involved in cell wall biosynthesis
Pyrazinamide 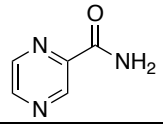	First-line	1952	Inhibits fatty acid synthase
Bedaquiline 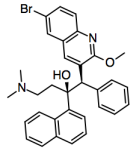	Second-line	2012	Inhibits ATP proton pump
Delamanid 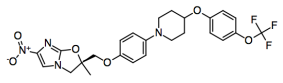	Second-line	2014	Inhibits mycolic acid biosynthesis

A new antibacterial strategy: targeting bacterial GroEL/ES chaperonin systems to disrupt protein folding.

With current medical efforts to combat tuberculosis becoming increasingly ineffective, it is necessary to develop novel approaches targeting different mechanisms of action to overcome multi-drug resistance. One such strategy that we are exploring is targeting bacterial protein homeostasis pathways. A network of molecular chaperones and proteases collectively functions to maintain protein homeostasis by assisting proteins to fold to their native, functional states, or ensuring their proper degradation

(Chapman 2006, Xu 1998). Since many molecular chaperones, which are also known as Heat Shock Proteins (HSPs), are essential under normal and stress conditions, targeting them with small molecule inhibitors should be an effective antibacterial strategy. *E. coli* GroEL, which is the prototypical member of the HSP60 chaperonin family, is a homo-tetradecameric protein that forms two, seven-subunit rings that stack back-to-back with one another (Figure 3). Through a series of events driven by ATP binding and hydrolysis (Figure 4), unfolded substrate polypeptides are bound within the central cavity of a GroEL ring and are encapsulated by the GroES co-chaperonin lid, allowing protein folding within the sequestered chamber (Horwich 2006).

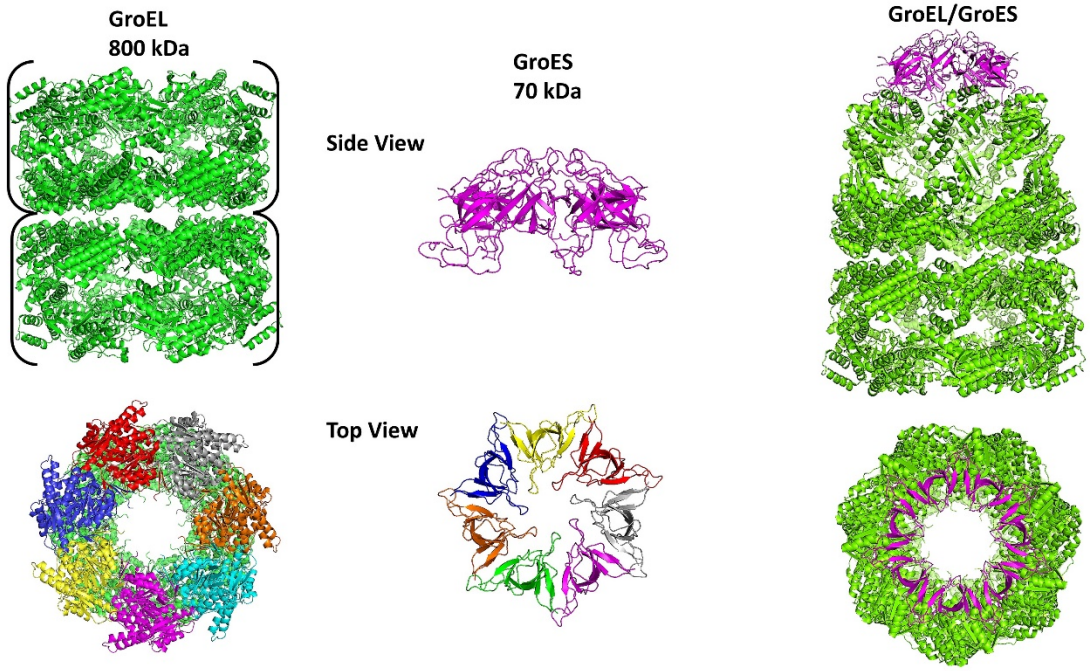

Figure 3 – GroEL/ES chaperonin structure. GroEL is as a homo-tetradecameric complex consisting of two, seven-subunit rings stacked back-to-back. To facilitate polypeptide folding, the 7-subunit GroES "lid" caps off the GroEL rings, where unfolded polypeptides are encapsulated and allowed to fold to their native states (schematic of the polypeptide folding cycle is shown in Figure 4). Images are adapted from the 4V43 and 1SX4 crystal structures (Chaudhry 2004).

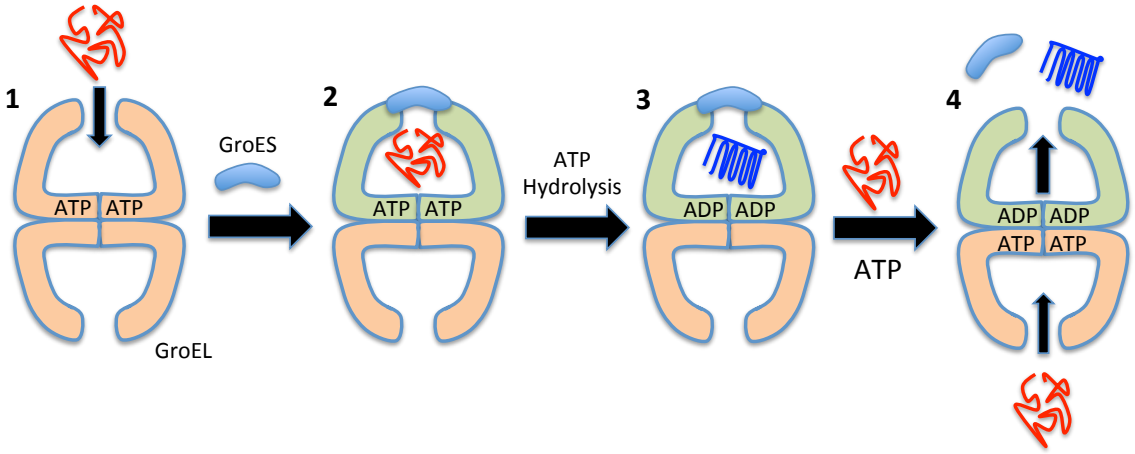

Figure 4 – Schematic of the GroEL/ES-mediated folding cycle. 1. Unfolded polypeptide binds to the GroEL apical domains, with ATP binding to the equatorial domains (seven ATPs bind per GroEL ring). 2. GroES binds to the GroEL apical domains and releases the unfolded polypeptide into the GroEL *cis*-cavity, where folding occurs. 3. ATP hydrolysis releases the negative cooperativity to the GroEL *trans*-ring. 4. ATP and another unfolded polypeptide bind to the GroEL *trans*-ring, signaling ejection of cargo from the initial *cis*-ring. The folding cycle then continues in the new *cis*-ring (Horwich 2006).

Mtb has two homologs of GroEL – GroEL1 and GroEL2. GroEL2 is an essential gene for the survival of *Mtb* and if knocked out, *Mtb* fails to grow (Hu 2008). Thus, targeting GroEL2 with small molecule inhibitors should be an effective strategy to kill mycobacteria. While GroEL1 is not essential, it is important in regulating cytokine-dependent granuloma formation (Hu 2008). When infected with GroEL1-deficient (Δ*cpn60.1*) mutant *Mtb*, both mice and guinea pigs produced equal number of bacteria as the WT-GroEL1; however, the mutant strain failed to produce granulomatous inflammation. Thus, targeting GroEL1 with small molecule inhibitors could also thwart granuloma formation. These enticing findings suggest that inhibitors that act on both of the *Mtb* GroEL homologs could treat both the active and latent stages of tuberculosis.

Previous studies identifying GroEL/ES inhibitors for hit-to-lead development as antibiotic candidates.

Towards our goal of exploiting HSP60/10 and GroEL/ES chaperonin systems as an antibiotic strategy, we previously reported a high-throughput screen for small

molecule inhibitors of the *E. coli* GroEL/ES chaperonin system (Johnson 2014). A schematic of the general GroEL/ES-mediated folding assay protocol is outlined in Figure 5. In general, a denatured reporter enzyme - we typically use malate dehydrogenase (MDH) or rhodanese (Rho) for our compound evaluations - is mixed to create a binary complex with GroEL. GroES and ATP are then added to initiate the folding cycle. After adequate incubation time to allow proper folding of the reporter enzyme, the amount of enzymatic activity by the refolded reporter enzyme is monitored by the addition of an enzyme assay solution. Using this general assay protocol, 235 GroEL inhibitors were identified by screening against a library of 700,000 molecules (Johnson 2014). In a subsequent study, we evaluated 22 of these GroEL/ES inhibitor hits for their antibacterial properties against bacteria termed the *ESKAPE* pathogens - an acronym that stands for *Enterococcus faecium*, *Staphylococcus aureus*, *Klebsiella pneumoniae*, *Acinetobacter baumannii*, *Pseudomonas aeruginosa*, and *Enterobacter* species. While ineffective against each of the bacterial species, these studies identified compound 1 (Figure 6) as one of the most potent inhibitors of both the refolding and ATPase functions of GroEL (Abdeen 2016).

A PubChem database search found a related compound **1** analog (the 2-phenylbenzoxazole **2e-*p***) that elicited antimicrobial functions against *Leishmania major* promastigotes while being reported active in only 8 out of 285 bioassays, showing inherent selectivity. Thus, in a follow up study, we evaluated a series of compound **1**-based GroEL/ES inhibitors for their antibiotic effects against a related parasite, *Trypanosoma brucei*, which are the causative agent of African sleeping sickness (Abdeen 2016). In an extension of those studies, we explored asymmetric compound **1** analogs for their antibiotic effects against the *ESKAPE* pathogens. In that study, while we found that inhibitors were largely ineffective against Gram-negative bacteria, many

exhibited potent inhibition of the proliferation of Gram-positive bacteria, in particular *Staphylococcus aureus* (Abdeen 2018).

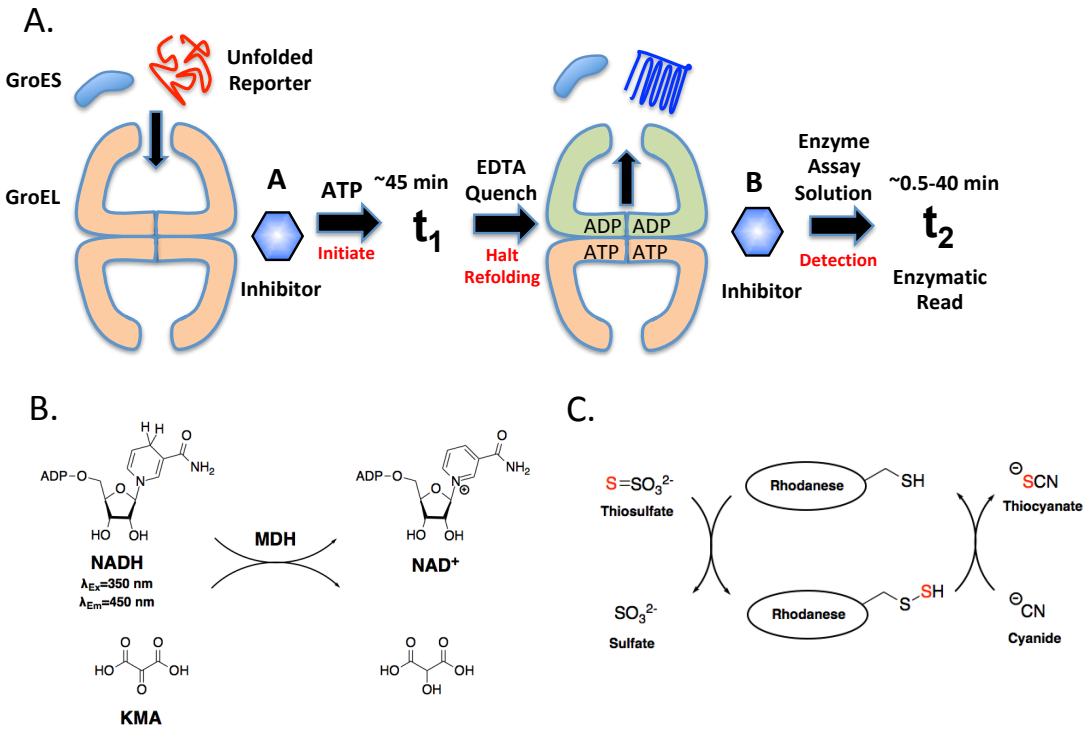

Figure 5 – Schematic of the general GroEL/ES-mediated folding assays used for evaluating test compounds. A. Compounds are added to a binary mixture of GroEL, GroES, and unfolded enzyme reporter. ATP is added to initiate the folding cycle, and after a short incubation time (30-60 min, depending on the particular enzyme to be folded), EDTA is added to quench the cycle (in the case of rhodanese as the reporter enzyme, no EDTA quench is added). Inhibitors are added at point A for the refolding assay plate while inhibitors are added at point B for the native counter-screen plate. This was done to determine if compounds inhibit native enzyme reporter activity instead of GroEL/ES. Reporter substrates are added to determine the activity of the reporter enzyme and thus the efficacy of the refolding mechanism (Johnson 2014). The enzymatic reporter reactions are shown for malate dehydrogenase (panel B) and rhodanese (panel C).

With our compound **1** analogs eliciting antibiotic effects against parasites and bacteria, and because GroEL is highly conserved across all organisms (Table 2), we reasoned that they may also exhibit antibiotic effects against *M. tuberculosis*. Thus, in the present study, we evaluated the previously developed compound **1** analogs for their ability to inhibit *M. tuberculosis* proliferation in liquid media. Because we were unsure

whether or not these compounds required both of the sulfonamide end-capping groups to maintain potent inhibition, we developed a new series of what we term “half-molecules” that contain only one sulfonamide on either the right or left-hand sides of the 2-phenylbenzoxazole core (Figure 6).

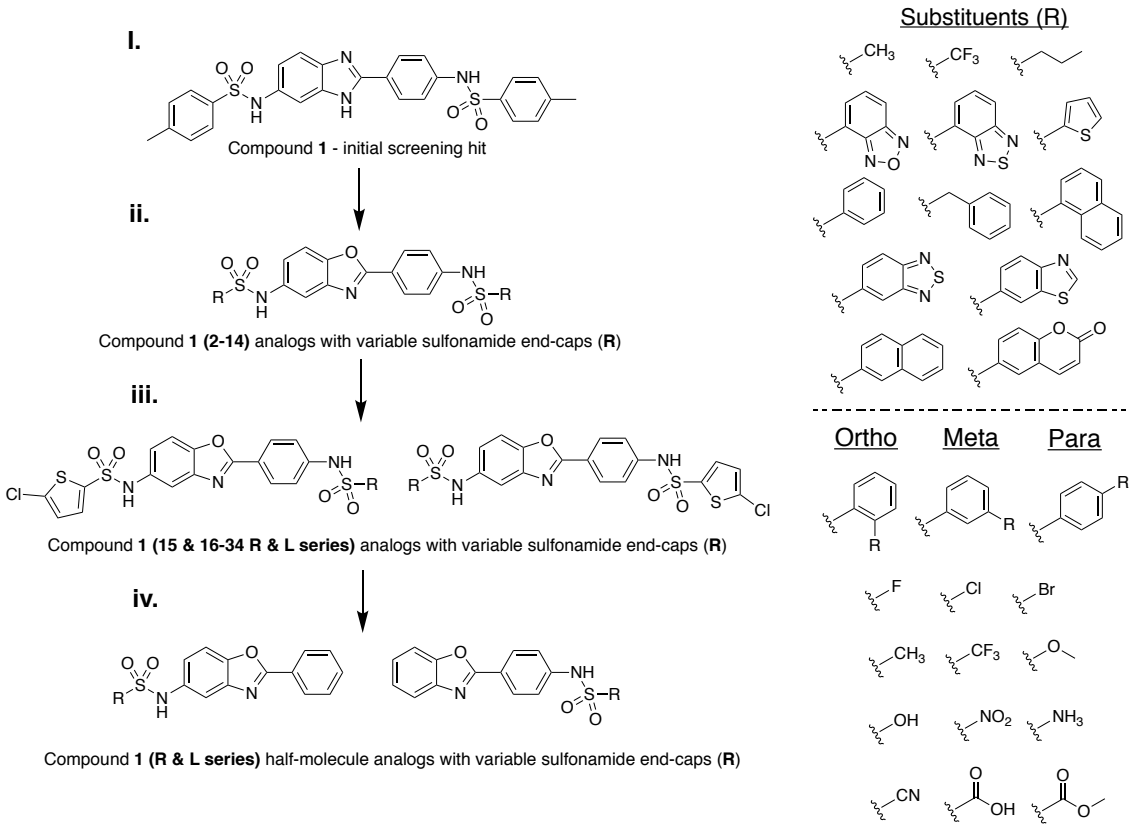

Figure 6 – Summary of progression of compound **1** testing and optimization from previous studies. i. Compound **1** was an initial hit that emerged from our recent high-throughput screening for GroEL/ES inhibitors (Abdeen 2016). ii. The related analog, **2e-*p***, was found in the PubChem database (CID #1098316) and had reported bioactivity in only 8 of the 285 assays it has been evaluated in. Analog inhibitors were found to be cytotoxic to *Trypanosoma brucei* parasites. In this study, 50 inhibitor analogs bearing this scaffold were tested. iii. Asymmetric compound **1** inhibitor analogs with both left and right-hand series were tested on the *ESKAPE* pathogens. Inhibitors were found to be cytotoxic to Gram-positive bacteria. In that study, 40 inhibitor analogs bearing this scaffold were tested. iv. Half-molecule compound **1** inhibitor analogs with both the left and right-hand series. The current study will look into the efficacy of these inhibitors. In this study, 58 inhibitor analogs bearing this scaffold were tested. Representative substituents in the R position for the inhibitor analogs are presented.

Table 2 – Conservation between GroEL (HSP60) chaperonins. Values represent % identical amino acids compared to *E. coli* GroEL.

Species	GroEL (HSP60)
E. coli	100%
S. aureus	57%
T. brucei (HSP60.1)	53%
T. brucei (HSP60.2)	43%
T. brucei (HSP60.3)	40%
M. tuberculosis (GroEL1)	54%
M. tuberculosis (GroEL2)	59%

Exploring the ability of compound 1 analogs to also inhibit *Mtb* protein tyrosine phosphatase B (PtpB), which could allow the targeting of intracellular bacteria evading host cell immune responses.

Another possible strategy to treat tuberculosis infections is by targeting a virulence factor that *Mtb* secretes into the cytoplasm of host macrophages, protein tyrosine phosphatase B (PtpB). By secreting PtpB into the cytosol of host macrophages, *Mtb* disrupts host cell immune responses by blocking ERK1/2 and p38 mediated IL-6 production and promoting host cell survival by acting on the Akt pathway (Zhou 2010). Deletion of PtpB has been shown to block intracellular survival of *Mtb* in IFN-γ activated macrophages and reduce the bacterial load in a guinea pig model (Zhou 2010). In a 2007 study by Grundner *et al.*, a crystal structure was reported of PtpB in complex with the selective PtpB inhibitor (oxalylamino-methylene)-thiophene sulfonamide (OMTS – Figure 7A). In this structure, while PtpB was seen to adopt a simplified PTP fold with features of conventional PTPs, two key differences were noted. First, PtpB contains a disordered, acidic loop and a flexible, two-helix lid that covers the active site, and inhibitor binding promotes a large hinge motion of one helix in the lid to form a hydrophobic hairpin and a channel that leads to the catalytic cysteine. Second, the 30-residue disordered loop folds to form a new helix bordering the active site. With such structural differences from other PTPs, there could be potential selectivity for targeting

PtpB over other phosphatases (Grundner 2005). Interestingly, two OMTS molecules were found bound in the crystal structure, raising the possibility of two phosphotyrosine binding sites (Grundner 2007). In these binding conformations, we noted that the sulfonamides of each OMTS molecule reside ~11-12 Å apart from one another (Figure 7B), making key polar interactions with water molecules and protein backbone amides and side chains (e.g. Arg59, Arg63, His94, Glu129, and Arg136). Since the two sulfonamides of our compound **1** analogs are also ~11-12 Å apart, we envisioned that this analog series might also be capable of inhibiting *Mtb* PtpB in a conformation that would bridge across the two OMTS molecules. This raises the possibility that this class of molecules could inhibit the two GroEL homologs to target actively replicating mycobacteria and dormant ones in granulomas, as well as inhibiting PtpB to target intracellular *Mtb* that are evading host cell immune responses. Thus, this class of inhibitors could be effective against all stages of *Mtb* infection. The present study was designed to explore the possibility of such dual-targeting GroEL/ES and PtpB inhibitors *in vitro* and in cell culture, with future studies envisioned to build from the established structure-activity relationships (SAR) to further optimize lead candidates for evaluating in animal infection models.

A)

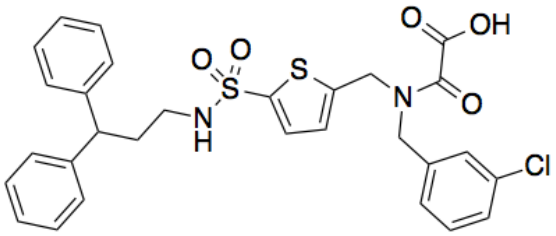

B)

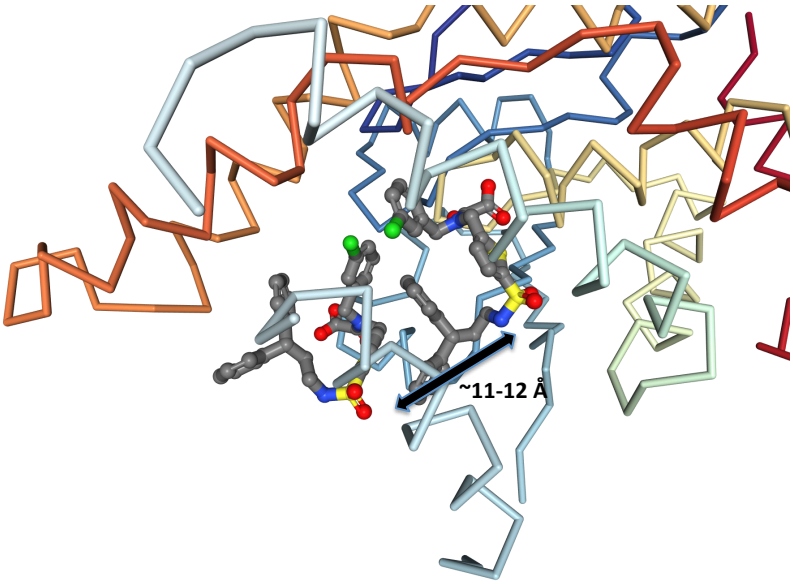

Figure 7 – Crystal structure of OMTS bound in PtpB. A. Structure of OMTS molecule. B. Two molecules of OMTS bound in the PtpB active site making key polar interactions. Image adapted from 2OZ5 crystal structure (Grundner 2007). When bound, the sulfonamides of each OMTS molecule reside ~11-12 Å apart, similar to our compound **1** analog inhibitors.

RESULTS AND DISCUSSION

Identifying the efficacies of compound 1 analogs for inhibiting the GroEL/ES-mediated folding cycle.

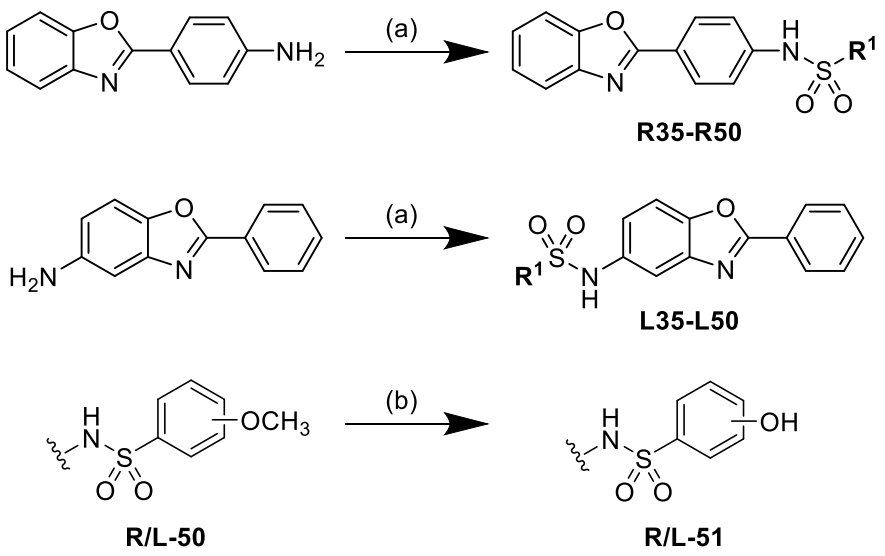

Scheme 1. Synthesis of the R- and L-series of half-molecules. (a) R^1-SO_2Cl, pyridine, CH_2Cl_2, rt.; (b) BBr_3, CH_2Cl_2, rt.

Extending from our previous studies that explored the bis-sulfonamide full-molecule series (compounds **1**-**34** – see Tables S1-S3 in the Appendix), a library of half-molecule analogs that had the R^1-substituted sulfonamide end caps on either the Right (R-series) or Left (L-series) sides of the 2-phenylbenzoxazole core (Scheme 1) was synthesized (Abdeen 2016, Abdeen 2018). Representative synthetic protocols and complete compound characterizations (^{1}H-NMR, MS, and RP-HPLC) are presented in the Experimental section. These syntheses resulted in the development of 58 new half-molecules – 29 of each of the R- and L-series analogs. As we previously found that aryl-sulfonamides were the most potent GroEL/ES inhibitors, we primarily developed analogs bearing substituted phenyl-sulfonamides. Furthermore, we biased the analogs to contain a variety of halide substituents and substitution patterns as our previous antibacterial

study indicated that halide-bearing compounds were typically more effective at inhibiting bacterial proliferation than compounds with other substituents (Abdeen 2018).

We next employed a series of well-established biochemical assays to evaluate the inhibitory effects of the new half-molecules against the GroEL/ES chaperonin system. For these assays, we used *E. coli* GroEL/ES as a surrogate as obtaining functional GroEL oligomeric rings from *Mtb* has so far proven elusive. As in previous studies (Abdeen 2016; Johnson 2014), we employed two chaperonin-mediated folding assays using malate dehydrogenase (MDH) and rhodanese (Rho) as the unfolded reporter enzymes. Schematics of these assays are outlined in Figure 5, with detailed protocols presented in the Experimental section. IC_{50} results for the testing of compounds in these two assays are shown in Tables 5-16 in the Appendix section. While the full-molecules had been evaluated in these assays in the previous studies, we have also included their IC_{50} results in Tables 5-16 in the Appendix section for completeness. As visualized in the correlation plot in Figure 8A, compounds were nearly equipotent at inhibiting both of the GroEL/ES-mediated folding assays. As structure-activity relationships (SAR) for full-molecule series have been more thoroughly discussed for these assays in the previous studies, we will primarily present SAR comparisons between the full- vs. half-molecule scaffolds herein. In this context, the full-molecules were significantly more potent than the half-molecules were. We further counter-screened and evaluated compounds for their ability to inhibit native MDH and Rho to identify false-positives that simply inhibit the enzymatic reporter reactions of the coupled folding assays. While some compounds were found to inhibit either the native MDH activity or the native rhodanese activity, only one compound, **28R,** inhibited in both native assays and the IC_{50} values for this compound, as well as the other compounds that inhibited in either native assay, were much larger than the IC_{50} values for the refolding assays (Tables 5-16 in the Appendix section and Figure 8B). These results

suggest that the inhibitors are on target for inhibiting the GroEL/ES-mediated folding cycle.

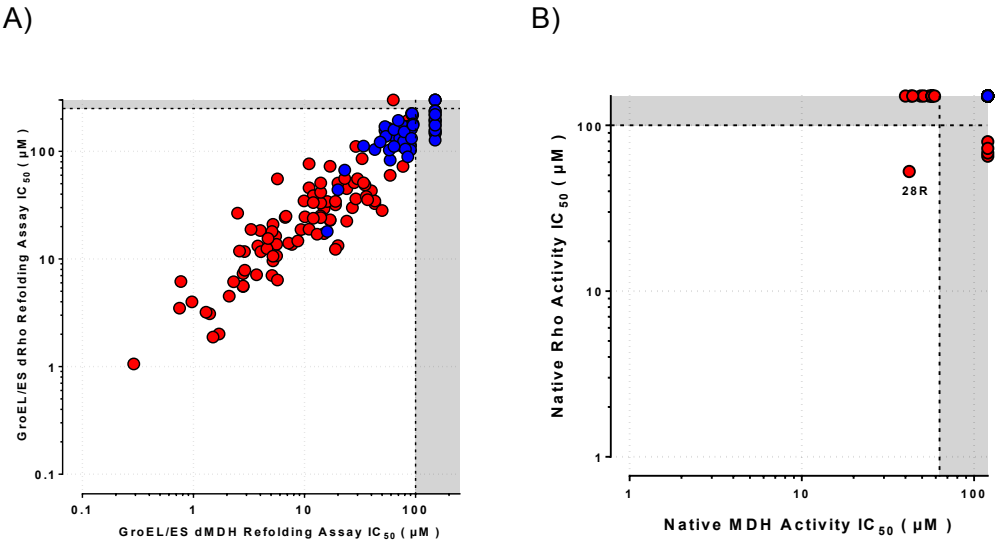

Figure 8 – Correlation plots comparing GroEL/ES-mediated substrate folding and native reporter enzyme inhibition results. A. Compounds inhibit nearly equipotently in both refolding assays, suggesting that compounds are on-target for inhibiting GroEL/ES. B. Correlation plot of IC_{50} values for compounds tested in the native MDH and native Rho reporter enzymatic counter-screens. Only compound **28R** inhibited in both native assay counter-screens and the IC_{50} along with the IC_{50} values for compounds that inhibited in either native assay counter-screen were much larger than those for the refolding assays, suggesting that compounds are on-target for GroEL/ES and not the enzymatic reporter reactions. Results plotted in the grey zones represent IC_{50} values higher than the maximum concentrations listed. Blue values represent half-molecules and red values represent full-molecules.

Compound 1 analogs are largely ineffective against *M. smegmatis*, but some modestly inhibit the proliferation of *M. tuberculosis*.

We next evaluated how effective our GroEL/ES inhibitors would be at inhibiting the proliferation of mycobacteria in liquid culture. In our own lab, we first screened our inhibitors against *M. smegmatis*, which is a non-pathogenic bacterium found in water and soil that is often used as a surrogate for initial high-throughput screening of *Mtb* inhibitors, albeit with varying levels of success (He 2010). Detailed procedures for the proliferation assay are presented in the Experimental section. Briefly, test compounds were incubated in dilution series with *M. smegmatis* for 24 h and an EC_{50} was

determined from OD_{600} readings. Unfortunately, very few compounds inhibited *M. smegmatis* growth, and the ones that did had high EC_{50} values (Tables 5-16 in the Appendix section). Intriguingly, while the half-molecules were poor GroEL/ES inhibitors, four were able to inhibit *M. smegmatis* proliferation (**L36**, **L38-*o***, **L39-*o***, and **L39-*p***), which may indicate off-target effects (Figure 9). While the results from the *M. smegmatis* proliferation testing were less encouraging than we had hoped for, previous studies have also found that *M. smegmatis* is not necessarily a good screening substitute for *M. tuberculosis* (Altaf 2010). This is emphasized by the fact that even current tuberculosis therapeutics are not very effective against *M. smegmatis* (e.g. pyrazinamide and isoniazid). Thus, we further evaluated these compounds in an established *M. tuberculosis* proliferation assay with our collaborators at the Infectious Disease Research Institute in Seattle, Washington. An overview of this assay protocol is presented in the Experimental section. Briefly, test compounds (single concentrations of 200 μM) were incubated with *Mtb* for 5 days and then plates were analyzed for mycobacterial growth and % inhibition values calculated (Tables 5-16 in the Appendix section). Compounds exhibiting >50% inhibition were then re-screened in dose-response format to determine EC_{50} values. On processing the results from this assay, we were happy to see that there were 36 analogs that were more potent at inhibiting *M. tuberculosis* proliferation than inhibiting *M. smegmatis* with 15 compounds having an EC_{50} under 100 μM. Compounds **20R** and **20L** were two of the most potent compounds against *Mtb,* having an EC_{50} value of 26 μM and 59 μM respectively (Tables 5-16 in the Appendix section and Figure 10). For inhibiting *Mtb*, the full-molecules were more effective than the half-molecules, which is consistent with the results for the GroEL/ES-mediated refolding assays. With this being an exploratory study, having compounds that act on *Mtb* at these potencies are promising initial results that future SAR studies can further optimized from.

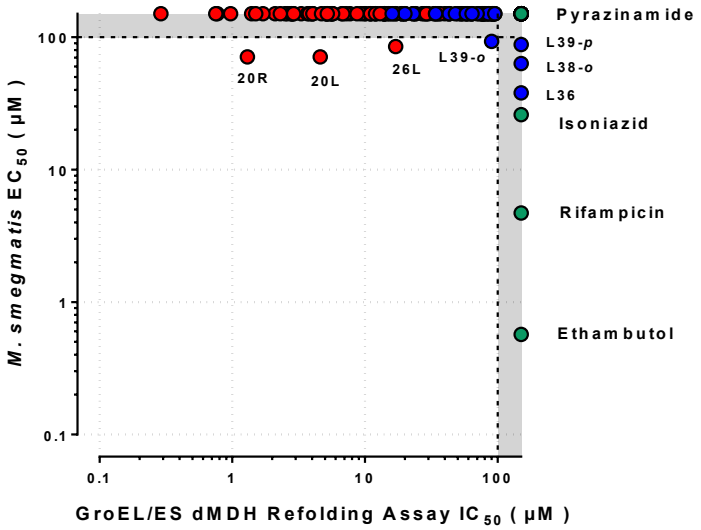

Figure 9 – Correlation plot comparing GroEL/ES-mediated substrate folding with *M. smegmatis* bacterial growth inhibition results. Green values represent tuberculosis antibiotics. While compound **1** analogs were mostly ineffective against *M. smegmatis*, many current tuberculosis antibiotics were not very effective as well. Thus, follow-up screening against *M. tuberculosis* was warranted to see if molecules would also be more effective against the human pathogen.

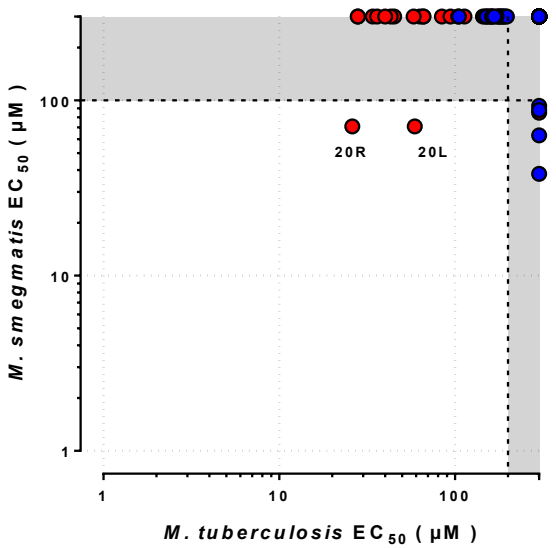

Figure 10 – Correlation plot comparing *M. smegmatis* with *M. tuberculosis* bacterial growth inhibition results. Compounds that had less than 50% inhibition in the single concentration *Mtb* testing were assumed to have EC_{50} values >200 µM. There are 36 compounds that are more potent towards *M. tuberculosis* with 15 compounds having EC_{50} values below 100 µM. Lead compounds **20R** and **20L** have an EC_{50} values of 26 µM and 59 µM respectively.

While compounds can inhibit the human HSP60/10 chaperonin system *in vitro*, many display moderate-to-low cytotoxicity to human cells in culture.

A caveat to targeting *Mtb* GroEL is that human HSP60 is moderately conserved (48% sequence identity with *E. coli* GroEL), which raises concern of potential off-target effects against human cells. However, the HSP60/10 chaperonin system is localized within the mitochondrial matrix of human cells, which is highly impermeable to penetration by small molecules. Thus, even if compounds can inhibit HSP60/10 biochemical functions *in-vitro*, they may never reach and inhibit the chaperonin system in the mitochondrial matrix, permitting selective targeting of bacteria over human cells (Cheng 1989). Nonetheless, we counter-screened compounds in our standard HSP60/10-dMDH folding assay, which was analogous to the GroEL/ES-dMDH assays so that IC_{50} results could be directly compared between the two chaperonin systems. A detailed protocol for this assay is presented in the Experimental section, with results presented in Tables 5-16 of the Appendix section. While compounds were able to inhibit human HSP60/10, there were inhibitors that showed a greater selectivity towards *E. coli* GroEL/ES over human HSP60/10, with ~20 compounds showing around a 10-fold greater selectivity towards *E. coli* GroEL/ES (Figure 11). As with GroEL/ES, the full-molecules were more potent at inhibiting HSP60/10 than the half-molecules were. Lead compounds in this study were compounds **20R**, and **20L**, having IC_{50} values under 5 μM for the GroEL/ES dMDH refolding mechanism. When compared to human HSP60/10 dMDH refolding, both these compounds have >8-fold selectivity for GroEL/ES over human. Future SAR studies will need to be performed to optimize this series of compounds, but the initial selectivity towards bacterial GroEL/ES is promising in the development of compound **1** inhibitor analogs.

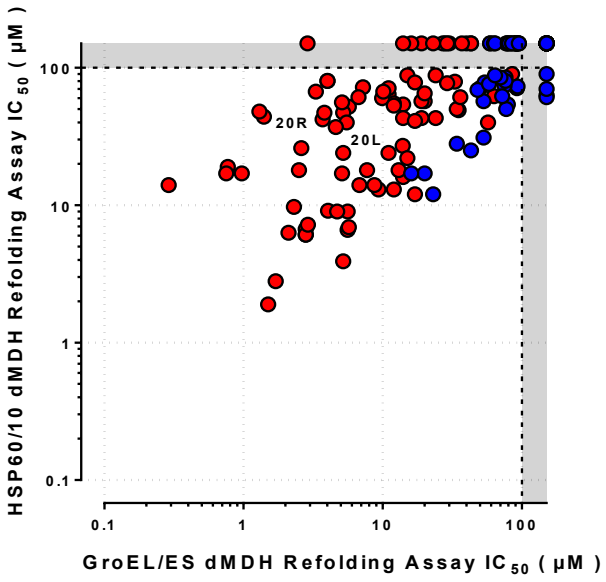

Figure 11 – Correlation plots comparing human HSP60/10-dMDH with GroEL/ES-dMDH folding inhibition. Compounds towards the top and left of the graph exhibit greater selectivity towards *E. coli* GroEL/ES over human HSP60/10.

We next evaluated all the compounds in two Alamar Blue-based cell viability assays, where compounds were incubated with human liver (THLE-3) or kidney (HEK 293) cells over a 48 h time period. A detailed protocol for these assays is presented in the Experimental section, with cell viability results (cytotoxicity CC_{50} values) presented in Tables 5-16 in the Appendix. In general, the half-molecules exhibited higher CC_{50} values than the full-molecules, which would not be surprising since they were also weaker HSP60/10 inhibitors; however, as evident in Figure 12, there is no correlation between HSP60/10 IC_{50} values and cell viability CC_{50} values, suggesting cytotoxicities could be from off-target effects.

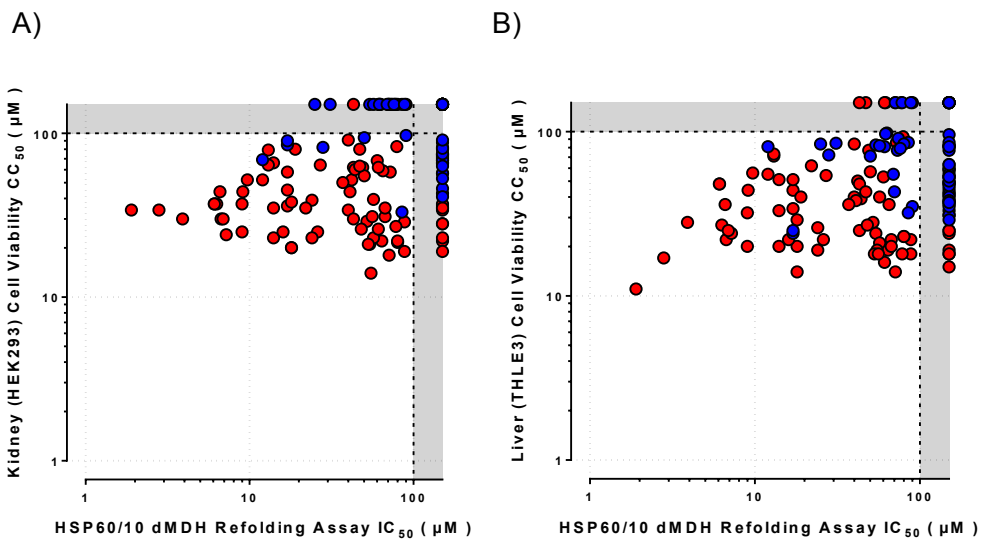

Figure 12 – Correlation plots comparing human HSP60/10-dMDH folding inhibition results with human liver and kidney cell viability results. A. HEK 293 kidney cells. B. THLE-3 liver cells. There is no correlation between HSP60/10 IC_{50} values and cell viability CC_{50} values. Compounds might not even inhibit HSP60 because it is located in the mitochondria and would have to cross the membrane. Cytotoxicities in cell assays could be from off target effects.

Identifying the efficacies of compound 1 analogs for inhibiting the *Mtb* protein tyrosine phosphatase B (PtpB) virulence factor.

While the above studies supported the feasibility of identifying GroEL/ES inhibitors that could kill actively replicating *Mtb* (e.g. **20R** and **20L**), we were particularly intrigued by the possibility of also targeting the protein tyrosine phosphatase B (PtpB) virulence factor that intracellular *Mtb* secretes into macrophages to evade host cell immune responses. To investigate this possibility, we obtained a His-tagged version of *Mtb* PtpB that was previously developed by Grundner *et al.* to generate recombinantly expressed and purified enzyme (Grundner 2007). Following previously reported procedures by Zhou *et al.*, which monitored for phosphatase activity using *para*-nitrophenyl phosphate (pNPP), we then proceeded to evaluate all compounds in dose-response format to obtain IC_{50} values (Zhou 2010). As a preliminary indication of selectively targeting *Mtb* PtpB, we counter-screened against three human phosphatases,

PTPN1 (PTP1B), PTPN2 (TCPTP), and PTPN5 (STEP), using analogous procedures (detailed protocols are presented in the Experimental section).

When tested against *M. tuberculosis* PtpB, while both the full and half-molecules acted on the phosphatase, the full-molecules were generally more potent at inhibiting phosphatase activity (Tables 5-16 in Appendix) (Figure 13A). An interesting discovery for many of the half-molecules was that as compound concentrations increase, they first appear to activate the phosphatase at lower concentrations then inhibit the phosphatase at higher concentrations (Figure 13B). This could be a result of two half-molecules binding to PtpB in a manner like that previously observed for OMTS. Thus, binding of the first molecule at the distal site may prop the alpha-helical lid open, allowing the pNPP to then occupy the proximal, active site. Then, at higher concentrations, the second half-molecule could competitively displace the pNPP from the active site, thus showing inhibition. It should be noted, though, that this could potentially be an artifact of this particular assay protocol, as we anticipate that binding to either site would compete with a phosphorylated peptide. Thus, IC_{50} values could be more potent in a physiological context than what we have reported, although future studies would need to confirm this.

A) B)

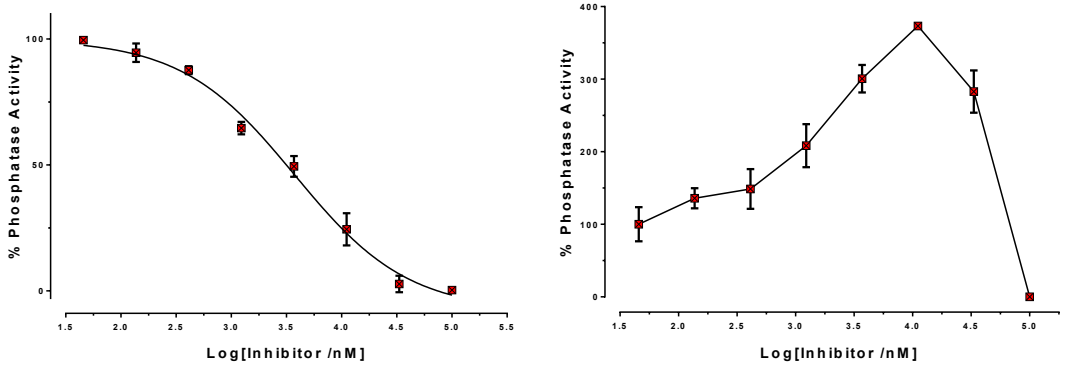

Figure 13 – Representative *Mtb* PtpB phosphatase dose-response curves. A. compound **2h-*p*** and B. compound **L51-*p***. Full-molecules inactivate the phosphatase activity while most half-molecules first activate the phosphatase at lower concentrations, then inhibit the phosphatase at higher concentrations.

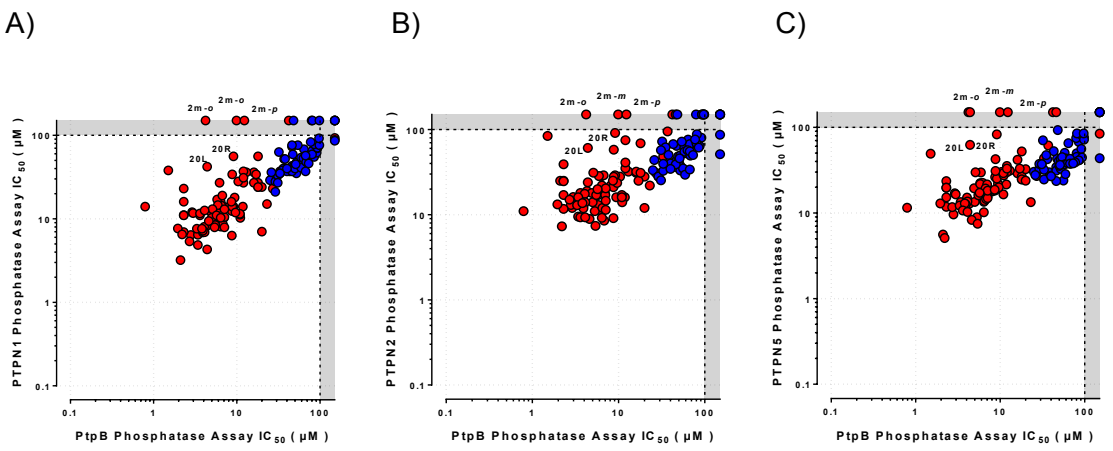

Figure 14 – Correlation plots comparing *Mtb* PtpB inhibition results with human PTP's. A. PTPN1 (PTP1B). B. PTPN2 (TCPTP). C. PTPN5 (STEP).

While the aggregate results for the compound **1** analogs as a whole were not very promising for being able to selectively inhibit *Mtb* PtpB over the three human phosphatases (Figure 14), a few noteworthy compounds stood out. In particular, SAR reveals 10 compounds that exhibit greater than 10-fold selectivity for *Mtb* PtpB over the human phosphatases (compounds **2d-*m*, 2h-*o***, **2h-*m***, **2m-*o***, **2m-*m***, **2m-*p***, **10**, **15**, **20L**, and **20R),** with two divergent series that could be further explored in future optimization studies. The first is a series of inhibitors that selectively inhibit PtpB over human phosphatases, but that do not inhibit GroEL/ES-mediated refolding functions. These are best represented by compounds **2m-*o***, **2m-*m***, and **2m-*p*** (Table 3). Thus, future studies could explore new analogs that contain a carboxylate on either the right or left-hand sulfonamides, while varying groups on the other side. The second contains inhibitors that selectively inhibit both *Mtb* GroEL/ES and PtpB over human HSP60/10 and phosphatases. This is particularly evident for analogs **20R** and **20L** (Table 4), which were also two of the most potent inhibitors of *Mtb* proliferation. These were unique compounds within this study as they were the only analogs to contain primary amines that would be charged under physiological conditions. Thus, future studies could explore new analogs that contain amines on either the right or left-hand sulfonamides, while

varying groups on the other side. In either case, additional areas of exploration to optimize inhibitors are varying the sulfonamide linkers and scaffolds other than the 2-phenylbenzoxazole core. Once we have developed more potent and selective GroEL/ES and/or PtpB inhibitors, we will pursue additional studies looking at the effects of inhibiting *Mtb* PtpB in macrophage models, as well as the antibiotic efficacy of lead candidates in an *in vivo* infection model.

CONCLUSIONS AND FUTURE DIRECTIONS

In this study, we evaluated whether or not a series of previously identified GroEL/ES inhibitors, based on the compound **1** scaffold, would be effective at inhibiting the proliferation of *M. tuberculosis*. Furthermore, we envisioned that these molecules could be a dual-targeting inhibitor series capable of inhibiting the *Mtb* GroEL/ES chaperonin systems as well as the PtpB phosphatase that they secrete into macrophages. From this study, our results have illuminated two potential avenues for future optimization studies. The first is a series of compound **1** inhibitors that act solely on PtpB (e.g. **2m-*o***, **2m-*m***, and **2m-*p***) and not GroEL/ES. These compounds showed a greater selectivity for *Mtb* PtpB than human phosphatases as presented in Table 3. This series of compounds would target bacteria evading the host cell immune response and could be used in conjunction with current TB therapeutics that could target actively replicating bacteria. The second is a series of compound **1** inhibitors that target both *Mtb* PtpB and the GroEL/ES chaperonin systems (e.g. **20L** and **20R**). These compounds showed a greater selectivity for *Mtb* PtpB over human phosphatases, as well as bacterial GroEL/ES over human HSP60/10 (Table 4). These compounds would putatively be able to concomitantly target actively replicating bacteria, intracellular bacteria that are evading host cell immune responses, and dormant bacteria that have formed granulomas. Thus, we are hopeful that this could be an effective strategy to treat all stages of tuberculosis. Testing of inhibitors on granuloma formation has not been evaluated yet, and such *in vivo* efficacy experiments are planned for future studies once compounds have been further optimized.

Table 3 – IC_{50} values for phosphatase-only inhibitors. These inhibitors could be used to target intracellular bacteria evading the host cell immune responses.

Assay	**2m-*o*** (IC_{50}) 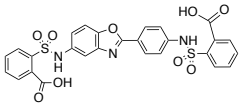	**2m-*m*** (IC_{50}) 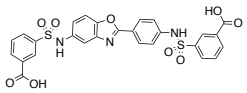	**2m-*p*** (IC_{50}) 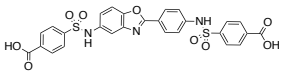
Kidney (HEK 293) cell viability	>100 μM	>100 μM	>100 μM
Liver (THLE-3) cell viability	>100 μM	>100 μM	>100 μM
Mtb PtpB	4.2 μM	9.9 μM	12 μM
Human PTPN1	>100 μM	>100 μM	>100 μM
Human PTPN2	>100 μM	>100 μM	>100 μM
Human PTPN5	>100 μM	>100 μM	>100 μM

Table 4 – IC_{50} values for dual-targeting phosphatase and GroEL/ES inhibitors. These compounds show a greater selectivity for *Mtb* PtpB over the human phosphatases and are also potent and selective GroEL/ES inhibitors. These compounds are envisioned to target actively replicating bacteria (i.e. inhibiting GroEL2), bacteria evading the host cell immune responses (i.e. inhibiting PtpB), and bacteria in granulomas contributing to latent disease (i.e. inhibiting GroEL1).

Assay	**20R** (IC_{50}) 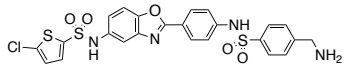	**20L** (IC_{50}) 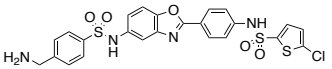
Kidney (HEK 293) cell viability	26 μM	50 μM
Liver (THLE-3) cell viability	27 μM	36 μM
Mtb PtpB	9.1 μM	4.4 μM
Human PTPN1	56 μM	42 μM
Human PTPN2	91 μM	61 μM
Human PTPN5	75 μM	62 μM
GroEL/ES-dMDH refolding	1.3 μM	4.6 μM
HSP60/10-dMDH refolding	48 μM	37 μM
Native MDH counter-screen	>100 μM	>100 μM
Native Rho counter-screen	>63 μM	>63 μM
M. smegmatis EC_{50}	71 μM	71 μM
M. tuberculosis EC_{50}	26 μM	59 μM

EXPERIMENTAL

Compound synthesis and characterization.

Unless otherwise stated, all chemicals were purchased from commercial suppliers and used without further purification. Reaction progress was monitored by thin-layer chromatography on silica gel 60 F254 coated glass plates (EM Sciences). Flash chromatography was performed using a Biotage Isolera One flash chromatography system and eluting through Biotage KP-Sil Zip or Snap silica gel columns for normal-phase separations (hexanes:EtOAc gradients), or Snap KP-C18-HS columns for reverse-phase separations (H_2O:MeOH gradients). Reverse-phase high-performance liquid chromatography (RP-HPLC) was performed using a Waters 1525 binary pump, 2489 tunable UV/Vis detector (254 and 280 nm detection), and 2707 autosampler. For preparatory HPLC purification, samples were chromatographically separated using a Waters XSelect CSH C18 OBD prep column (part number 186005422, 130 Å pore size, 5 mm particle size, 19x150 mm), eluting with a H_2O:CH_3CN gradient solvent system. Linear gradients were run from either 100:0, 80:20, or 60:40 A:B to 0:100 A:B (A = 95:5 H_2O:CH_3CN, 0.05% TFA; B = 5:95 H_2O:CH_3CN, 0.05% TFA. Products from normal-phase separations were concentrated directly, and reverse-phase separations were concentrated, diluted with H_2O, frozen, and lyophilized. For primary compound purity analyses (HPLC-1), samples were chromatographically separated using a Waters XSelect CSH C18 column (part number 186005282, 130 Å pore size, 5 mm particle size, 3.0x150 mm), eluting with the above H_2O:CH_3CN gradient solvent systems. For secondary purity analyses (HPLC-2) of final test compounds, samples were chromatographically separated using a Waters XBridge C18 column (either part number 186003027, 130 Å pore size, 3.5 mm particle size, 3.0x100 mm, or part number 186003132, 130 Å pore size, 5.0 mm particle size, 3.0x100 mm), eluting with a H_2O:MeOH gradient solvent system. Linear gradients were run from

either 100:0, 80:20, 60:40, or 20:80 A:B to 0:100 A:B (A = 95:5 H_2O:MeOH, 0.05% TFA; B = 5:95 H_2O:MeOH, 0.05% TFA). Test compounds were found to be >95% in purity from both RP-HPLC analyses. Mass spectrometry data were collected using either an Agilent analytical LC-MS at the IU Chemical Genomics Core Facility (CGCF), or a Thermo-Finnigan LTQ LC-MS in-lab. ^{1}H-NMR spectra were recorded on either Bruker 300 MHz or 500 MHz spectrometers. Chemical shifts are reported in parts per million and calibrated to the d_6-DMSO solvent peaks at 2.50 ppm. We previously synthesized compounds **1-14** (including the *ortho*-, *meta*-, and *para*-analogs of 2a-m), as well as **15**, **16R-34R**, and **16L-34L** (Abdeen 2016 and Kunkle 2018). For the new half-molecules synthesized and evaluated in this study, the general sulfonamide coupling step is presented immediately below, followed by compound characterizations for each analog synthesized.

General procedure for the sulfonamide coupling step.

To stirring mixtures of either 4-(1,3-benzoxazol-2-yl)aniline or 2-phenyl-1,3-bezoxazol-5-amine (1 eq.) in anhydrous CH_2Cl_2 (5 mL) were added the respective R^1-sulfonyl chlorides (1.3 eq.), followed by anhydrous pyridine (1.3 eq.). The reactions were allowed to stir at room temperature for 18 h, then chromatographed over silica (hexanes:EtOAc gradient), and concentrated. If necessary, the products were further purified by preparatory RP-HPLC (H_2O:CH_3CN gradient), concentrated, and lyophilized. Refer below for individual compound characterization data.

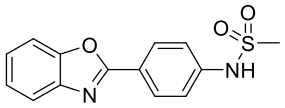

R35: *N*-(4-(benzo[*d*]oxazol-2-yl)phenyl)methanesulfonamide. ^{1}H-NMR (300 MHz, d_6-DMSO) δ 10.35 (br s, 1H), 8.13-8.20 (m, 2H), 7.74-7.81 (m, 2H), 7.36-7.44 (m, 4H), 3.13 (s, 3H); MS (ESI) $C_{14}H_{12}N_2O_3S$ $[M-H]^-$ *m/z* expected = 287.1, observed = 286.9; HPLC-1 = 98%; HPLC-2 = 99%.

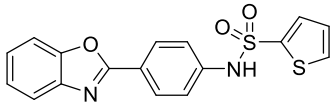

R36: *N*-(4-(benzo[*d*]oxazol-2-yl)phenyl)thiophene-2-sulfonamide. ^{1}H-NMR (300 MHz, d_6-DMSO) δ 11.01 (br s, 1H), 8.08-8.15 (m, 2H), 7.94 (dd, *J* = 5.0, 1.4 Hz, 1H), 7.72-7.80 (m, 2H), 7.68 (dd, *J* = 3.8, 1.4 Hz, 1H), 7.34-7.44 (m, 4H), 7.14 (dd, *J* = 5.0, 3.8 Hz, 1H); MS (ESI) $C_{17}H_{12}N_2O_3S_2$ $[M-H]^-$ *m/z* expected = 355.0, observed = 354.9; HPLC-1 = >99%; HPLC-2 = >99%.

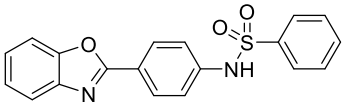

R37: *N*-(4-(benzo[*d*]oxazol-2-yl)phenyl)benzenesulfonamide. ^{1}H-NMR (500 MHz, d_6-DMSO) δ 10.91 (br s, 1H), 8.05-8.09 (m(*para*), 2H), 7.84-7.88 (m, 2H), 7.72-7.78 (m, 2H), 7.61-7.66 (m, 1H), 7.56-7.61 (m, 2H), 7.36-7.42 (m, 2H), 7.31-7.35 (m(*para*), 2H); MS (ESI) $C_{19}H_{14}N_2O_3S$ $[M-H]^-$ *m/z* expected = 349.1, observed = 349.0; HPLC-1 = >99%; HPLC-2 = >99%.

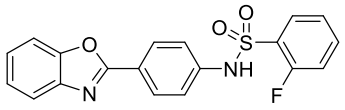

R38-*o*: *N*-(4-(benzo[*d*]oxazol-2-yl)phenyl)-2-fluorobenzenesulfonamide. ^{1}H-NMR (500 MHz, d_6-DMSO) δ 11.22 (br s, 1H), 8.04-8.09 (m, 2H), 7.95 (td, *J* = 7.6, 1.7 Hz, 1H), 7.68-7.78 (m, 3H), 7.36-7.46 (m, 4H), 7.29-7.35 (m, 2H); MS (ESI) $C_{19}H_{13}FN_2O_3S$ $[M-H]^-$ *m/z* expected = 367.1, observed = 367.0; HPLC-1 = 99%; HPLC-2 = 97%.

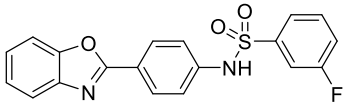

R38-*m*: *N*-(4-(benzo[*d*]oxazol-2-yl)phenyl)-3-fluorobenzenesulfonamide. ^{1}H-NMR (500 MHz, d_6-DMSO) δ 10.98 (br s, 1H), 8.07-8.12 (m, 2H), 7.73-7.79 (m, 2H), 7.63-7.71 (m, 3H), 7.50-7.56 (m, 1H), 7.37-7.43 (m, 2H), 7.33-7.36 (m, 2H); MS (ESI) $C_{19}H_{13}FN_2O_3S$ $[M-H]^-$ *m/z* expected = 367.1, observed = 366.9; HPLC-1 = >99%; HPLC-2 = 99%.

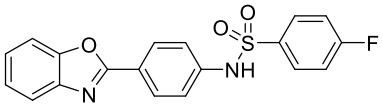

R38-*p*: *N*-(4-(benzo[*d*]oxazol-2-yl)phenyl)-4-fluorobenzenesulfonamide. ^{1}H-NMR (500 MHz, d_6-DMSO) δ 10.97 (br s, 1H), 8.11-8.16 (m, 2H), 7.94-7.99 (m, 2H), 7.78-7.84 (m, 2H), 7.42-7.52 (m, 4H), 7.36-7.41 (m, 2H); MS (ESI) $C_{19}H_{13}FN_2O_3S$ $[M-H]^-$ *m/z* expected = 367.1, observed = 366.9; HPLC-1 = 98%; HPLC-2 = 96%.

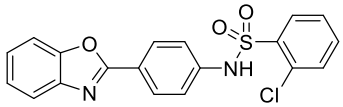

R39-*o*: *N*-(4-(benzo[*d*]oxazol-2-yl)phenyl)-2-chlorobenzenesulfonamide. ^{1}H-NMR (500 MHz, d_6-DMSO) δ 11.22 (br s, 1H), 8.14-8.18 (m, 1H), 8.04-8.08 (m, 2H), 7.72-7.77 (m, 2H), 7.66 (d, *J* = 3.8 Hz, 2H), 7.54-7.60 (m, 1H), 7.36-7.42 (m, 2H), 7.28-7.33 (m, 2H); MS (ESI) $C_{19}H_{13}ClN_2O_3S$ $[M-H]^-$ *m/z* expected = 383.0, observed = 382.9; HPLC-1 = >99% HPLC-2 = 99%.

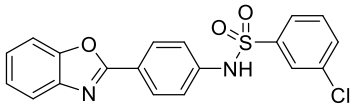

R39-*m*: *N*-(4-(benzo[*d*]oxazol-2-yl)phenyl)-3-chlorobenzenesulfonamide. ^{1}H-NMR (500 MHz, d_6-DMSO) δ 10.98 (br s, 1H), 8.08-8.13 (m, 2H), 7.86 (t, *J* = 1.9 Hz, 1H), 7.80 (dq, *J* = 7.9, 0.8 Hz, 1H), 7.72-7.78 (m, 3H), 7.63 (t, *J* = 7.9 Hz, 1H), 7.37-7.43 (m, 2H), 7.33-7.37 (m, 2H); MS (ESI) $C_{19}H_{13}ClN_2O_3S$ $[M-H]^-$ *m/z* expected = 383.0, observed = 382.9; HPLC-1 = >99%; HPLC-2 = >99%.

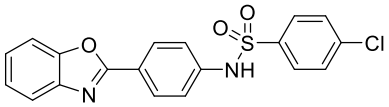

R39-*p*: *N*-(4-(benzo[*d*]oxazol-2-yl)phenyl)-4-chlorobenzenesulfonamide. ^{1}H-NMR (500 MHz, d_6-DMSO) δ 10.96 (br s, 1H), 8.07-8.11 (m, 2H), 7.83-7.87 (M, 2H), 7.73-7.79 (m, 2H), 7.65-7.69 (m, 2H), 7.36-7.43 (m, 2H), 7.31-7.35 (m, 2H); MS (ESI) $C_{19}H_{13}ClN_2O_3S$ $[M-H]^-$ *m/z* expected = 383.0, observed = 382.9; HPLC-1 = 99%.

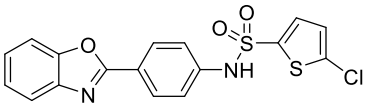

R40: *N*-(4-(benzo[*d*]oxazol-2-yl)phenyl)-5-chlorothiophene-2-sulfonamide. ^{1}H-NMR (300 MHz, d_6-DMSO) δ 11.15 (br s, 1H), 8.10-8.17 (m, 2H), 7.73-7.81 (m, 2H), 7.57 (d, *J* = 4.1 Hz, 1H), 7.35-7.45 (m, 4H), 7.23 (d, *J* = 4.1 Hz, 1H); MS (ESI) $C_{17}H_{11}ClN_2O_3S_2$ [M-H]$^-$ *m/z* expected = 389.0, observed = 388.9; HPLC-1 = 99%; HPLC-2 = 99%.

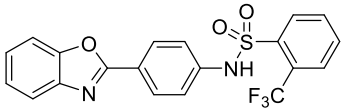

R41-*o*: *N*-(4-(benzo[*d*]oxazol-2-yl)phenyl)-2-(trifluoromethyl)benzenesulfonamide. ^{1}H-NMR (500 MHz, d_6-DMSO) δ 11.25 (br s, 1H), 8.18 (d, *J* = 7.6 Hz, 1H), 8.08-8.12 (m, 2H), 8.02-8.05 (m, 1H), 7.84-7.93 (m, 2H), 7.73-7.79 (m, 2H), 7.36-7.43 (m, 2H), 7.31-7.35 (m, 2H); MS (ESI) $C_{20}H_{13}F_3N_2O_3S$ [M-H]$^-$ *m/z* expected = 417.1, observed = 416.9; HPLC-1 = >99%; HPLC-2 = >99%.

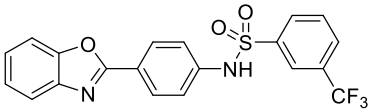

R41-*m*: *N*-(4-(benzo[*d*]oxazol-2-yl)phenyl)-3-(trifluoromethyl)benzenesulfonamide. ^{1}H-NMR (500 MHz, d_6-DMSO) δ 11.02 (br s, 1H), 8.08-8.15 (m, 4H), 8.06 (d, *J* = 7.9 Hz, 1H), 7.85 (t, *J* = 7.9 Hz, 1H), 7.74-7.78 (m, 2H), 7.37-7.43 (m, 2H), 7.33-7.37 (m, 2H); MS (ESI) $C_{20}H_{13}F_3N_2O_3S$ [M-H]$^-$ *m/z* expected = 417.1, observed = 416.9; HPLC-1 = >99%; HPLC-2 = 99%.

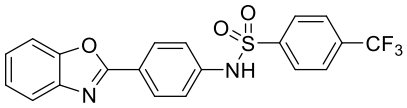

R41-*p*: *N*-(4-(benzo[*d*]oxazol-2-yl)phenyl)-4-(trifluoromethyl)benzenesulfonamide. ^{1}H-NMR (500 MHz, d_6-DMSO) δ 11.11 (br s, 1H), 8.08-8.12 (m, 2H), 8.04-8.08 (m, 2H), 7.97-8.01 (m, 2H), 7.73-7.79 (m, 2H), 7.37-7.43 (m, 2H), 7.33-7.37 (m, 2H); MS (ESI) $C_{20}H_{13}F_3N_2O_3S$ $[M-H]^-$ *m/z* expected = 417.1, observed = 416.9; HPLC-1 = >99%; HPLC-2 = >99%.

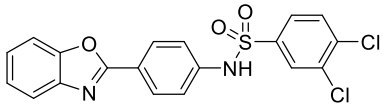

R42: *N*-(4-(benzo[*d*]oxazol-2-yl)phenyl)-3,4-dichlorobenzenesulfonamide. ^{1}H-NMR (500 MHz, d_6-DMSO) δ 10.55 (br s, 1H), 8.13-8.18 (m, 2H), 7.94 (d, *J* = 1.9 Hz, 1H), 7.82 (d, *J* = 8.2 Hz, 1H), 7.71 (d, *J* = 8.8 Hz, 1H), 7.57-7.67 (m, 4H), 7.49 (d, *J* = 1.6 Hz, 1H), 7.12 (dd, *J* = 8.7 Hz, 1H); MS (ESI) $C_{19}H_{12}Cl_2N_2O_3S$ $[M-H]^-$ *m/z* expected = 417.0, observed = 416.8; HPLC-1 = >99%; HPLC-2 = >99%.

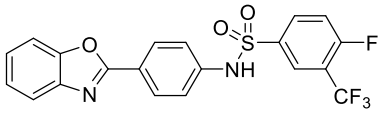

R43: *N*-(4-(benzo[*d*]oxazol-2-yl)phenyl)-4-fluoro-3-(trifluoromethyl)benzenesulfonamide. ^{1}H-NMR (500 MHz, d_6-DMSO) δ 11.01 (br s, 1H), 8.19 (dd, *J* = 8.4, 4.3 Hz, 1H), 8.16 (d, *J* = 6.3 Hz, 1H), 8.07-8.13 (m, 2H), 7.72-7.79 (m, 3H), 7.36-7.43 (m, 2H), 7.32-7.36 (m, 2H); MS (ESI) $C_{20}H_{12}F_4N_2O_3S$ $[M-H]^-$ *m/z* expected = 435.0, observed = 434.9; HPLC-1 = >99%; HPLC-2 = >99%.

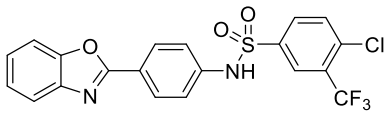

R44: *N*-(4-(benzo[*d*]oxazol-2-yl)phenyl)-4-chloro-3-(trifluoromethyl)benzenesulfonamide. ^{1}H-NMR (500 MHz, d_6-DMSO) δ 11.06 (br s, 1H), 8.16-8.19 (m, 1H), 8.06-8.13 (m, 3H), 7.97 (d, *J* = 8.2 Hz, 1H), 7.73-7.79 (m, 2H), 7.36-7.43 (m, 2H), 7.32-7.36 (m, 2H); MS (ESI) $C_{20}H_{12}ClF_3N_2O_3S$ $[M-H]^-$ *m/z* expected = 451.0, observed = 450.8; HPLC-1 = >99%; HPLC-2 = >99%.

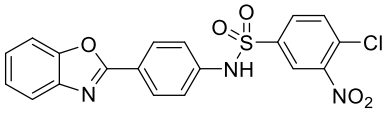

R45: *N*-(4-(benzo[*d*]oxazol-2-yl)phenyl)-4-chloro-3-nitrobenzenesulfonamide. ^{1}H-NMR (500 MHz, d_6-DMSO) δ 11.17 (br s, 1H), 8.52 (d, *J* = 2.2 Hz, 1H), 8.09-8.13 (m, 2H), 8.06 (dd, *J* = 8.5, 1.9 Hz, 1H), 8.00 (d, *J* = 8.5 Hz, 1H), 7.72-7.79 (m, 2H), 7.38-7.43 (m, 2H), 7.33-7.38 (m, 2H); MS (ESI) $C_{19}H_{12}ClN_3O_5S$ $[M-H]^-$ *m/z* expected = 428.0, observed = 427.9; HPLC-1 = 99%; HPLC-2 = 99%.

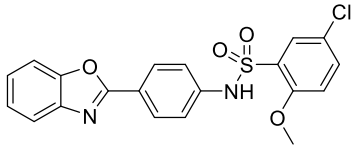

R46: *N*-(4-(benzo[*d*]oxazol-2-yl)phenyl)-5-chloro-2-methoxybenzenesulfonamide. ^{1}H-NMR (500 MHz, d_6-DMSO) δ 10.78 (br s, 1H), 8.03-8.08 (m, 2H), 7.81 (d, *J* = 2.5 Hz, 1H), 7.71-7.77 (m, 2H), 7.66 (dd, *J* = 9.0, 2.7 Hz, 1H), 7.34-7.42 (m, 2H), 7.29-7.33 (m, 2H), 7.22 (d, *J* = 8.8 Hz, 1H), 3.87 (s, 3H); MS (ESI) $C_{20}H_{15}ClN_2O_4S$ $[M-H]^-$ *m/z* expected = 413.0, observed = 412.9; HPLC-1 = >99%; HPLC-2 = >99%.

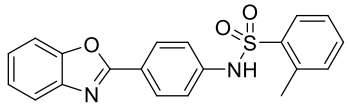

R47-*o*: *N*-(4-(benzo[*d*]oxazol-2-yl)phenyl)-2-methylbenzenesulfonamide. ^{1}H-NMR (300 MHz, d_6-DMSO) δ 11.02 (br s, 1H), 8.01-8.07 (m, 2H), 7.96-8.01 (m, 1H), 7.70-7.77 (m, 2H), 7.49-7.56 (m, 1H), 7.35-7.44 (m, 4H), 7.25-7.30 (m, 2H), 2.62 (s, 3H); MS (ESI) $C_{20}H_{16}N_2O_3S$ $[M-H]^-$ *m/z* expected = 363.1, observed = 363.0; HPLC-1 = >99%; HPLC-2 = >99%.

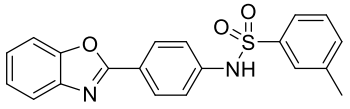

R47-*m*: *N*-(4-(benzo[*d*]oxazol-2-yl)phenyl)-3-methylbenzenesulfonamide. ^{1}H-NMR (300 MHz, d_6-DMSO) δ 10.85 (br s, 1H), 8.04-8.10 (m, 2H), 7.71-7.78 (m, 2H), 7.68 (br s, 1H), 7.61-7.67 (m, 1H), 7.43-7.48 (m, 2H), 7.36-7.41 (m, 2H), 7.29-7.35 (m, 2H), 2.35 (s, 3H); MS (ESI) $C_{20}H_{16}N_2O_3S$ $[M-H]^-$ *m/z* expected = 363.1, observed = 363.0; HPLC-1 = >99%; HPLC-2 = >99%.

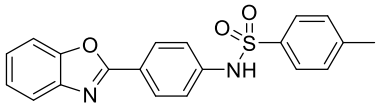

R47-*p*: *N*-(4-(benzo[*d*]oxazol-2-yl)phenyl)-4-methylbenzenesulfonamide. ^{1}H-NMR (500 MHz, d_6-DMSO) δ 10.83 (br s, 1H), 8.04-8.09 (m, 2H), 7.72-7.78 (m, 4H), 7.36-7.43 (m, 4H), 7.30-7.34 (m, 2H), 2.33 (s, 3H); MS (ESI) $C_{20}H_{16}N_2O_3S$ $[M-H]^-$ *m/z* expected = 363.1, observed = 363.0; HPLC-1 = >99%; HPLC-2 = >99%.

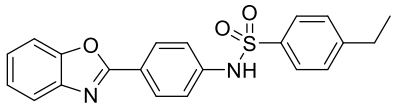

R48: *N*-(4-(benzo[*d*]oxazol-2-yl)phenyl)-4-ethylbenzenesulfonamide. ^{1}H-NMR (500 MHz, d_6-DMSO) δ 10.83 (br s, 1H), 8.04-8.08 (m, 2H), 7.71-7.79 (m, 4H), 7.35-7.43 (m, 4H), 7.30-7.35 (m, 2H), 2.63 (q, *J* = 7.6 Hz, 2H), 1.14 (t, *J* = 7.6 Hz, 3H); MS (ESI) $C_{21}H_{18}N_2O_3S$ $[M-H]^-$ *m/z* expected = 375.1, observed = 377.0; HPLC-1 = >99%; HPLC-2 = 99%.

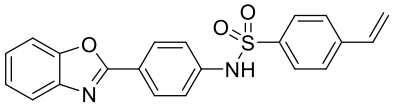

R49: *N*-(4-(benzo[*d*]oxazol-2-yl)phenyl)-4-vinylbenzenesulfonamide. ^{1}H-NMR (500 MHz, d_6-DMSO) δ 10.87 (br s, 1H), 8.05-8.09 (m, 2H), 7.78-7.82 (m, 2H), 7.72-7.77 (m, 2H), 7.64-7.68 (m, 2H), 7.35-7.41 (m, 2H), 7.30-7.34 (m, 2H), 6.76 (dd, *J* = 17.7, 11.0 Hz, 1H), 5.97 (d, *J* = 17.7 Hz, 1H), 5.42 (d, *J* = 11.0 Hz, 1H); MS (ESI) $C_{21}H_{16}N_2O_3S$ $[M-H]^-$ *m/z* expected = 377.1, observed = 375.0; HPLC-1 = 98%; HPLC-2 = 98%.

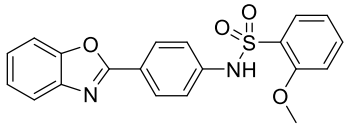

R50-*o*: *N*-(4-(benzo[*d*]oxazol-2-yl)phenyl)-2-methoxybenzenesulfonamide. ^{1}H-NMR (500 MHz, d_6-DMSO) δ 10.64 (br s, 1H), 8.01-8.05 (m, 2H), 7.88 (dd, *J* = 7.9, 1.6 Hz, 1H), 7.71-7.77 (m, 2H), 7.56-7.62 (m, 1H), 7.35-7.41 (m, 2H), 7.28-7.32 (m, 2H), 7.18 (d, *J* = 7.9 Hz, 1H), 7.06-7.11 (m, 1H), 3.87 (s, 3H); MS (ESI) $C_{20}H_{16}N_2O_4S$ $[M-H]^-$ *m/z* expected = 379.1, observed = 378.9; HPLC-1 = >99%; HPLC-2 = >99%.

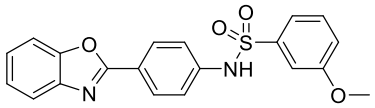

R50-*m*: *N*-(4-(benzo[*d*]oxazol-2-yl)phenyl)-3-methoxybenzenesulfonamide. ^{1}H-NMR (500 MHz, d_6-DMSO) δ 10.86 (br s, 1H), 8.06-8.11 (m, 2H), 7.73-7.78 (m, 2H), 7.50 (t, *J* = 8.2 Hz, 1H), 7.38-7.43 (m, 3H), 7.33-7.37 (m, 3H), 7.20 (ddd, *J* = 8.2, 2.5, 0.9 Hz, 1H), 3.79 (s, 3H); MS (ESI) $C_{20}H_{16}N_2O_4S$ $[M-H]^-$ *m/z* expected = 379.1, observed = 378.9; HPLC-1 = >99%; HPLC-2 = >99%.

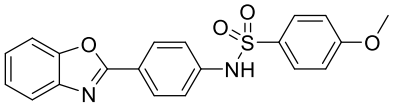

R50-*p*: *N*-(4-(benzo[*d*]oxazol-2-yl)phenyl)-4-methoxybenzenesulfonamide. ^{1}H-NMR (500 MHz, d_6-DMSO) δ 10.00 (br s, 1H), 7.89-7.93 (m, 2H), 7.40-7.46 (m, 3H), 7.33-7.40 (m, 3H), 7.21 (d, *J* = 1.6 Hz, 1H), 6.88 (dd, *J* = 8.8, 2.2 Hz, 1H), 6.78-6.82 (m, 2H), 3.53 (s, 3H); MS (ESI) $C_{20}H_{16}N_2O_4S$ $[M-H]^-$ *m/z* expected = 379.1, observed = 379.0; HPLC-1 = 95%; HPLC-2 = 95%.

General procedure for the methoxy-to-hydroxy de-protection step.

To stirring mixtures of the respective compound **50** methoxy-bearing analogs (1 eq.) in anhydrous CH_2Cl_2 (5 mL) was added BBr_3 (3 eq. of 1 M BBr_3 solution in anhydrous CH_2Cl_2). The reactions were allowed to stir at room temperature for 18 h (under argon), quenched with MeOH, then chromatographed over silica (hexanes:EtOAc gradient), and concentrated. If necessary, the products were further purified by preparatory RP-HPLC (H_2O:CH_3CN gradient), concentrated, and lyophilized. Refer below for individual compound characterization data.

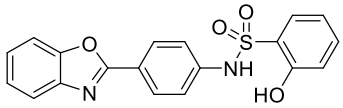

R51-*o*: *N*-(4-(benzo[*d*]oxazol-2-yl)phenyl)-2-hydroxybenzenesulfonamide. ^{1}H-NMR (300 MHz, d_6-DMSO) δ 10.81 (br s, 2H), 7.98-8.05 (m, 2H), 7.80 (dd, *J* = 8.1, 1.7 Hz, 1H), 7.69-7.76 (m, 2H), 7.34-7.46 (m, 3H), 7.26-7.33 (m, 2H), 6.89-6.97 (m, 2H); MS (ESI) $C_{19}H_{14}N_2O_4S$ $[M-H]^-$ *m/z* expected = 365.1, observed = 364.9; HPLC-1 = 97%; HPLC-2 = >99%.

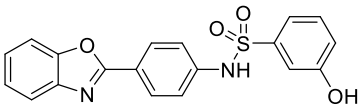

R51-*m*: *N*-(4-(benzo[*d*]oxazol-2-yl)phenyl)-3-hydroxybenzenesulfonamide. ^{1}H-NMR (300 MHz, d_6-DMSO) δ 10.77 (br s, 1H), 10.12 (s, 1H), 7.97-8.05 (m, 2H), 7.64-7.73 (m, 2H), 7.17-7.37 (m, 6H), 7.11-7.15 (m, 1H), 6.89-6.95 (m, 1H); MS (ESI) $C_{19}H_{14}N_2O_4S$ $[M-H]^-$ *m/z* expected = 365.1, observed = 365.0; HPLC-1 = >99%; HPLC-2 = >99%.

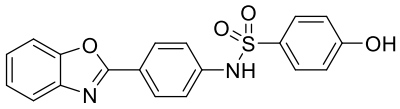

R51-*p*: *N*-(4-(benzo[*d*]oxazol-2-yl)phenyl)-4-hydroxybenzenesulfonamide. ^{1}H-NMR (300 MHz, d_6-DMSO) δ 10.43 (s, 1H), 10.15 (s, 1H), 8.12-8.19 (m, 2H), 7.54-7.69 (m, 6H), 7.44 (d, *J* = 2.0 Hz, 1H), 7.11 (dd, *J* = 8.8, 2.0 Hz, 1H), 6.79-6.87 (m, 2H); MS (ESI) $C_{19}H_{14}N_2O_4S$ $[M-H]^-$ *m/z* expected = 365.1, observed = 365.0;

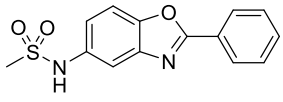

L35: *N*-(2-phenylbenzo[*d*]oxazol-5-yl)methanesulfonamide. ^{1}H-NMR (300 MHz, d_6-DMSO) δ 9.82 (br s, 1H), 8.16-8.23 (m, 2H), 7.78 (d, *J* = 8.8 Hz, 1H), 7.58-7.67 (m, 4H), 7.28 (dd, *J* = 8.7, 2.2 Hz, 1H), 2.99 (s, 3H); MS (ESI) $C_{14}H_{12}N_2O_3S$ $[M-H]^-$ *m/z* expected = 287.1, observed = 287.0; HPLC-1 = >99%; HPLC-2 = >99%.

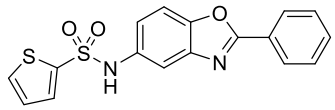

L36: *N*-(2-phenylbenzo[*d*]oxazol-5-yl)thiophene-2-sulfonamide. ^{1}H-NMR (300 MHz, d_6-DMSO) δ 10.51 (br s, 1H), 8.17 (dd, *J* = 7.7, 1.8 Hz, 2H), 7.88 (dd, *J* = 5.0, 1.3 Hz, 1H), 7.72 (d, *J* = 8.8 Hz, 1H), 7.56-7.66 (m, 3H), 7.47-7.55 (m, 2H), 7.16 (dd, *J* = 8.8, 2.1 Hz, 1H), 7.10 (dd, *J* = 4.9, 3.8 Hz, 1H); MS (ESI) $C_{17}H_{12}N_2O_3S_2$ $[M-H]^-$ *m/z* expected = 355.0, observed = 354.9; HPLC-1 = 99%; HPLC-2 = 99%.

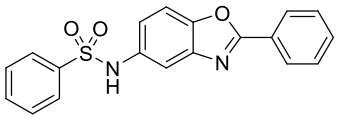

L37: *N*-(2-phenylbenzo[*d*]oxazol-5-yl)benzenesulfonamide. ^{1}H-NMR (300 MHz, d_6-DMSO) δ 10.39 (br s, 1H), 8.11-8.18 (m, 2H), 7.75 (d, *J* = 7.0 Hz, 2H), 7.49-7.70 (m 7H), 7.45 (d, *J* = 1.8 Hz, 1H), 7.12 (dd, *J* = 8.7, 2.0 Hz, 1H); MS (ESI) $C_{19}H_{14}N_2O_3S$ $[M-H]^-$ *m/z* expected = 349.1, observed = 349.0; HPLC-1 = >99%; HPLC-2 = >99%.

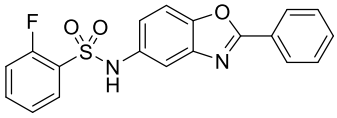

L38-*o*: 2-fluoro-*N*-(2-phenylbenzo[*d*]oxazol-5-yl)benzenesulfonamide. ^{1}H-NMR (500 MHz, d_6-DMSO) δ 10.71 (br s, 1H), 8.13-8.17 (m, 2H), 7.83 (td, *J* = 7.6, 1.7 Hz, 1H), 7.57-7.70 (m, 5H), 7.47-7.49 (m, 1H), 7.39-7.44 (m, 1H), 7.34 (td, *J* = 7.6, 1.1 Hz, 1H), 7.15-7.18 (m, 1H); MS (ESI) $C_{19}H_{13}FN_2O_3S$ $[M-H]^-$ *m/z* expected = 367.1, observed = 367.0; HPLC-1 = >99%; HPLC-2 = >99%.

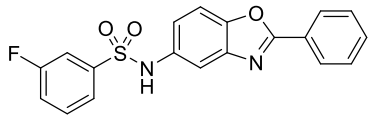

L38-*m*: 3-fluoro-*N*-(2-phenylbenzo[*d*]oxazol-5-yl)benzenesulfonamide. ^{1}H-NMR (500 MHz, d_6-DMSO) δ 10.53 (br s, 1H), 8.13-8.18 (m, 2H), 7.68 (d, *J* = 8.8 Hz, 1H), 7.56-7.66 (m, 5H), 7.55 (dt, *J* = 8.0, 1.7 Hz, 1H), 7.47-7.51 (m, 1H), 7.47 (d, *J* = 1.9 Hz, 1H), 7.12 (dd, *J* = 8.8, 2.2 Hz, 1H); MS (ESI) $C_{19}H_{13}FN_2O_3S$ $[M-H]^-$ *m/z* expected = 367.1, observed = 367.0; HPLC-1 = >99%; HPLC-2 = >99%.

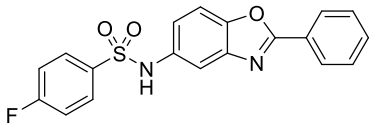

L38-*p*: 4-fluoro-*N*-(2-phenylbenzo[*d*]oxazol-5-yl)benzenesulfonamide. ^{1}H-NMR (500 MHz, d_6-DMSO) δ 10.41 (br s, 1H), 8.13-8.18 (m, 2H), 7.77-7.82 (m, 2H), 7.68 (d, *J* = 8.8 Hz, 1H), 7.58-7.66 (m, 3H), 7.46 (d, *J* = 1.9 Hz, 1H), 7.35-7.42 (m, 2H), 7.11 (dd, *J* = 8.7, 2.0 Hz, 1H); MS (ESI) $C_{19}H_{13}FN_2O_3S$ $[M-H]^-$ *m/z* expected = 367.1, observed = 366.9; HPLC-1 = 99%; HPLC-2 = 99%.

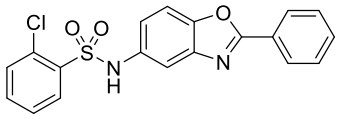

L39-*o*: 2-chloro-*N*-(2-phenylbenzo[*d*]oxazol-5-yl)benzenesulfonamide. ^{1}H-NMR (500 MHz, d_6-DMSO) δ 10.74 (br s, 1H), 8.11-8.16 (m, 2H), 8.05 (dd, *J* = 8.0, 1.4 Hz, 1H), 7.67 (d, *J* = 8.8 Hz, 1H), 7.57-7.65 (m, 5H), 7.50 (td, *J* = 7.6, 1.6 Hz, 1H), 7.46 (d, *J* = 1.9 Hz, 1H), 7.17 (dd, *J* = 8.8, 2.2 Hz, 1H); MS (ESI) $C_{19}H_{13}ClN_2O_3S$ $[M-H]^-$ *m/z* expected = 383.0, observed = 382.9; HPLC-1 = >99%; HPLC-2 = >99%.

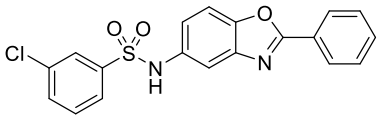

L39-*m*: 3-chloro-*N*-(2-phenylbenzo[*d*]oxazol-5-yl)benzenesulfonamide. ^{1}H-NMR (500 MHz, d_6-DMSO) δ 10.50 (br s, 1H), 8.13-8.18 (m, 2H), 7.77 (t, *J* = 1.7 Hz, 1H), 7.66-7.72 (m, 3H), 7.54-7.65 (m, 4H), 7.47 (d, *J* = 2.2 Hz, 1H), 7.12 (dd, *J* = 8.7, 2.0 Hz, 1H); MS (ESI) $C_{19}H_{13}ClN_2O_3S$ $[M-H]^-$ *m/z* expected = 383.0, observed = 382.9; HPLC-1 = >99%; HPLC-2 = >99%.

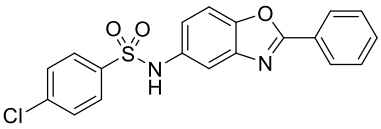

L39-*p*: 4-chloro-*N*-(2-phenylbenzo[*d*]oxazol-5-yl)benzenesulfonamide. ^{1}H-NMR (500 MHz, d_6-DMSO) δ 10.46 (br s, 1H), 8.13-8.18 (m, 2H), 7.71-7.76 (m, 2H), 7.66-7.70 (m, 1H), 7.57-7.66 (m, 5H), 7.47 (s, 1H), 7.09-7.14 (m, 1H); MS (ESI) $C_{19}H_{13}ClN_2O_3S$ $[M-H]^-$ *m/z* expected = 383.0, observed = 382.9; HPLC-1 = >99%; HPLC-2 = >99%.

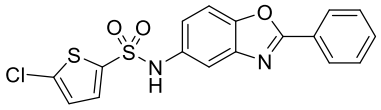

L40: 5-chloro-*N*-(2-phenylbenzo[*d*]oxazol-5-yl)thiophene-2-sulfonamide. ^{1}H-NMR (300 MHz, d_6-DMSO) δ 10.67 (br s, 1H), 8.14-8.21 (m, 2H), 7.75 (d, *J* = 8.8 Hz, 1H), 7.57-7.68 (m, 3H), 7.53 (d, *J* = 2.0 Hz, 1H), 7.41 (d, *J* = 4.0 Hz, 1H), 7.15-7.21 (m, 2H); MS (ESI) $C_{17}H_{11}ClN_2O_3S_2$ $[M-H]^-$ *m/z* expected = 389.0, observed =

1 = >99%; HPLC-2 = >99%.

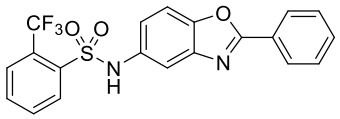

L41-*o*: *N*-(2-phenylbenzo[*d*]oxazol-5-yl)-2-(trifluoromethyl)benzenesulfonamide.

^{1}H-NMR (500 MHz, d_6-DMSO) δ 10.78 (br s, 1H), 8.13-8.17 (m, 2H), 8.12 (d, *J* = 7.9 Hz, 1H), 7.97-8.02 (m, 1H), 7.79-7.89 (m, 2H), 7.70 (d, *J* = 8.8 Hz, 1H), 7.57-7.66 (m, 3H), 7.47 (d, *J* = 2.2 Hz, 1H), 7.17 (dd, *J* = 8.8, 2.2 Hz, 1H); MS (ESI) $C_{20}H_{13}F_3N_2O_3S$ $[M-H]^-$ *m/z* expected = 417.1, observed = 416.9; HPLC-1 = >99%; HPLC-2 = >99%.

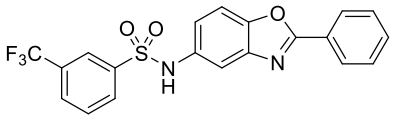

L41-*m*: *N*-(2-phenylbenzo[*d*]oxazol-5-yl)-3-(trifluoromethyl)benzenesulfonamide.

^{1}H-NMR (500 MHz, d_6-DMSO) δ 10.55 (br s, 1H), 8.13-8.18 (m, 2H), 7.97-8.04 (m, 3H), 7.76-7.81 (m, 1H), 7.69 (d, *J* = 8.8 Hz, 1H), 7.57-7.67 (m, 3H), 7.46 (d, *J* = 1.9 Hz, 1H), 7.11 (d, *J* = 8.8, 2.2 Hz, 1H); MS (ESI) $C_{20}H_{13}F_3N_2O_3S$ $[M-H]^-$ *m/z* expected = 417.1, observed = 416.9; HPLC-1 = 99%; HPLC-2 = 99%.

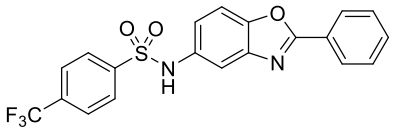

L41-*p*: *N*-(2-phenylbenzo[*d*]oxazol-5-yl)-4-(trifluoromethyl)benzenesulfonamide.

^{1}H-NMR (500 MHz, d_6-DMSO) δ 10.64 (br s, 1H), 8.13-8.17 (m, 2H), 7.95 (app s, 4H), 7.69 (d, *J* = 8.5 Hz, 1H), 7.58-7.66 (m, 3H), 7.49 (d, *J* = 1.9 Hz, 1H), 7.12 (d, *J* = 8.8, 2.2 Hz, 1H); MS (ESI) $C_{20}H_{13}F_3N_2O_3S$ $[M-H]^-$ *m/z* expected = 417.1, observed = 416.9; HPLC-1 = >99%; HPLC-2 = >99%.

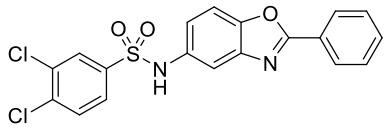

L42: 3,4-dichloro-*N*-(2-phenylbenzo[*d*]oxazol-5-yl)benzenesulfonamide. ^{1}H-NMR (500 MHz, d_6-DMSO) δ 11.02 (br s, 1H), 8.08-8.13 (m, 2H), 8.03 (d, *J* = 1.9 Hz, 1H), 7.87 (d, *J* = 8.5 Hz, 1H), 7.73-7.79 (m, 3H), 7.36-7.43 (m, 2H), 7.32-7.36 (m, 2H); MS (ESI) $C_{19}H_{12}Cl_2N_2O_3S$ $[M-H]^-$ *m/z* expected = 417.0, observed = 416.8; HPLC-1 = >99%; HPLC-2 = >99%.

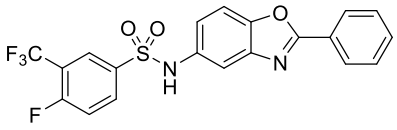

L43: 4-fluoro-*N*-(2-phenylbenzo[*d*]oxazol-5-yl)-3-(trifluoromethyl)benzenesulfonamide. ^{1}H-NMR (500 MHz, d_6-DMSO) δ 10.53 (br s, 1H), 8.15 (d, *J* = 7.3 Hz, 2H), 8.02-8.09 (m, 2H), 7.66-7.7.3 (m, 2H), 7.57-7.66 (m, 3H), 7.48 (s, 1H), 7.11 (dd, *J* = 8.7, 1.7 Hz, 1H); MS (ESI) $C_{20}H_{12}F_4N_2O_3S$ $[M-H]^-$ *m/z* expected = 435.0, observed = 434.9; HPLC-1 = >99%; HPLC-2 = >99%.

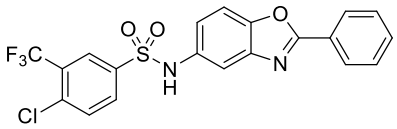

L44: 4-chloro-*N*-(2-phenylbenzo[*d*]oxazol-5-yl)-3-(trifluoromethyl)benzenesulfonamide. ^{1}H-NMR (500 MHz, d_6-DMSO) δ 10.60 (br s, 1H), 8.16 (d, *J* = 6.9 Hz, 2H), 8.10 (s, 1H), 7.88-7.97 (m, 2H), 7.71 (d, *J* = 8.8 Hz, 1H), 7.58-7.67 (m, 3H), 7.46-7.49 (m, 1H), 7.10 (dd, *J* = 8.8, 1.9 Hz, 1H); MS (ESI) $C_{20}H_{12}ClF_3N_2O_3S$ $[M-H]^-$ *m/z* expected = 451.0, observed = 450.9; HPLC-1 = >99%; HPLC-2 = >99%.

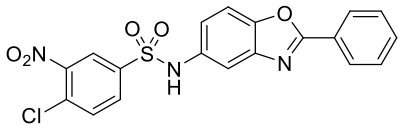

L45: 4-chloro-3-nitro-*N*-(2-phenylbenzo[*d*]oxazol-5-yl)benzenesulfonamide. ^{1}H-NMR (500 MHz, d_6-DMSO) δ 10.69 (br s, 1H), 8.42 (d, *J* = 1.3 Hz, 1H), 8.16 (d, *J* = 6.6 Hz, 2H), 7.91-7.97 (m, 2H), 7.72 (d, *J* = 8.5 Hz, 1H), 7.58-7.67 (m, 3H), 7.52 (d, *J* = 1.6 Hz, 1H), 7.13 (dd, *J* = 8.7, 2.0 Hz, 1H); MS (ESI) $C_{19}H_{12}ClN_3O_5S$ $[M-H]^-$ *m/z* expected = 428.0, observed = 427.9; HPLC-1 = 99%; HPLC-2 = 99%.

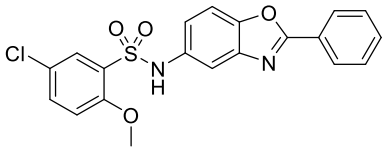

L46: 5-chloro-2-methoxy-*N*-(2-phenylbenzo[*d*]oxazol-5-yl)benzenesulfonamide. ^{1}H-NMR (300 MHz, d_6-DMSO) δ 10.29 (br s, 1H), 8.11-8.17 (m, 2H), 7.65-7.69 (m, 2H), 7.55-7.64 (m, 4H), 7.45 (d, *J* = 2.0 Hz, 1H), 7.23 (d, *J* = 8.9 Hz, 1H), 7.16 (dd, *J* = 8.8, 2.1 Hz, 1H), 3.92 (s, 3H); MS (ESI) $C_{20}H_{15}ClN_2O_4S$ $[M-H]^-$ *m/z*

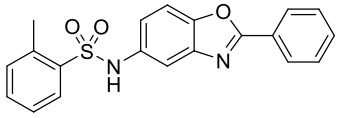

L47-*o*: 2-methyl-*N*-(2-phenylbenzo[*d*]oxazol-5-yl)benzenesulfonamide. ^{1}H-NMR (300 MHz, d_6-DMSO) δ 10.52 (br s, 1H), 8.14 (dd, *J* = 7.5, 1.8 Hz, 2H), 7.89 (d, *J* = 7.5 Hz, 1H), 7.66 (d, *J* = 8.8 Hz, 1H), 7.55-7.64 (m, 3H), 7.44-7.52 (m, 1H), 7.42 (d, *J* = 2.1 Hz, 1H), 7.30-7.39 (m, 2H), 7.12 (dd, *J* = 8.8, 2.1 Hz, 1H), 2.61 (s, 3H); MS (ESI) $C_{20}H_{16}N_2O_3S$ $[M-H]^-$ *m/z* expected = 363.1, observed = 363.0; HPLC-1 = >99%; HPLC-2 = >99%.

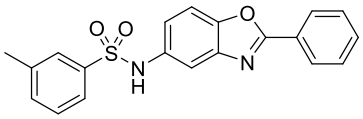

L47-*m*: 3-methyl-*N*-(2-phenylbenzo[*d*]oxazol-5-yl)benzenesulfonamide. ^{1}H-NMR (300 MHz, d_6-DMSO) δ 10.36 (br s, 1H), 8.12-8.18 (m, 2H), 7.67 (d, *J* = 8.7 Hz, 1H), 7.51-7.64 (m, 5H), 7.46 (d, *J* = 2.0 Hz, 1H), 7.38-7.43 (m, 2H), 7.12 (dd, *J* = 8.8, 2.1 Hz, 1H), 2.32 (s, 3H); MS (ESI) $C_{20}H_{16}N_2O_3S$ $[M-H]^-$ *m/z* expected = 363.1, observed = 363.0; HPLC-1 = >99%; HPLC-2 = >99%.

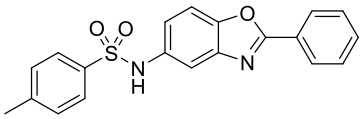

L47-*p*: 4-methyl-*N*-(2-phenylbenzo[*d*]oxazol-5-yl)benzenesulfonamide. ^{1}H-NMR (500 MHz, d_6-DMSO) δ 10.32 (br s, 1H), 8.12-8.17 (m, 2H), 7.57-7.68 (m, 6H), 7.45 (d, *J* = 1.9 Hz, 1H), 7.30-7.36 (m, 2H), 7.12 (dd, *J* = 8.7, 2.0 Hz, 1H), 2.31 (s, 3H); MS (ESI) $C_{20}H_{16}N_2O_3S$ $[M-H]^-$ *m/z* expected = 363.1, observed = 362.9; HPLC-

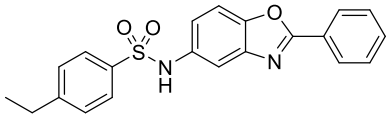

L48: 4-ethyl-*N*-(2-phenylbenzo[*d*]oxazol-5-yl)benzenesulfonamide. ^{1}H-NMR (500 MHz, d_6-DMSO) δ 10.35 (br s, 1H), 8.15 (dd, *J* = 7.9, 1.6 Hz, 2H), 7.64-7.70 (m, 3H), 7.57-7.64 (m, 3H), 7.46 (d, *J* = 2.2 Hz, 1H), 7.37 (d, *J* = 8.2 Hz, 2H), 7.13 (dd, *J* = 8.7, 2.0 Hz, 1H), 2.62 (q, *J* = 7.6 Hz, 2H), 1.13 (t, *J* = 7.6 Hz, 3H); MS (ESI) $C_{21}H_{18}N_2O_3S$ $[M-H]^-$ *m/z* expected = 377.1, observed = 377.0; HPLC-1 = 99%; HPLC-2 = 99%.

388.9; HPLC-1 = 98%; HPLC-2 = 99%.

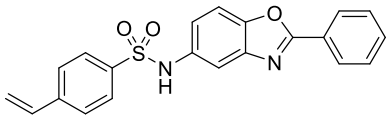

L49: *N*-(2-phenylbenzo[*d*]oxazol-5-yl)-4-vinylbenzenesulfonamide. ^{1}H-NMR (500 MHz, d_6-DMSO) δ 10.38 (br s, 1H), 8.15 (dd, *J* = 8.0, 1.4 Hz, 2H), 7.71 (d, *J* = 8.5 Hz, 2H), 7.67 (d, *J* = 8.8 Hz, 1H), 7.57-7.65 (m, 5H), 7.46 (d, *J* = 1.9 Hz, 1H), 7.12 (dd, *J* = 8.8, 2.2 Hz, 1H), 6.75 (dd, *J* = 17.7, 11.0 Hz, 1H), 5.95 (d, *J* = 17.7 Hz, 1H), 5.41 (d, *J* = 11.0 Hz, 1H); MS (ESI) $C_{21}H_{16}N_2O_3S$ $[M-H]^-$ *m/z* expected = 375.1, observed = 374.9; HPLC-1 = 97%; HPLC-2 = 96%.

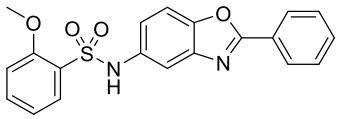

L50-*o*: 2-methoxy-*N*-(2-phenylbenzo[*d*]oxazol-5-yl)benzenesulfonamide. ^{1}H-NMR (500 MHz, d_6-DMSO) δ 10.10 (br s, 1H), 8.11-8.15 (m, 2H), 7.76 (d, *J* = 7.9, 1.6 Hz, 1H), 7.56-7.65 (m, 4H), 7.51-7.56 (m, 1H), 7.45 (d, *J* = 1.9 Hz, 1H), 7.16 (dd, *J* = 8.8, 1.9 Hz, 2H), 6.98-7.03 (m, 1H), 3.92 (s, 3H); MS (ESI) $C_{20}H_{16}N_2O_4S$ $[M-H]^-$ *m/z* expected = 379.1, observed = 378.9; HPLC-1 = >99%; HPLC-2 = 99%.

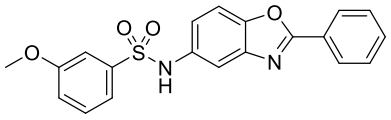

L50-*m*: 3-methoxy-*N*-(2-phenylbenzo[*d*]oxazol-5-yl)benzenesulfonamide. ^{1}H-NMR (500 MHz, d_6-DMSO) δ 10.37 (br s, 1H), 8.13-8.17 (m, 2H), 7.68 (d, *J* = 8.8 Hz, 1H), 7.57-7.66 (m, 3H), 7.4.7 (d, *J* = 1.9 Hz, 1H), 7.44 (t, *J* = 8.0 Hz, 1H), 7.29-7.32 (m, 1H), 7.25-7.28 (m, 1H), 7.12-7.18 (m, 2H), 3.75 (s, 3H); MS (ESI) $C_{20}H_{16}N_2O_4S$ $[M-H]^-$ *m/z* expected = 379.1, observed = 379.0; HPLC-1 = >99%; HPLC-2 = >99%.

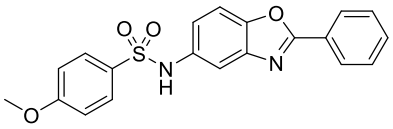

L50-*p*: 4-methoxy-*N*-(2-phenylbenzo[*d*]oxazol-5-yl)benzenesulfonamide. ^{1}H-NMR (300 MHz, d_6-DMSO) δ 10.25 (br s, 1H), 8.15 (dd, *J* = 7.7, 1.8 Hz, 2H), 7.64-7.71 (m, 3H), 7.56-7.63 (m, 3H), 7.45 (d, *J* = 2.0 Hz, 1H), 7.12 (dd, *J* = 8.8, 2.1 Hz, 1H), 7.04 (d, *J* = 8.9 Hz, 2H), 3.76 (s, 3H); MS (ESI) $C_{20}H_{16}N_2O_4S$ $[M-H]^-$ *m/z* expected = 379.1, observed = 378.9; HPLC-1 = >99%; HPLC-2 = >99%.

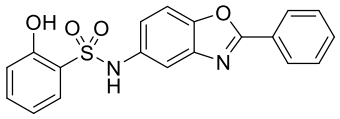

L51-*o*: 2-hydroxy-*N*-(2-phenylbenzo[*d*]oxazol-5-yl)benzenesulfonamide. ^{1}H-NMR (300 MHz, d_6-DMSO) δ 10.52 (br s, 2H), 8.10-8.18 (m, 2H), 7.55-7.72 (m, 5H), 7.48 (d, *J* = 2.0 Hz, 1H), 7.33-7.42 (m, 1H), 7.20 (dd, *J* = 8.8, 2.1 Hz, 1H), 6.93 (d, *J* = 8.1 Hz, 1H), 6.86 (t, *J* = 7.6 Hz, 1H); MS (ESI) $C_{19}H_{14}N_2O_4S$ $[M-H]^-$ *m/z* expected = 365.1, observed = 365.0; HPLC-1 = 96%; HPLC-2 = 98%.

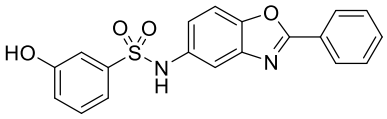

L51-*m*: 3-hydroxy-*N*-(2-phenylbenzo[*d*]oxazol-5-yl)benzenesulfonamide. ^{1}H-NMR (300 MHz, d_6-DMSO) δ 10.33 (br s, 1H), 10.10 (br s, 1H), 8.16 (dd, *J* = 7.7, 1.9 Hz, 2H), 7.68 (d, *J* = 8.8 Hz, 1H), 7.56-7.66 (m, 3H), 7.46 (d, *J* = 2.0 Hz, 1H), 7.32 (t, *J* = 8.0 Hz, 1H), 7.18 (d, *J* = 8.1 Hz, 1H), 7.09-7.15 (m, 2H), 6.94 (dd, *J* = 7.8, 2.0 Hz, 1H); MS (ESI) $C_{19}H_{14}N_2O_4S$ $[M-H]^-$ *m/z* expected = 365.1, observed = 365.0; HPLC-1 = >99%; HPLC-2 = 98%.

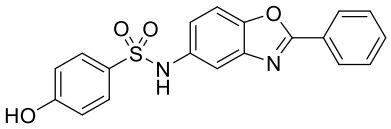

L51-*p*: 4-hydroxy-*N*-(2-phenylbenzo[*d*]oxazol-5-yl)benzenesulfonamide. ^{1}H-NMR (300 MHz, d_6-DMSO) δ 10.67 (br s, 1H), 10.52 (br s, 1H), 8.06 (d, *J* = 8.8 Hz, 2H), 7.71-7.79 (m, 2H), 7.64-7.71 (m, 2H), 7.34-7.44 (m, 2H), 7.30 (d, *J* = 8.8 Hz, 2H), 6.84-6.91 (m, 2H); MS (ESI) $C_{19}H_{14}N_2O_4S$ $[M-H]^-$ *m/z* expected = 365.1, observed = 365.0; HPLC-1 = 98%; HPLC-2 = 97%.

General materials and methods for biochemical & cell-based experiments.

DH5α and BL21 (DE3) *E. coli* cells were purchased from New England Biolabs, and Rosetta™ 2 (DE3) E. coli cells from EMD Millipore. The *Mycobacterium smegmatis* proliferation assay used the (Trevisan) Lehmann and Neumann strain, which was obtained from the ATCC (#700084). The *Mycobacterium tuberculosis* proliferation assay used an H37Rv strain that researchers at the Infectious Disease Research Institute (Seattle, WA, USA) previously engineered to express a codon-optimized mCherry fluorescent protein (TOPred).[REF] The human cell viability assays used HEK 293 kidney cells (CRL-1573) and THLE-3 liver cells (CRL-11233) obtained from the ATCC. Antibiotics were used in following concentrations when appropriate; Kanamycin (34 μg/mL), Ampicillin (50 μg/mL), Chloramphenicol (30 μg/mL) and Streptomycin (100 μg/mL).

NOTE: While the following experimental protocols have been reported in previous studies, by us and others, we have reported detailed descriptions of each here to maintain rigor, reproducibility, and transparency throughout our studies.

***E. coli* GroEL and GroES protein expression and purification**

E. coli GroEL was expressed from a trc-promoted and Amp(+) resistance marker plasmid in DH5α. *E. coli* cells. GroES was expressed from a T7-promoted and Amp(+)

resistance plasmid in *E. coli* BL21 (DE3) cells. Transformed colonies were plated onto Ampicillin-treated LB agar and incubated for 24 h at 37°C. Cells were then grown at 37°C in Ampicillin-treated LB medium until an OD_{600} of 0.5 was reached, then were induced with 0.8 mM IPTG and continued to grow for 2-3 h at 37°C. The cultures were centrifuged at 8,000 rpm and the cell pellets were collected and re-suspended in Buffer A (50 mM Tris-HCl, pH 7.4, and 20 mM NaCl) supplemented with EDTA-free complete protease inhibitor cocktail (Roche). The combined suspension was lysed by sonication, the lysate was centrifuged at 14,000 rpm, and the clarified lysate was passed through a 0.45 µM filter (Millipore).

Anion exchange purification:

The filtered lysate was loaded onto a GE HiScale Anion exchange column (Q Sepharose fast flow anion exchange resin) that was equilibrated with 2 column volumes of Buffer A. The loaded column was washed with 4 column volumes of Buffer A containing 30% of Buffer B (50 mM Tris-HCl, pH 7.4, and 1 M NaCl), then bound protein was eluted with a 30-60% gradient elution of Buffer B. Protein-containing fractions, as identified by SDS-PAGE, were collected, spin concentrated using a 10 kDa Amicon Ultra-15 centrifugal filter (EMD Millipore), and dialyzed overnight with 10 kDa SnakeSkin™ dialysis tubing (Thermo Scientific) at 4°C in 2 L of 50 mM Tris-HCl, pH 7.4, and 150 mM NaCl solution.

Size exclusion chromatography:

The dialyzed protein was loaded onto a Superdex 200 column (HiLoad 26/600, GE) column that was equilibrated with 2 column volumes of 50 mM Tris-HCl, pH 7.4 and 150 mM NaCl solution. The loaded column was eluted with 1 column volume of 100% 50 mM Tris-HCl, pH 7.4 and 150 mM NaCl solution and the column was washed with 2 column volumes of the same solution. Protein-containing fractions, as identified by SDS-PAGE, were collected, spin concentrated using a 10 kDa Amicon Ultra-15 centrifugal

filter (EMD Millipore), and dialyzed overnight with 10 kDa SnakeSkin™ dialysis tubing (Thermo Scientific) at 4°C in 2 L of 50 mM Tris-HCl, pH 7.4, and 150 mM NaCl solution. The final protein concentration was determined by Coomassie Protein Assay Kit (Thermo Scientific). Batches of protein for testing were stored at 4°C for up to one month then discarded.

Human HSP60 and HSP10 protein expression and purification

Human HSP60 purification:

For generating human mitochondrial HSP60 (mtHSP60), a previously reported pET21-*HSP60* plasmid with an *N*-terminal octa-Histidine tag was transformed into Rosetta™ 2 (DE3) pLysS *E. coli* cells for over-expression (Abdeen 2016). Cells were grown at 37°C in LB / ampicillin / chloramphenicol medium until an OD_{600} of 0.5 was reached, then cultures were induced with 0.5 mM IPTG and continued to grow for 2-3 h at 25°C. Cells were centrifuged at 14,000 rpm, and the cell pellet was suspended in 50 mL of lysis buffer composed of 100 mM Tris-HCl, pH 7.7, 10 mM $MgSO_4$, 1 mM β-ME, 5% glycerol, 0.1% triton X-100, 1500 Units DNAase, 50 mg/ml lysozyme, and one tablet of EDTA-free complete protease inhibitor cocktail (Roche). Cells were homogenized and passed through a microfluidizer, washing with buffer containing 10 mM Tris-HCl, pH 7.7, 5% glycerol, and 0.1% triton X-100.

1st nickel column purification and His-tag cleavage:

The cell lysate was centrifuged at 14,000 rpm, then the clarified lysate was supplemented with 10 mM imidazole, passed through a 0.2 µM filter (Millipore), and loaded onto a nickel-agarose resin column that was equilibrated with 2 column volumes of 20 mM Tris-HCl pH, 7.7, 5% glycerol, 200 mM NaCl, and 10 mM imidazole. The loaded column was washed with 6 column volumes of 50 mM imidazole, then bound HSP60 was eluted with 500 mM imidazole. Fractions that were enriched with the His-tagged mtHSP60 were collected, concentrated, dialyzed at room temperature for 2 h in 4

L of 20 mM Tris-HCl, pH 7.7, 200 mM NaCl, and 5% glycerol. Proteolytic cleavage of the His-tag was next performed by addition of His-tagged TEV protease at a 1:10 (w:w) ratio, while dialyzing over night at 4°C against 4 L of 20 mM Tris-HCl, pH 7.7, 200 mM NaCl, and 5% glycerol buffer.

2nd nickel column purification:

The protein sample was loaded onto a second nickel-agarose resin column that was equilibrated with 20 mM Tris-HCl, pH 7.7, 5% glycerol, 10 mM NaCl, and 10 mM imidazole. With this column, undigested His-tagged mtHSP60 can be separated from digested His-tag removed mtHSP60. The unbound fractions enriched with His-tag cleaved mtHSP60 were collected, and anion exchange chromatography was performed on the same day.

Anion exchange purification of His-tag removed mtHSP60:

The protein sample was next loaded onto an anion-exchange column that was equilibrated with 20 mM Tris-HCl, pH 7.7, and 5% glycerol. Bound proteins were eluted from the column with a linear gradient of 100-400 mM NaCl. Fractions enriched with mtHSP60 were collected, concentrated, and dialyzed in storage buffer (20 mM Tris-HCl, pH 7.7, 300 mM NaCl, 5% glycerol, and 10 mM $MgCl_2$) using 10 kDa SnakeSkin™ dialysis tubing (Thermo Scientific). The concentration of protein was determined by Coomassie Protein Assay Kit (Thermo Scientific). Batches of HSP60 protein for testing were stored at 4°C for up to two weeks, then discarded.

Human HSP10 purification:

Human HSP10 (mtHSP10) was expressed from a *T7*-promoted (pET3a-*HSP10*) plasmid in Rosetta™ 2 (DE3) cells. Cells were grown at 37°C in LB / kanamycin / chloramphenicol medium until an OD_{600} of 0.5 was reached, then were induced with 0.5 mM IPTG and continued to grow for 2-3 h at 37°C. Cells were centrifuged at 8,000 rpm, and the cell pellet was suspended in 50 mL of lysis buffer composed of 50 mM NaOAc,

pH 7.4, 20 mM NaCl, and one tablet of EDTA-free complete protease inhibitor cocktail (Roche). Once re-suspended, the sample was lysed by sonication.

Cation exchange purification:

The cell lysate was centrifuged at 14,000 rpm and the cell pellet was re-suspended in Buffer A (50 mM NaOAc, pH 4.5, and 20 mM NaCl), supplemented with EDTA-free complete protease inhibitor cocktail (Roche) and lysed by sonication. Clarified cell lysate was loaded on a cation exchange column (SP Sepharose fast flow resin, GE) and eluted with a linear NaCl gradient using Buffer B (50 mM NaOAc, pH 4.5, and 1 M NaCl). Fractions containing HSP10 were collected, spin concentrated using a 10 kDa filter canonicals, and dialyzed overnight with 10 kDa SnakeSkin™ dialysis tubing (Thermo Scientific) in a storage buffer composed of 50 mM Tris-HCl, pH 7.4 and 150 mM NaCl.

Size exclusion chromatography:

The dialyzed protein was loaded onto a GE HiScale Size Exclusion column that was equilibrated with 2 column volumes of 50 mM Tris-HCl, pH 7.4 and 150 mM NaCl solution. The loaded column was eluted with 1 column volume of 100% 50 mM Tris-HCl, pH 7.4 and 150 mM NaCl solution and the column was washed with 2 column volumes of the same elution buffer. Fractions were analyzed under a gel stain and fractions that contained protein were collected, were collected, spin concentrated using a 10 kDa filter canonicals, and dialyzed overnight with 10 kDa SnakeSkin™ dialysis tubing (Thermo Scientific) at 4°C in 2L of 50 mM Tris-HCl, pH 7.4, 300 mM NaCl, and 1 mM DTT solution. The concentration of protein was determined by Coomassie Protein Assay Kit (Thermo Scientific). Batches of HSP10 protein for testing were stored at 4°C for up to three weeks, then discarded.

Evaluating compounds for inhibition in the GroEL/ES and HSP60/10 mediated dMDH refolding assays.

Reagent preparation:

For these assays, four primary reagent stocks were prepared: 1) GroEL/ES-dMDH or HSP60/10-dMDH binary complex stock; 2) ATP initiation stock; 3) EDTA quench stock; 4) MDH enzymatic assay stock. Denatured MDH (dMDH) was prepared by 2-fold dilution of MDH (5 mg/ml, soluble pig heart MDH from Roche, product #10127248001) with denaturant buffer (7 M guanidine-HCl, 200 mM Tris, pH 7.4, and 50 mM DTT). MDH was completely denatured by incubating at room temperature for 45 min. The binary complex solutions were prepared by slowly adding the dMDH stock to a stirring stock with GroEL (or HSP60) in folding buffer (50 mM Tris-HCl, pH 7.4, 50 mM KCl, 10 mM $MgCl_2$, and 1 mM DTT), followed by addition of GroES (or HSP10). The binary complex stocks were prepared immediately prior to dispensing in to the assay plates and had final protein concentrations of 83.3 nM GroEL (*Mr* 800 kDa) or HSP60 (*Mr* 400 kDa), 100 nM GroES or HSP10 (*Mr* 70 kDa), and 20 nM dMDH in folding buffer. For the ATP initiation stock, ATP solid was diluted into folding buffer to a final concentration of 2.5 mM. Quench solution contained 600 mM EDTA (pH 8.0). The MDH enzymatic assay stock consisted of 20 mM sodium mesoxalate and 2.4 mM NADH in reaction buffer (50 mM Tris-HCl, pH 7.4, 50 mM KCl, and 1 mM DTT).

Assay protocol:

First, 30 µL aliquots of the GroEL/ES-dMDH or HSP60/10-dMDH binary complex stocks were dispensed into clear, 384-well polystyrene plates. Next, 0.5 µL of the compound stocks (10 mM to 4.6 µM, 3-fold dilutions series in DMSO) were added by pin-transfer (V&P Scientific). The chaperonin-mediated refolding cycles were initiated by addition of 20 µL of ATP stock (reagent concentrations during refolding cycle: 50 nM GroEL or HSP60, 60 nM GroES or HSP10, 12 nM dMDH, 1 mM ATP, and compounds of

100 μM to 46 nM, 3-fold dilution series), and the refolding reactions incubated at 37°C. The incubation times were determined from refolding time-course control experiments until they reached ~90% completion of refolding of the denatured MDH – generally ~20-40 min for GroEL/ES, and ~40-60 min for HSP60/10. Next, the assays were quenched by addition of 10 μL of the EDTA stock, to final concentration of 100 mM. Enzymatic activity of the refolded MDH was initiated by addition of 20 μL MDH enzymatic assay stock (20 mM sodium mesoxalate and 2.4 mM NADH in reaction buffer, 50 mM Tris pH 7.4, 50 mM KCl, 1 mM DTT), and followed by measuring the NADH absorbance in each well at 340 nm using a Molecular Devices, SpectraMax Plus384 microplate reader (NADH absorbs at 340 nm, while NAD^+ does not). $A_{340\ nm}$ measurements were recorded at 0.5 minutes (start point) and at successive time points until the amount of NADH consumed reached ~90% (end point, generally between 20-35 minutes). The differences between the start and end point A_{340} values were used to calculate the % inhibition of the GroEL/ES or HSP60/10 machinery by the compounds. IC_{50} values for the test compounds were obtained by plotting the % inhibition results in GraphPad Prism 6 and analyzing by non-linear regression using the log (inhibitor) vs. response (variable slope) equation. Results presented represent the averages of IC_{50} values obtained from at least four replicates.

Counter-screening compounds for inhibition of native MDH enzymatic activity.

Reagent preparations and assay protocol:

This assay was performed as described above for the GroEL/ES-dMDH refolding assay; however, the assay protocol differed in the sequence of compound addition to the assay plates. The refolding reactions were allowed to proceed for 45 min at 37°C in the absence of test compounds (complete refolding of MDH occurs), then quenched with the EDTA stock. Compounds were then pin-transferred into the plates after the EDTA quenching step; thus, compounds effects are only possible by inhibiting the fully refolded

MDH reporter substrate. Next enzymatic activity of the refolded MDH was initiated by addition of 20 µL MDH enzymatic assay stock (20 mM sodium mesoxalate and 2.4 mM NADH in reaction buffer, 50 mM Tris pH 7.4, 50 mM KCl, 1 mM DTT), and followed by measuring the NADH absorbance in each well at 340 nm using a Molecular Devices SpectraMax Plus384 microplate reader (NADH absorbs at 340 nm, while NAD^+ does not). A340 nm measurements were recorded at 0.5 minutes (start point) and at successive time points until the amount of NADH consumed reached ~90% (end point, generally between 20-35 minutes). Compounds were tested in 8-point, 3-fold dilution series (62.5 µM to 29 nM during the reporter reaction) in clear, flat-bottom 384-well microtiter plates. DMSO was used as negative control, and previously discovered native MDH inhibitors were used as positive controls. IC_{50} values for the test compounds were obtained by plotting the % inhibition results in GraphPad Prism 6 and analyzing by non-linear regression using the log (inhibitor) vs. response (variable slope) equation. Results presented represent the averages of IC50 values obtained from at least four replicates.

Evaluating compounds for inhibition in the GroEL/ES-dRho refolding assay.

Reagent preparation:

For this assay, five primary reagent stocks were prepared: 1) GroEL/ES-dRho binary complex stock; 2) ATP initiation stock; 3) Enzyme solution; 4) Formaldehyde quench solution; 5) $Fe(NO_3)_3$ assay stock. Denatured Rho (dRho) was prepared by 3-fold dilution of Rho (Roche product #R1756, stock diluted to 10 mg/ml with H_2O) with denaturant buffer (12 M Urea, 50 mM Tris, pH 7.4, and 10 mM DTT). Rho was completely denatured by incubating at room temperature for 45 min. The binary complex solution was prepared by slowly adding the dRho stock to a stirring solution of concentrated GroEL in modified folding buffer (50 mM Tris-HCl, pH 7.4, 50 mM KCl, 10 mM $MgCl_2$, 5 mM $Na_2S_2O_3$ and 1 mM DTT). The solution was centrifuged at 16,000 x g for 5 minutes, and the supernatant was collected and added to a solution of GroES in

modified folding buffer to give final protein concentrations of 100 nM GroEL, 120 nM GroES, and 80 nM dRho in modified folding buffer. The binary complex stock was prepared immediately prior to use. For the ATP initiation stock, ATP solid was diluted into modified folding buffer to a final concentration of 2.0 mM. The thiocyanate enzymatic assay stock was prepared to contain 70 mM KH_2PO_4, 80 mM KCN, and 80 mM $Na_2S_2O_3$ in water. The formaldehyde quench solution contained 30% formaldehyde in water. The ferric nitrate reporter stock contained 8.5% w/v $Fe(NO_3)_3$ and 11.3% v/v HNO_3 in water.

Assay protocol:

First, 10 mL aliquots of the GroEL/ES-dRho complex stock was dispensed into clear, 384-well polystyrene plates. Next, 0.5 mL of the compound stocks (10 mM to 4.6 mM, 3-fold dilutions in DMSO) were added by pin-transfer. The chaperonin-mediated refolding cycle was initiated by addition of 10 mL of ATP stock (reagent concentrations during refolding cycle: 50 nM GroEL, 60 nM GroES, 40 nM dRho, 1 mM ATP, and compounds of 250 mM to 114 nM, 3-fold dilution series). After incubating for 45 minutes at 37°C for the refolding cycle, 30 mL of the thiocyanate enzymatic assay stock was added and incubated for 60 min at room temperature for the refolded rhodanese enzymatic reporter reaction. The rhodanese-catalyzed thiosulfate-cyanide reaction was quenched by adding 10 mL of the formaldehyde quench solution, and then 40 mL of the ferric nitrate reporter stock was added to quantify the amount of thiocyanate produced during the enzymatic reporter reaction, which is proportional to the amount of dRho refolded by GroEL/ES. After incubating at room temperature for 15 min, the absorbance by $Fe(SCN)_3$ was measured at 460 nm using a Molecular Devices, SpectraMax Plus384 microplate reader. A second set of baseline control plates were prepared analogously, but without binary solution, to correct for possible interference from compound absorbance or turbidity. IC_{50} values for the test compounds were obtained by plotting the A_{460} results in GraphPad Prism 6 and analyzing by non-linear regression using the

log(inhibitor) vs. response (variable slope) equation. Results presented represent the averages of IC_{50} values obtained from at least four replicates.

Counter-screening compounds for inhibition of native Rho enzymatic activity.

Reagent preparations and assay protocol:

Reagents were identical to those used in the GroEL/ES-dRho refolding assay described above; however, the assay protocol differed in the sequence of compound addition to the wells. Compounds were pin-transferred after the 60-minute incubation for the refolding cycle, but prior to the addition of the thiocyanate enzymatic assay stock. Thus, the refolding reactions were allowed to proceed for 60 min at 37°C in the absence of test compounds, but the enzymatic activity of the refolded rhodanese reporter enzyme was monitored in the presence of test compounds (inhibitor concentration range during the enzymatic reporter reaction is 100 mM to 46 nM – 3-fold dilutions). IC_{50} values for the rhodanese reporter enzyme were determined as described above. Results presented represent the averages of IC_{50} values obtained from at least three replicates.

Evaluating compounds for inhibition of *M. smegmatis* proliferation.

Mycobacterium smegmatis – (Trevisan) Lehmann and Neumann strain (ATCC 700084). *M. smegmatis* was grown in Middlebrook complete media (Becton, Dickinson and Company). The liquid culture was grown in Middlebrook complete media supplemented with 0.05% Tween 80. Stock bacterial cultures were streaked onto agar plates and grown for 72 h at 37°C. Fresh aliquots of broth were inoculated with single bacterial colonies and the cultures were grown overnight at 37°C with shaking (240 rpm) in media. The following morning, the overnight cultures were sub-cultured (1:5 dilution) into fresh aliquots of media and grown at 37°C for 1-2 h with shaking. After 2 h, cultures were diluted into fresh media to achieve final OD_{600} readings of 0.05. Aliquots of these diluted cultures (20 µL) were added to clear, flat-bottom, 384-well polystyrene plates that were stamped with 1 µL of test compounds in 20 µL media. Compounds were tested in

dose-response format where the inhibitor concentration range during the proliferation assay was 100 μM to 46 nM (3-fold dilution series). Plates were sealed with "Breathe Easy" oxygen permeable membranes (Diversified Biotech) and left to incubate at 37°C without shaking (stagnant assay). A second set of baseline control plates were prepared analogously, but without any bacteria added, to correct for possible compound absorbance and/or precipitation. After 24 h, plates were then read at 600 nm using a Molecular Devices SpectraMax Plus384 microplate reader. EC_{50} values for the test compounds were obtained by plotting the OD_{600} results in GraphPad Prism 6 and analyzing by non-linear regression using the log(inhibitor) vs. response (variable slope) equation. Results presented represent the averages of EC_{50} values obtained from at least triplicate experiments.

Evaluating compounds for inhibition of *M. tuberculosis* proliferation.

Evaluation of compound inhibition of *M. tuberculosis* proliferation in liquid culture was performed as per previously reported procedures (Ollinger 2013). *M. tuberculosis* (strain H37Rv) was grown in Middlebrook 7H9 medium supplemented with 0.05% Tween 80, 10% v/v oleic acid, and albumin dextrose catalase (OADC) supplement (Becton Dickinson) (7H9-Tw-OADC). Stock bacterial cultures were inoculated in a startup culture and grown to a logarithmic phase of OD_{590} ~0.7. This was sub-cultured in fresh media (1:10 dilution) and grown to an OD_{590} 1.0, then diluted again into fresh media to achieve a final OD_{590} reading of 0.04 (just prior to dispensing into plates). Compound plates were prepared by adding 4 μL of compound stocks to 96 μL of fresh medium in 96-well plates. Aliquots of the diluted *Mtb* cultures (100 μL) were then added to the compound plates, which were incubated in sealed bags at 37ºC for 5 days. All compounds were first evaluated in singlicate at a single concentration of 200 μM, with compounds showing >50% inhibition re-evaluated in dose-response format (inhibitor concentration range of 200 μM to 390 nM – 2-fold dilutions) to determine EC_{50} values. After 5 days, OD_{590}

values were read and % growth inhibition for each well were calculated. EC_{50} values for compounds tested in dose-response format were obtained by plotting the % inhibition results in GraphPad Prism 6 and analyzing by non-linear regression using the log (inhibitor) vs. response (variable slope) equation. Results presented represent the averages of EC_{50} values obtained from duplicate experiments.

Evaluating compounds for effects on liver and kidney cell viability.

Evaluation of compound cytotoxicity's to THLE-3 liver and HEK 293 kidney cells was performed using Alamar Blue-based viability assays. THLE-3 cells were maintained in Clonetics BEBM medium (Lonza, CC-3171) supplemented with the BEGM bullet kit (Lonza, CC-3170) and 10% FBS. HEK 293 cells were maintained in MEM medium (Corning Cellgro, 10-009 CV) supplemented with 10% FBS (Sigma, F2242). All assays were carried out in 384-well plates (BRAND cell culture grade plates, 781980). Cells at 80% confluence were harvested and diluted in growth medium, then 45 µL of the THLE-3 cells (1,500 cells/well) or HEK 293 cells (1,500 cells/well) were dispensed per well, and plates were sealed with "Breathe Easy" oxygen permeable membranes (Diversified Biotech) and incubated at 37°C, 5% CO_2, for 24 h. The following day, 1 µL of the compound stocks (10 mM to 4.6 µM, 3-fold dilutions in DMSO) were pre-diluted by pin-transfer into 25 µL of the relevant growth mediums. Then, 15 µL aliquots of the diluted compounds were added to the cell assay plates to give inhibitor concentration ranges of 100 µM to 46 nM during the assay (final DMSO concentration of 0.1% was maintained during the assay). Plates were sealed with "Breathe Easy" oxygen permeable membranes and incubated for an additional 48 h at 37°C and 5% CO_2. The Alamar Blue reporter reagents were then added to a final concentration of 10%, the plates incubated at 37°C and 5% CO_2, and sample fluorescence (535 nm excitation, 590 nm emission) was read using a Molecular Devices FlexStation II 384-well plate reader (readings taken between 4-24 h of incubation so as to achieve signals in the 30-60% range for

conversion of resazurin to resorufin). Cell viability was calculated as per vendor instructions (Thermo Fisher - Alamar Blue cell viability assay manual). Cytotoxicity CC_{50} values for the test compounds were obtained by plotting the % resazurin reduction results in GraphPad Prism 6 and analyzing by non-linear regression using the log(inhibitor) vs. response (variable slope) equation. Results presented represent the averages of CC_{50} values obtained from at least three replicates for THLE-3 liver cells and four replicates for HEK 293 kidney cells.

Mtb PtpB & human PTPN1 (PTP1B), PTPN2 (TCPTP), and PTPN5 (STEP) protein expression and purification

Mtb PtpB:

His-tagged *Mycobacterium tuberculosis* PtpB was expressed from a *T7*-promoted (pET21b-PtpB) and ampicillin resistance plasmid in Rosetta™ 2 (DE3) *E. coli* cells. Transformed cells were grown at 37°C in LB / ampicillin / chloramphenicol medium until an OD_{600} of ~0.3 was reached, then were induced with 20 µM IPTG and incubated overnight at 20°C. The culture was centrifuged at 8,000 rpm, and the cell pellet was re-suspended in Buffer A (20 mM Tris-Cl, pH 7.4, 200 mM NaCl, 10 mM Imidazole, and 5% glycerol) supplemented with EDTA-free complete protease inhibitor cocktail (Roche). The cells were lysed by sonication, centrifuged, and the clarified cell lysate was loaded on a nickel-agarose resin column. The His-tagged PtpB protein was eluted using a linear gradient of 100% Buffer A to 100% Buffer B (20 mM Tris-Cl, pH 7.4, 200 mM NaCl, 500 mM Imidazole, 5% glycerol). Fractions containing the PtpB phosphatase were spin concentrated, then dialyzed (20 mM Tris-HCl, pH 7.4, 150 mM NaCl, 1 mM EDTA, 1 mM DTT, and 5% glycerol) using 10 kDa SnakeSkin™ dialysis tubing (Thermo Scientific). The concentration of protein was determined by Coomassie Protein Assay Kit (Thermo Scientific). Batches of protein were stored at 4°C in 20 mM Tris-Cl, pH 7.4, 150 mM NaCl, 1 mM EDTA, 1 mM DTT, and 20% glycerol for up to three weeks, then discarded.

Human PTPN1 (PTP1B), PTPN2 (TCPTP), and PTPN5 (STEP):

Each of the human phosphatases was expressed from *T7*-promoted (pSPEED-ET) and kanamycin resistant plasmids in Rosetta™ 2 (DE3) *E. coli* cells. Transformed bacteria were grown at 37ºC in LB / kanamycin medium until an OD_{600} of ~0.3 was reached, then were induced with 20 μM IPTG and incubated overnight at 20°C. The cultures were centrifuged at 8,000 rpm, and the cell pellets were re-suspended in Buffer A (20 mM Tris-Cl, pH 7.4, 200 mM NaCl, 10 mM Imidazole, and 5% glycerol) supplemented with EDTA-free complete protease inhibitor cocktail (Roche). The cells were lysed by sonication, centrifuged, and the clarified cell lysates were loaded on a nickel-agarose resin column. The His-tagged proteins were eluted using linear gradients of 100% Buffer A to 100% Buffer B (20 mM Tris-Cl, pH 7.4, 200 mM NaCl, 500 mM Imidazole, 5% glycerol). Fractions containing the phosphatases were spin concentrated, then dialyzed with storage buffer (20 mM Tris-HCl, pH 7.4, 150 mM NaCl, 1 mM EDTA, 1 mM DTT, and 5% glycerol) using 10 kDa SnakeSkin™ dialysis tubing (Thermo Scientific). The concentration of each phosphatase was determined by Coomassie Protein Assay Kit (Thermo Scientific). Batches of the proteins were stored at 4°C in 20 mM Tris-Cl, pH 7.4, 150 mM NaCl, 1 mM EDTA, 1 mM DTT, 5% glycerol for up to three weeks, then discarded.

Evaluating compounds for inhibition of the *Mtb* PtpB and human phosphatases.

Reagent preparation:

For these assays, three primary reagent stocks were prepared: 1) phosphatase enzyme solutions, containing *M. tuberculosis* PtpB or human PTPN1 (PTP1B), PTPN2 (TCPTP), or PTPN5 (STEP); 2) pNPP solution; and 3) NaOH developing solution. The phosphatase enzyme solutions contained 50 nM of either of the four phosphatases in assay buffer (50 mM 3,3-dimethyl glutarate, pH 7.0, 150 mM NaCl, 1 mM EDTA, and 1

mM DTT). The pNPP solution contained 4.16 mM of *para*-nitrophenyl phosphate in assay buffer. The NaOH developing solution contained 6 M NaOH.

General assay protocol:

First, 20 µL aliquots of the phosphatase enzyme solutions were dispensed into clear, 384-well polystyrene plates. Next, 0.5 µL of the compound stocks (10 mM to 4.6 µM, 3-fold dilutions series in DMSO) were added by pin-transfer. The phosphatase enzymatic reactions were then initiated by addition of 30 µL of the pNPP solution. The plates were incubated 37°C for either 30 min (Mtb PtpB) or 45 min (human phosphatases), then 10 µL of the NaOH developing solution was added. The absorbance at 405 nm was measured in each well (monitoring for the phenolate product) using a Molecular Devices, SpectraMax Plus384 microplate reader. A second set of baseline control plates were prepared analogously, but without any phosphatases present, to correct for possible interference from compound absorbance or turbidity. IC_{50} values for the test compounds were obtained by plotting the A_{405} results in GraphPad Prism 6 and analyzing by non-linear regression using the log(inhibitor) vs. response (variable slope) equation. Results presented represent the averages of IC_{50} values obtained from at least six replicates for each phosphatase.

Control compounds, calculation of IC_{50} values, and statistical considerations.

For the chaperonin-mediated biochemical assays, DMSO was used as negative control, and a panel of our previously discovered and reported chaperonin inhibitors were used as positive controls: e.g. compounds **8**, **9**, and **18** from Johnson *et. al* 2014 and Abdeen *et. al* 2016; suramin and compound **2h-*p*** from Abdeen *et. al* 2016; compounds **20R**, **20L**, and **28R** from Abdeen *et. al* 2018. All IC_{50} results reported are averages of values determined from individual dose-response curves in assay replicates as follows: 1) Individual IC_{50} values from assay replicates were first log-transformed and the average log(IC_{50}) values and standard deviations (SD) calculated; 2) Replicate

log(IC_{50}) values were evaluated for outliers using the ROUT method in GraphPad Prism 6 (Q of 10%); and 3) Average IC_{50} values were then back-calculated from the average log(IC_{50}) values. For compounds where log(IC_{50}) values were greater than the maximum compound concentrations tested (i.e. >1.8, >2.0, and >2.4 – or >63, >100, and >250 mM, respectively), results were represented as 0.1 log units higher than the maximum concentrations tested (i.e. 1.9, 2.1, and 2.5 – or 79, 126, and 316 mM, respectively) so as not to overly bias comparisons because of the unavailability of definitive values for these inactive compounds.

APPENDIX

Table 5A – IC_{50} and EC_{50} biochemical assay results for analogs **1** and **2a-m**. Compounds that were tested in the PTPN2 phosphatase assay for which their dose-response curve baselines did not go to zero, but appeared to plateau between 10-30% inhibition, are labeled with a superscript "bp".

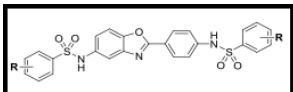

Compounds & Substituents			Biochemical Assay IC_{50} (μM)								
			Reporter Counter-Screens:		GroEL/ES refolding of:		HSP60/10-dMDH refolding	*Mtb* PtpB	Human PTPN1 (PTP1B)	Human PTPN2 (TCPTP)	Human PTPN5 (STEP)
			nRho	nMDH	dRho	dMDH					
$-CH_3$	1		>100	>63	45	24	88	23	15	22^{bp}	13
-H	2a		>100	>63	18	4.0	80	18	24	29	23
-F	2b	- *o*	>100	>63	51	20	57	16	36	31	26
		- *m*	>100	>63	56	5.7	52	13	36	32	31
		- *p*	>100	>63	19	3.3	67	18	27	28	23
-Cl	2c	- *o*	>100	>63	43	40	>100	6.4	16	22^{bp}	17
		- *m*	>100	>63	46	11	64	2.3	16	17^{bp}	13
		- *p*	>100	>63	29	15	88	4.3	8.1	19^{bp}	12
-Br	2d	- *o*	>100	>63	60	59	>100	20	24	28	31
		- *m*	>100	>63	32	19	>100	0.79	14	11^{bp}	11
		- *p*	>100	>63	34	16	>100	3.6	11	18^{bp}	11
$-CH_3$	2e	- *o*	>100	>63	73	77	>100	4.9	12	18^{bp}	14
		- *m*	>100	>63	51	28	>100	5.8	13	17	16
		- *p*	>100	>63	30	27	>100	6.9	14	18^{bp}	14
$-CF_3$	2f	- *o*	>100	>63	56	23	>100	8.1	14	22	15
		- *m*	>100	>63	33	14	54	2.9	12	12	16
		- *p*	>100	>63	34	19	57	2.8	6.4	13^{bp}	7.9
$-OCH_3$	2g	- *o*	>100	>63	33	43	>100	8.7	12	21^{bp}	19
		- *m*	>100	>63	73	17	78	9.4	18	16^{bp}	22
		- *p*	>100	>63	56	30	>100	12	14	16	15
-OH	2h	- *o*	>100	49	14	7.7	18	2.3	23	39	25
		- *m*	>100	55	4.0	0.97	17	1.5	38	84	47
		- *p*	>100	>63	1.1	0.29	14	12	27	75	35
$-NO_2$	2i	- *o*	>100	>63	9.6	5.2	47	10	28	28	29
		- *m*	>100	>63	7.1	3.7	42	9.1	14	29	24
		- *p*	>100	>63	22	24	43	6.2	27	28	18
$-NH_2$	2j	- *o*	>100	>63	39	12	55	17	34	25	51
		- *m*	N/A	N/A	N/A	N/A	N/A	N/A	N/A	N/A	N/A
		- *p*	>100	>63	3.1	1.4	44	16	27	32	41
-CN	2k	- *o*	>100	>63	86	33	79	18	56	69	47
		- *m*	>100	>63	14	7.2	72	33	37	48	44
		- *p*	>100	>63	49	35	49	12	37	35	27
$-CO_2CH_3$	2l	- *o*	>100	>63	36	29	77	11	10	14	21
		- *m*	>100	>63	35	9.9	60	5.8	17	13	16
		- *p*	>100	>63	13	20	65	11	11	17	22
$-CO_2H$	2m	- *o*	>100	>63	222	>100	>100	4.2	>100	>100	>100
		- *m*	>100	51	>250	63	62	9.9	>100	>100	>100
		- *p*	>100	>63	194	85	90	12	>100	>100	>100

Table 5B – Log(IC_{50} and EC_{50}) biochemical assay results ± SD for analogs **1** and **2a**-**m**.

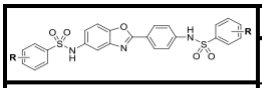			Biochemical Assay IC_{50} (μM)								
			Reporter Counter-Screens:		GroEL/ES refolding of:		HSP60/10-dMDH refolding	*Mtb* PtpB	Human PTPN1 (PTP1B)	Human PTPN2 (TCPTP)	Human PTPN5 (STEP)
Compounds & Substituents			nRho	nMDH	dRho	dMDH					
-CH_3	1		>2	>1.8	1.66 ± 0.27	1.36 ± 0.57	1.92 ± 0.19	1.36 ± 0.08	1.19 ± 0.28	1.35 ± 0.19	1.10 ± 0.13
-H	2a		>2	>1.8	1.26 ± 0.16	0.60 ± 0.28	1.90 ± 0.13	1.24 ± 0.14	1.38 ± 0.12	1.49 ± 0.02	1.35 ± 0.09
-F	2b	- *o*	>2	>1.8	1.71 ± 0.03	1.3 ± 0.23	1.76 ± 0.18	1.19 ± 0.15	1.55 ± 0.22	1.49 ± 0.02	1.41 ± 0.09
		- *m*	>2	>1.8	1.74 ± 0.09	0.74 ± 0.17	1.71 ± 0.22	1.11 ± 0.23	1.55 ± 0.16	1.51 ± 0.02	1.49 ± 0.07
		- *p*	>2	>1.8	1.27 ± 0.08	0.51 ± 0.24	1.83 ± 0.20	1.26 ± 0.20	1.43 ± 0.12	1.45 ± 0.05	1.36 ± 0.12
-Cl	2c	- *o*	>2	>1.8	1.63 ± 0.15	1.61 ± 0.18	>2	0.81 ± 0.29	1.20 ± 0.26	1.33 ± 0.19	1.22 ± 0.04
		- *m*	>2	>1.8	1.66 ± 0.12	1.07 ± 0.41	1.81 ± 0.24	0.37 ± 0.26	1.20 ± 0.30	1.23 ± 0.17	1.12 ± 0.12
		- *p*	>2	>1.8	1.47 ± 0.09	1.19 ± 0.33	1.94 ± 0.14	0.64 ± 0.44	0.91 ± 0.12	1.28 ± 0.19	1.09 ± 0.04
-Br	2d	- *o*	>2	>1.8	1.78 ± 0.16	1.77 ± 0.15	>2	1.30 ± 0.27	1.38 ± 0.17	1.44 ± 0.07	1.49 ± 0.05
		- *m*	>2	>1.8	1.50 ± 0.16	1.27 ± 0.21	>2	-0.10 ± 0.46	1.15 ± 0.43	1.06 ± 0.10	1.05 ± 0.06
		- *p*	>2	>1.8	1.53 ± 0.08	1.22 ± 0.30	>2	0.56 ± 0.40	1.03 ± 0.37	1.26 ± 0.18	1.02 ± 0.13
-CH_3	2e	- *o*	>2	>1.8	1.86 ± 0.08	1.88 ± 0.19	>2	0.69 ± 0.41	1.08 ± 0.14	1.26 ± 0.19	1.15 ± 0.20
		- *m*	>2	>1.8	1.71 ± 0.15	1.45 ± 0.28	>2	0.77 ± 0.36	1.12 ± 0.14	1.22 ± 0.18	1.20 ± 0.23
		- *p*	>2	>1.8	1.48 ± 0.14	1.43 ± 0.24	>2	0.84 ± 0.39	1.14 ± 0.19	1.25 ± 0.20	1.16 ± 0.18
-CF_3	2f	- *o*	>2	>1.8	1.75 ± 0.12	1.34 ± 0.22	>2	0.91 ± 0.15	1.14 ± 0.13	1.34 ± 0.20	1.18 ± 0.13
		- *m*	>2	>1.8	1.52 ± 0.18	1.12 ± 0.28	1.73 ± 0.40	0.46 ± 0.17	1.07 ± 0.11	1.08 ± 0.08	1.22 ± 0.05
		- *p*	>2	>1.8	1.54 ± 0.16	1.27 ± 0.23	1.76 ± 0.28	0.44 ± 0.21	0.81 ± 0.13	1.13 ± 0.13	0.90 ± 0.14
-OCH_3	2g	- *o*	>2	>1.8	1.51 ± 0.18	1.64 ± 0.22	>2	0.94 ± 0.24	1.09 ± 0.08	1.32 ± 0.13	1.28 ± 0.21
		- *m*	>2	>1.8	1.86 ± 0.06	1.24 ± 0.51	1.93 ± 0.7	0.97 ± 0.22	1.25 ± 0.19	1.26 ± 0.18	1.35 ± 0.44
		- *p*	>2	>1.8	1.75 ± 0.08	1.46 ± 0.19	>2	1.07 ± 0.29	1.16 ± 0.12	1.21 ± 0.15	1.18 ± 0.23
-OH	2h	- *o*	>2	1.73 ± 0.09	1.14 ± 0.14	0.88 ± 0.17	1.07 ± 0.18	0.35 ± 0.25	1.37 ± 0.22	1.59 ± 0.05	1.40 ± 0.08
		- *m*	>2	1.46 ± 0.31	0.60 ± 0.65	-0.020 ± 0.29	1.24 ± 0.14	0.18 ± 0.16	1.58 ± 0.07	1.92 ± 0.03	1.68 ± 0.10
		- *p*	>2	>1.8	0.048 ± 0.27	-0.54 ± 0.38	1.15 ± 0.17	1.07 ± 0.42	1.43 ± 0.19	1.87 ± 0.07	1.55 ± 0.06
-NO_2	2i	- *o*	>2	>1.8	0.98 ± 0.13	0.71 ± 0.30	1.67 ± 0.17	1.02 ± 0.16	1.45 ± 0.30	1.44 ± 0.09	1.46 ± 0.05
		- *m*	>2	>1.8	0.85 ± 0.17	0.55 ± 0.14	1.63 ± 0.12	0.96 ± 0.12	1.16 ± 0.10	1.46 ± 0.02	1.37 ± 0.07
		- *p*	>2	>1.8	1.35 ± 0.08	1.38 ± 0.17	1.64 ± 0.28	0.79 ± 0.08	1.43 ± 0.44	1.45 ± 0.07	1.27 ± 0.13
-NH_2	2j	- *o*	>2	>1.8	1.59 ± 0.14	1.06 ± 0.24	1.74 ± 0.29	1.23 ± 0.12	1.54 ± 0.24	1.39 ± 0.08	1.71 ± 0.28
		- *m*	N/A	N/A	N/A	N/A	N/A	N/A	N/A	N/A	N/A
		- *p*	>2	>1.8	0.49 ± 0.22	0.16 ± 0.37	1.65 ± 0.25	1.20 ± 0.42	1.43 ± 0.24	1.51 ± 0.08	1.61 ± 0.04
-CN	2k	- *o*	>2	>1.8	1.93 ± 0.04	1.51 ± 0.15	1.90 ± 0.11	1.27 ± 0.13	1.75 ± 0.21	1.84 ± 0.13	1.67 ± 0.09
		- *m*	>2	>1.8	1.15 ± 0.14	0.86 ± 0.18	1.86 ± 0.15	1.51 ± 0.02	1.57 ± 0.12	1.69 ± 0.09	1.64 ± 0.13
		- *p*	>2	>1.8	1.69 ± 0.08	1.54 ± 0.10	1.70 ± 0.18	1.07 ± 0.13	1.57 ± 0.30	1.55 ± 0.18	1.43 ± 0.07
-CO_2CH_3	2l	- *o*	>2	>1.8	1.56 ± 0.07	1.47 ± 0.18	1.89 ± 0.14	1.05 ± 0.10	1.01 ± 0.21	1.15 ± 0.05	1.32 ± 0.02
		- *m*	>2	>1.8	1.54 ± 0.13	1.00 ± 0.46	1.78 ± 0.22	0.76 ± 0.23	1.22 ± 0.35	1.13 ± 0.15	1.21 ± 0.21
		- *p*	>2	>1.8	1.12 ± 0.08	1.31 ± 0.22	1.81 ± 0.20	1.04 ± 0.15	1.05 ± 0.15	1.22 ± 0.16	1.34 ± 0.19
-CO_2H	2m	- *o*	>2	>1.8	2.35 ± 0.10	>2	>2	0.62 ± 0.10	>2	>2	>2
		- *m*	>2	1.59 ± 0.11	>2.4	1.80 ± 0.14	1.79 ± 0.13	1.00 ± 0.53	>2	>2	>2
		- *p*	>2	>1.8	2.29 ± 0.05	1.93 ± 0.13	1.96 ± 0.07	1.09 ± 0.65	>2	>2	>2

Table 6A – EC_{50} and CC_{50} cell viability results for analogs **1** and **2a-m**.

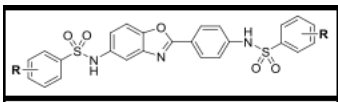 Compounds & Substituents			Cell Viability EC_{50} or CC_{50} (μM) or % Inhibition at 200 μM				
			M. smegmatis	*M. tuberculosis*		THLE3 (Liver)	HEK 293 (Kidney)
				% Inhibition	EC_{50}		
$-CH_3$	1		>100	14		22	29
-H	2a		>100	76	28	23	22
-F	2b	- *o*	>100	54	45	40	39
		- *m*	>100	48	>200	28	29
		- *p*	>100	48	66	22	31
-Cl	2c	- *o*	>100	0		25	43
		- *m*	>100	0		19	22
		- *p*	>100	0		18	19
-Br	2d	- *o*	>100	50	>200	37	36
		- *m*	>100	17		24	28
		- *p*	>100	0		18	22
$-CH_3$	2e	- *o*	>100	0		25	28
		- *m*	>100	0		19	35
		- *p*	>100	0		15	37
$-CF_3$	2f	- *o*	>100	35		63	66
		- *m*	>100	0		24	21
		- *p*	>100	0		21	23
$-OCH_3$	2g	- *o*	>100	12		48	34
		- *m*	>100	0		18	27
		- *p*	>100	0		60	57
-OH	2h	- *o*	>100	79	63	20	20
		- *m*	>100	80	84	44	45
		- *p*	>100	66	94	51	66
$-NO_2$	2i	- *o*	>100	39		>100	80
		- *m*	>100	0		50	52
		- *p*	>100	0		48	62
$-NH_2$	2j	- *o*	>100	58	>200	19	14
		- *m*	N/A	N/A		N/A	N/A
		- *p*	>100	51	>200	39	60
-CN	2k	- *o*	>100	85	113	93	83
		- *m*	>100	65	>200	86	58
		- *p*	>100	95	43	77	62
$-CO_2CH_3$	2l	- *o*	>100	0		>100	>100
		- *m*	>100	0		53	68
		- *p*	>100	0		36	59
$-CO_2H$	2m	- *o*	>100	22		>100	>100
		- *m*	>100	7		>100	>100
		- *p*	>100	10		>100	>100

Table 6B – Log(EC_{50} and CC_{50}) cell viability results ± SD for analogs **1** and **2a**-**m**.

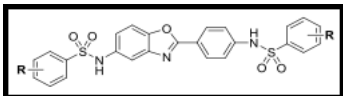 Compounds & Substituents			Cell Viability EC_{50} or CC_{50} (μM) or % Inhibition at 200 μM				
			M. smegmatis	*M. tuberculosis*		THLE3 (Liver)	HEK 293 (Kidney)
				% Inhibition	EC_{50}		
-CH_3	1		>2	14		1.34 ± 0.09	1.58 ± 0.26
-H	2a		>2	76	1.45 ± 0.04	1.35 ± 0.10	1.40 ± 0.25
-F	2b	- *o*	>2	54	1.65 ± 0.01	1.60 ± 0.15	1.63 ± 0.24
		- *m*	>2	48	>2.3	1.45 ± 0.21	1.51 ± 0.19
		- *p*	>2	48	1.82 ± 0.01	1.34 ± 0.25	1.51 ± 0.24
-Cl	2c	- *o*	>2	0		1.39 ± 0.14	1.66 ± 0.27
		- *m*	>2	0		1.28 ± 0.14	1.38 ± 0.21
		- *p*	>2	0		1.26 ± 0.16	1.27 ± 0.22
-Br	2d	- *o*	>2	50	>2.3	1.57 ± 0.04	1.60 ± 0.21
		- *m*	>2	17		1.38 ± 0.14	1.48 ± 0.19
		- *p*	>2	0		1.26 ± 0.17	1.39 ± 0.27
-CH_3	2e	- *o*	>2	0		1.37 ± 0.24	1.49 ± 0.22
		- *m*	>2	0		1.26 ± 0.12	1.59 ± 0.33
		- *p*	>2	0		1.18 ± 0.33	1.60 ± 0.36
-CF_3	2f	- *o*	>2	35		1.80 ± 0.16	1.84 ± 0.14
		- *m*	>2	0		1.37 ± 0.14	1.36 ± 0.23
		- *p*	>2	0		1.31 ± 0.18	1.47 ± 0.29
-OCH_3	2g	- *o*	>2	12		1.70 ± 0.29	1.57 ± 0.45
		- *m*	>2	0		1.27 ± 0.14	1.46 ± 0.26
		- *p*	>2	0		1.78 ± 0.27	1.78 ± 0.26
-OH	2h	- *o*	>2	79	1.80 ± 0.01	1.28 ± 0.12	1.32 ± 0.19
		- *m*	>2	80	1.93 ± 0.03	1.64 ± 0.15	1.58 ± 0.07
		- *p*	>2	66	1.98 ± 0.01	1.73 ± 0.16	1.92 ± 0.12
-NO_2	2i	- *o*	>2	39		>2	>2
		- *m*	>2	0		1.70 ± 0.18	1.74 ± 0.18
		- *p*	>2	0		1.68 ± 0.22	1.81 ± 0.19
-NH_2	2j	- *o*	>2	58	>2.3	1.27 ± 0.13	1.20 ± 0.20
		- *m*	N/A	N/A		N/A	N/A
		- *p*	>2	51	>2.3	1.59 ± 0.22	1.80 ± 0.18
-CN	2k	- *o*	>2	85	2.05 ± 0.07	1.96 ± 0.06	1.93 ± 0.14
		- *m*	>2	65	>2.3	1.94 ± 0.07	1.79 ± 0.18
		- *p*	>2	95	1.64 ± 0.02	1.89 ± 0.13	1.81 ± 0.17
-CO_2CH_3	2l	- *o*	>2	0		>2	>2
		- *m*	>2	0		1.71 ± 0.19	1.84 ± 0.22
		- *p*	>2	0		1.56 ± 0.49	1.79 ± 0.27
-CO_2H	2m	- *o*	>2	22		>2	>2
		- *m*	>2	7		>2	>2
		- *p*	>2	10		>2	>2

Table 7A – IC_{50} and EC_{50} biochemical assay results for analogs **2-14**. Compounds that were tested in the PTPN2 phosphatase assay for which their dose-response curve baselines did not go to zero, but appeared to plateau between 10-30% inhibition, are labeled with a superscript “bp”.

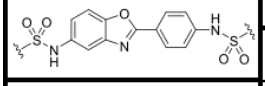		Biochemical Assay IC_{50} (μM)								
		Reporter Counter-Screens:		GroEL/ES refolding of:		HSP60/10-dMDH refolding	*Mtb* PtpB	Human PTPN1 (PTP1B)	Human PTPN2 (TCPTP)	Human PTPN5 (STEP)
Compounds & Substituents		nRho	nMDH	dRho	dMDH					
	**2a**	>100	>63	18	4.0	80	18	24	31	23
	**3**	>100	>63	>250	>100	>100	>100	>100	>100	>100
	**4**	>100	>63	28	50	71	42	>100	>100	>100
	**5**	>100	>63	>250	>100	>100	>100	>100	>100	83
	**6**	>100	>63	16	5.5	40	12	31	41	33
	**7**	>100	>63	111	29	>100	27	23	31	25
	**8**	>100	>63	51	34	50	8.8	34	58	40
	**9**	>100	>63	38	36	61	7.0	10	17^{bp}	17
	**10**	>100	>63	35	43	>100	2.1	3.2	25^{bp}	4.9
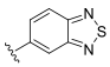	**11**	65	>63	13	3.8	47	6.4	8.0	11^{bp}	11
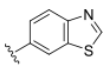	**12**	>100	>63	6.2	0.77	19	20	7.0	12^{bp}	20
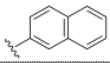	**13**	>100	>63	36	37	>100	4.4	4.3	24^{bp}	6.2
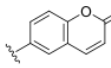	**14**	>100	>63	12	19	43	8.7	6.3	9.1^{bp}	17

Table 7B – Log(IC_{50} and EC_{50}) biochemical assay results ± SD for analogs **2**-**14**.

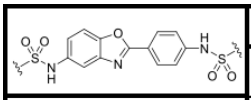		Biochemical Assay IC_{50} (μM)								
		Reporter Counter-Screens:		GroEL/ES refolding of:		HSP60/10-dMDH refolding	*Mtb* PtpB	Human PTPN1 (PTP1B)	Human PTPN2 (TCPTP)	Human PTPN5 (STEP)
Compounds & Substituents		nRho	nMDH	dRho	dMDH					
	**2a**	>2	>1.8	1.26 ± 0.16	0.60 ± 0.28	1.90 ± 0.13	1.24 ± 0.14	1.38 ± 0.12	1.49 ± 0.02	1.35 ± 0.09
	**3**	>2	>1.8	>2.4	>2	>2	>2	>2	>2	>2
	**4**	>2	>1.8	1.45 ± 0.30	1.69 ± 0.24	1.85 ± 0.16	1.62 ± 0.13	>2	>2	>2
	**5**	>2	>1.8	>2.4	>2	>2	>2	>2	>2	1.92 ± 0.03
	**6**	>2	>1.8	1.21 ± 0.12	0.73 ± 0.23	1.60 ± 0.13	1.07 ± 0.19	1.50 ± 0.06	1.62 ± 0.06	1.51 ± 0.02
	**7**	>2	>1.8	2.05 ± 0.11	1.46 ± 0.36	>2	1.43 ± 0.18	1.36 ± 0.11	1.49 ± 0.08	1.40 ± 0.08
	**8**	>2	>1.8	1.71 ± 0.03	1.53 ± 0.17	1.70 ± 0.16	0.94 ± 0.09	1.54 ± 0.10	1.76 ± 0.17	1.60 ± 0.05
	**9**	>2	>1.8	1.58 ± 0.08	1.56 ± 0.18	1.79 ± 0.22	0.85 ± 0.11	1.02 ± 0.25	1.23 ± 0.12	1.22 ± 0.19
	**10**	>2	>1.8	1.54 ± 0.07	1.63 ± 0.23	>2	0.32 ± 0.23	0.51 ± 0.11	1.39 ± 0.17	0.69 ± 0.10
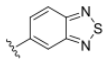	**11**	>2	>1.8	1.12 ± 0.04	0.57 ± 0.45	1.68 ± 0.24	0.81 ± 0.09	0.91 ± 0.08	1.06 ± 0.09	1.04 ± 0.14
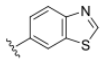	**12**	>2	>1.8	0.79 ± 0.31	-0.11 ± 0.38	1.27 ± 0.38	1.30 ± 0.17	0.85 ± 0.12	1.06 ± 0.09	1.30 ± 0.14
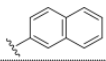	**13**	>2	>1.8	1.55 ± 0.11	1.57 ± 0.17	>2	0.64 ± 0.30	0.64 ± 0.08	1.38 ± 0.13	0.80 ± 0.21
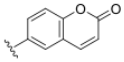	**14**	>2	>1.8	1.09 ± 0.17	1.26 ± 0.18	1.63 ± 0.29	0.94 ± 0.11	0.80 ± 0.08	0.96 ± 0.21	1.23 ± 0.08

Table 8A – EC_{50} and CC_{50} cell viability results for analogs **2-14**.

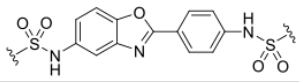 Compounds & Substituents		Cell Viability EC_{50} or CC_{50} (μM) or % Inhibition at 200 μM				
		M. smegmatis	*M. tuberculosis*		THLE3 (Liver)	HEK 293 (Kidney)
			% Inhibition	EC_{50}		
	**2a**	>100	76	28	23	22
	**3**	>100	62	>200	>100	>100
	**4**	>100	28		>100	>100
	**5**	>100	13		>100	>100
	**6**	>100	59	34	40	34
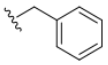	**7**	>100	0		31	23
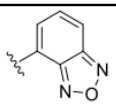	**8**	>100	76	>200	57	55
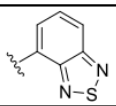	**9**	>100	0		>100	62
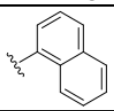	**10**	>100	0		49	>100
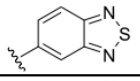	**11**	>100	0		43	63
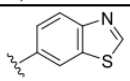	**12**	>100	0		40	80
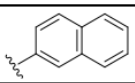	**13**	>100	0		36	35
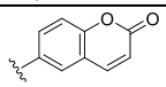	**14**	>100	23		>100	>100

Table 8B – Log(EC_{50} and CC_{50}) cell viability results ± SD for analogs **2**-**14**.

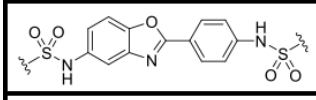 Compounds & Substituents		Cell Viability EC_{50} or CC_{50} (μM) or % Inhibition at 200 μM				
		M. smegmatis	*M. tuberculosis*		THLE3 (Liver)	HEK 293 (Kidney)
			% Inhibition	EC_{50}		
	**2a**	>2	76	1.45 ± 0.04	1.35 ± 0.10	1.40 ± 0.25
	**3**	>2	62	>2.3	>2	>2
	**4**	>2	28		>2	>2
	**5**	>2	13		>2	>2
	**6**	>2	59	1.53 ± 0.07	1.60 ± 0.18	1.59 ± 0.22
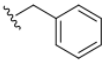	**7**	>2	0		1.49 ± 0.15	1.38 ± 0.15
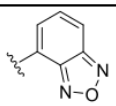	**8**	>2	76	>2.3	1.75 ± 0.23	1.76 ± 0.23
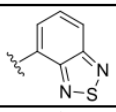	**9**	>2	0		>2	1.81 ± 0.17
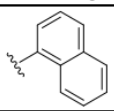	**10**	>2	0		1.69 ± 0.30	>2
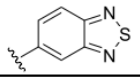	**11**	>2	0		1.63 ± 0.19	1.82 ± 0.18
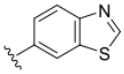	**12**	>2	0		1.61 ± 0.23	1.91 ± 0.17
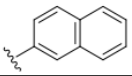	**13**	>2	0		1.56 ± 0.28	1.54 ± 0.07
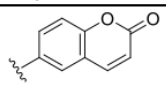	**14**	>2	23		>2	>2

Table 9A – IC_{50} and EC_{50} biochemical assay results for analogs **15** and **16R-34R**. Compounds that were tested in the PTPN2 phosphatase assay for which their dose-response curve baselines did not go to zero, but appeared to plateau between 10-30% inhibition, are labeled with a superscript "bp".

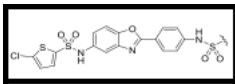		Biochemical Assay IC_{50} (μM)								
		Reporter Counter-Screens:		GroEL/ES refolding of:		HSP60/10-dMDH refolding	*Mtb* PtpB	Human PTPN1 (PTP1B)	Human PTPN2 (TCPTP)	Human PTPN5 (STEP)
Compounds & Substituents		nRho	nMDH	dRho	dMDH					
	**15**	>100	57	5.6	2.8	6.1	2.3	11	25	15
	**16R**	68	>63	42	14	43	37	52	95	52
	**17R**	>100	>63	23	17	41	3.4	4.9	9.5^{bp}	9.3
	**18R**	>100	>63	12	2.6	26	6.7	19	29^{bp}	17
	**19R**	>100	>63	21	5.2	24	5.3	8.8	11^{bp}	8.8
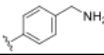	**20R**	>100	>63	3.2	1.3	48	9.1	56	91	75
	**21R**	>100	>63	33	12	53	5.0	10	14	13
	**22R**	>100	>63	51	14	>100	6.5	14	12^{bp}	12
	**23R**	>100	>63	24	6.7	61	11	11	16	16
	**24R**	>100	>63	4.5	2.1	6.3	3.0	12	16	16
	**25R**	>100	>63	7.0	5.1	17	2.3	6.9	12	9.8
	**26R**	>100	>63	77	11	71	6.8	8.6	8.5	14
	**27R**	>100	>63	7.3	2.8	6.7	2.0	7.6	13	12
	**28R**	53	42	2.0	1.7	2.8	4.0	8.0	18	15
	**29R**	>100	>63	27	2.5	18	3.4	6.4	16^{bp}	11
	**30R**	80	>63	3.5	0.75	17	7.1	7.9	11	13
	**31R**	>100	>63	25	10	67	3.9	6.9	13	11
	**32R**	>100	>63	25	14	27	5.5	8.4	17^{bp}	15
	**33R**	72	>63	19	9.3	13	5.9	15	28	24
	**34R**	>100	>63	18	5.1	56	2.7	5.4	15^{bp}	9.1

Table 9B – Log(IC_{50} and EC_{50}) biochemical assay results ± SD for analogs **15** and **16R**-**34R**.

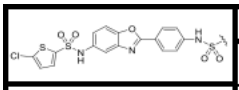 Compounds & Substituents		Biochemical Assay IC_{50} (μM)								
		Reporter Counter-Screens:		GroEL/ES refolding of:		HSP60/10-dMDH refolding	*Mtb* PtpB	Human PTPN1 (PTP1B)	Human PTPN2 (TCPTP)	Human PTPN5 (STEP)
		nRho	nMDH	dRho	dMDH					
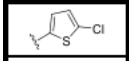	**15**	>2	1.71 ± 0.06	0.75 ± 0.07	0.44 ± 0.16	0.79 ± 0.16	0.37 ± 0.19	1.05 ± 0.07	1.39 ± 0.13	1.18 ± 0.18
	**16R**	1.83 ± 0.09	>1.8	1.62 ± 0.13	1.16 ± 0.09	1.63 ± 0.05	1.57 ± 0.07	1.72 ± 0.15	1.98 ± 0.13	1.72 ± 0.11
	**17R**	>2	>1.8	1.36 ± 0.12	1.23 ± 0.22	1.61 ± 0.23	0.54 ± 0.23	0.69 ± 0.06	0.98 ± 0.14	0.97 ± 0.17
	**18R**	>2	>1.8	1.07 ± 0.27	0.42 ± 0.22	1.41 ± 0.19	0.82 ± 0.20	1.28 ± 0.32	1.46 ± 0.05	1.22 ± 0.12
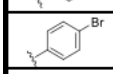	**19R**	>2	>1.8	1.33 ± 0.10	0.72 ± 0.20	1.38 ± 0.14	0.72 ± 0.15	0.94 ± 0.24	1.06 ± 0.30	0.95 ± 0.20
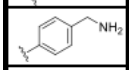	**20R**	>2	>1.8	0.50 ± 0.22	0.11 ± 0.30	1.68 ± 0.10	0.96 ± 0.30	1.75 ± 0.14	1.96 ± 0.02	1.88 ± 0.08
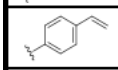	**21R**	>2	>1.8	1.52 ± 0.12	1.08 ± 0.09	1.73 ± 0.21	0.70 ± 0.25	1.02 ± 0.09	1.15 ± 0.13	1.12 ± 0.03
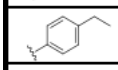	**22R**	>2	>1.8	1.71 ± 0.16	1.16 ± 0.12	>2	0.81 ± 0.27	1.16 ± 0.32	1.09 ± 0.12	1.07 ± 0.11
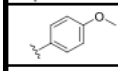	**23R**	>2	>1.8	1.39 ± 0.24	0.82 ± 0.34	1.78 ± 0.23	1.04 ± 0.18	1.06 ± 0.07	1.20 ± 0.14	1.20 ± 0.04
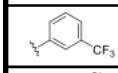	**24R**	>2	>1.8	0.65 ± 0.10	0.32 ± 0.15	0.80 ± 0.32	0.47 ± 0.10	1.07 ± 0.05	1.21 ± 0.13	1.21 ± 0.02
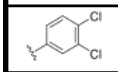	**25R**	>2	>1.8	0.85 ± 0.08	0.66 ± 0.32	1.23 ± 0.21	0.37 ± 0.23	0.84 ± 0.08	1.07 ± 0.18	0.99 ± 0.12
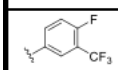	**26R**	>2	>1.8	1.89 ± 0.09	1.04 ± 0.33	1.85 ± 0.16	0.83 ± 0.18	0.94 ± 0.14	0.93 ± 0.07	1.16 ± 0.02
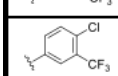	**27R**	>2	>1.8	0.92 ± 0.03	0.44 ± 0.39	0.82 ± 0.38	0.29 ± 0.12	0.88 ± 0.08	1.12 ± 0.11	1.08 ± 0.06
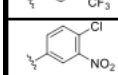	**28R**	1.72 ± 0.29	1.58 ± 0.10	0.30 ± 0.09	0.22 ± 0.10	0.44 ± 0.23	0.61 ± 0.19	0.90 ± 0.08	1.25 ± 0.19	1.16 ± 0.05
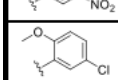	**29R**	>2	>1.8	1.43 ± 0.14	0.40 ± 0.32	1.25 ± 0.28	0.53 ± 0.12	0.81 ± 0.10	1.20 ± 0.15	1.05 ± 0.11
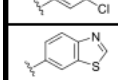	**30R**	1.90 ± 0.10	>1.8	0.54 ± 0.21	-0.13 ± 0.18	1.23 ± 0.16	0.85 ± 0.16	0.90 ± 0.11	1.06 ± 0.18	1.11 ± 0.12
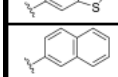	**31R**	>2	>1.8	1.39 ± 0.10	1.01 ± 0.22	1.83 ± 0.22	0.59 ± 0.13	0.84 ± 0.19	1.10 ± 0.20	1.04 ± 0.04
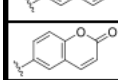	**32R**	>2	>1.8	1.40 ± 0.05	1.14 ± 0.16	1.43 ± 0.13	0.74 ± 0.10	0.93 ± 0.11	1.24 ± 0.17	1.19 ± 0.06
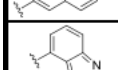	**33R**	1.86 ± 0.12	>1.8	1.27 ± 0.11	0.97 ± 0.12	1.10 ± 0.12	0.77 ± 0.14	1.16 ± 0.07	1.45 ± 0.09	1.39 ± 0.13
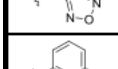	**34R**	>2	>1.8	1.27 ± 0.18	0.71 ± 0.44	1.75 ± 0.15	0.43 ± 0.21	0.73 ± 0.06	1.16 ± 0.13	0.96 ± 0.17

Table 10A – EC_{50} and CC_{50} cell viability results for analogs **15** and **16R-34R**.

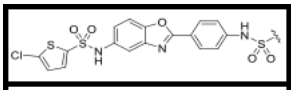 Compounds & Substituents		Cell Viability EC_{50} or CC_{50} (μM) or % Inhibition at 200 μM				
		M. smegmatis	*M. tuberculosis*		THLE3 (Liver)	HEK 293 (Kidney)
			% Inhibition	EC_{50}		
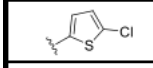	**15**	>100	41		48	37
	**16R**	>100	74	66	25	30
	**17R**	>100	0		38	44
	**18R**	>100	41		22	25
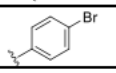	**19R**	>100	0		19	23
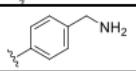	**20R**	71	94	26	27	26
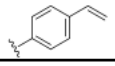	**21R**	>100	14		18	21
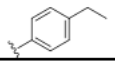	**22R**	>100	11		18	19
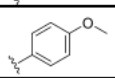	**23R**	>100	25		16	26
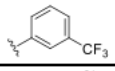	**24R**	>100	36		27	37
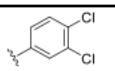	**25R**	>100	0		34	36
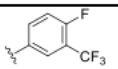	**26R**	>100	0		14	18
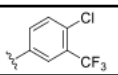	**27R**	>100	0		22	30
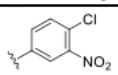	**28R**	>100	29		17	34
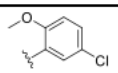	**29R**	>100	33		14	20
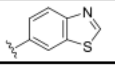	**30R**	>100	33		51	58
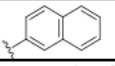	**31R**	>100	0		20	35
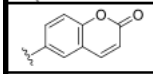	**32R**	>100	0		54	64
	**33R**	>100	46	58	71	64
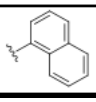	**34R**	>100	0		18	31

Table 10B – Log(EC_{50} and CC_{50}) cell viability results ± SD for analogs **15** and **16R**-**34R**.

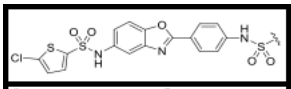 Compounds & Substituents		Cell Viability EC_{50} or CC_{50} (μM) or % Inhibition at 200 μM				
		M. smegmatis	*M. tuberculosis*		THLE3 (Liver)	HEK 293 (Kidney)
			% Inhibition	EC_{50}		
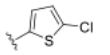	**15**	>2	41		1.68 ± 0.29	1.61 ± 0.23
	**16R**	>2	74	1.82 ± 0.05	1.41 ± 0.24	1.54 ± 0.32
	**17R**	>2	0		1.55 ± 0.14	1.70 ± 0.20
	**18R**	>2	41		1.33 ± 0.13	1.47 ± 0.32
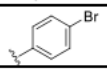	**19R**	>2	0		1.24 ± 0.18	1.54 ± 0.27
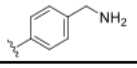	**20R**	1.85 ± 0.21	94	1.41 ± 0.08	1.40 ± 0.19	1.36 ± 0.14
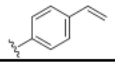	**21R**	>2	14		1.23 ± 0.18	1.41 ± 0.32
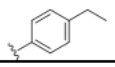	**22R**	>2	11		1.24 ± 0.17	1.37 ± 0.29
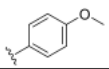	**23R**	>2	25		1.19 ± 0.16	1.49 ± 0.26
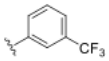	**24R**	>2	36		1.38 ± 0.29	1.62 ± 0.23
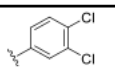	**25R**	>2	0		1.54 ± 0.30	1.61 ± 0.26
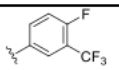	**26R**	>2	0		1.25 ± 0.17	1.47 ± 0.40
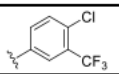	**27R**	>2	0		1.32 ± 0.29	1.53 ± 0.35
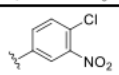	**28R**	>2	29		1.24 ± 0.26	1.48 ± 0.15
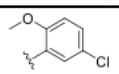	**29R**	>2	33		1.14 ± 0.14	1.37 ± 0.31
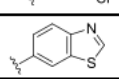	**30R**	>2	33		1.69 ± 0.17	1.80 ± 0.18
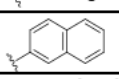	**31R**	>2	0		1.30 ± 0.15	1.60 ± 0.23
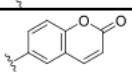	**32R**	>2	0		1.69 ± 0.19	1.84 ± 0.15
	**33R**	>2	46	1.76 ± 0.02	1.81 ± 0.13	1.84 ± 0.15
	**34R**	>2	0		1.25 ± 0.20	1.58 ± 0.29

Table 11A – IC_{50} and EC_{50} biochemical assay results for analogs **15** and **16L-34L**. Compounds that were tested in the PTPN2 phosphatase assay for which their dose-response curve baselines did not go to zero, but appeared to plateau between 10-30% inhibition, are labeled with a superscript "bp".

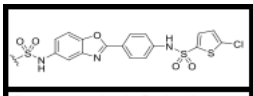		Biochemical Assay IC_{50} (μM)								
		Reporter Counter-Screens:		GroEL/ES refolding of:		HSP60/10-dMDH refolding	*Mtb* PtpB	Human PTPN1 (PTP1B)	Human PTPN2 (TCPTP)	Human PTPN5 (STEP)
Compounds & Substituents		nRho	nMDH	dRho	dMDH					
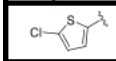	**15**	>100	57	5.6	2.8	6.1	2.3	11	25	15
	**16L**	>100	>63	164	57	40	46	73	>100	>100
	**17L**	>100	57	12	4.0	9.1	5.1	13	31	23
	**18L**	>100	57	14	5.6	9.0	8.8	14	28	24
	**19L**	>100	>63	7.9	2.9	7.2	4.1	6.9	14[bp]	12
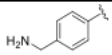	**20L**	>100	>63	13	4.6	37	4.4	42	61	62
	**21L**	>100	>63	15	4.7	9.0	3.9	7.2	12	12
	**22L**	>100	>63	15	8.7	14	7.1	11	15	15
	**23L**	>100	>63	25	6.8	14	9.6	12	24	16
	**24L**	>100	43	11	5.6	6.6	7.1	13	20	16
	**25L**	>100	>63	6.4	5.7	6.9	3.3	7.6	13	11
	**26L**	>100	57	23	17	12	5.7	11	20	14
	**27L**	>100	40	11	5.2	3.9	3.8	7.6	14	11
	**28L**	>100	44	1.9	1.5	1.9	4.6	9.4	8.9[bp]	8.4
	**29L**	>100	>63	24	14	16	6.4	10	9.2[bp]	11
	**30L**	>100	57	6.1	2.3	9.7	3.6	12	9.3[bp]	11
	**31L**	>100	>63	19	11	24	5.4	7.9	7.4[bp]	7.7
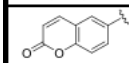	**32L**	>100	>63	17	15	22	4.1	13	9.3	11
	**33L**	>100	59	24	12	13	8.6	16	25	19
	**34L**	>100	>63	17	13	18	2.2	6.5	7.3[bp]	5.1

Table 11B – Log(IC_{50} and EC_{50}) biochemical assay results ± SD for analogs **15** and **16L**-**34L**.

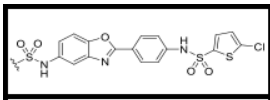		Biochemical Assay IC_{50} (μM)								
		Reporter Counter-Screens:		GroEL/ES refolding of:		HSP60/10-dMDH refolding	*Mtb* PtpB	Human PTPN1 (PTP1B)	Human PTPN2 (TCPTP)	Human PTPN5 (STEP)
Compounds & Substituents		nRho	nMDH	dRho	dMDH					
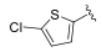	**15**	>2	1.71 ± 0.06	0.75 ± 0.07	0.44 ± 0.16	0.79 ± 0.16	0.37 ± 0.19	1.05 ± 0.07	1.39 ± 0.13	1.18 ± 0.18
	**16L**	>2	>1.8	2.21 ± 0.18	1.76 ± 0.15	1.61 ± 0.03	1.66 ± 0.12	1.87 ± 0.11	>2	>2
	**17L**	>2	1.76 ± 0.04	1.07 ± 0.04	0.61 ± 0.13	0.96 ± 0.14	0.70 ± 0.21	1.12 ± 0.07	1.49 ± 0.05	1.36 ± 0.18
	**18L**	>2	1.75 ± 0.06	1.58 ± 0.45	0.75 ± 0.19	0.96 ± 0.18	0.94 ± 0.26	1.15 ± 0.06	1.45 ± 0.07	1.37 ± 0.18
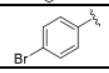	**19L**	>2	>1.8	0.90 ± 0.24	0.46 ± 0.23	0.86 ± 0.37	0.62 ± 0.08	0.84 ± 0.08	1.14 ± 0.15	1.07 ± 0.10
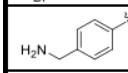	**20L**	>2	>1.8	1.10 ± 0.16	0.66 ± 0.14	1.57 ± 0.10	0.65 ± 0.23	1.62 ± 0.11	1.79 ± 0.11	1.79 ± 0.12
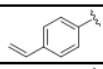	**21L**	>2	>1.8	1.19 ± 0.16	0.67 ± 0.25	0.96 ± 0.30	0.59 ± 0.09	0.86 ± 0.09	1.07 ± 0.12	1.09 ± 0.02
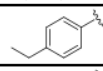	**22L**	>2	>1.8	1.17 ± 0.23	0.94 ± 0.17	1.14 ± 0.35	0.85 ± 0.07	1.02 ± 0.08	1.16 ± 0.13	1.17 ± 0.02
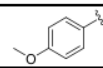	**23L**	>2	>1.8	1.40 ± 0.05	0.83 ± 0.27	1.15 ± 0.26	0.98 ± 0.31	1.08 ± 0.08	1.37 ± 0.14	1.21 ± 0.13
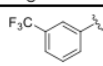	**24L**	>2	1.64 ± 0.14	1.03 ± 0.04	0.75 ± 0.25	0.82 ± 0.28	0.85 ± 0.12	1.10 ± 0.05	1.31 ± 0.14	1.21 ± 0.08
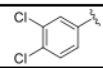	**25L**	>2	>1.8	0.81 ± 0.10	0.75 ± 0.14	0.84 ± 0.37	0.52 ± 0.11	0.88 ± 0.07	1.11 ± 0.14	1.04 ± 0.09
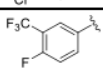	**26L**	>2	1.76 ± 0.05	1.36 ± 0.23	1.23 ± 0.37	1.07 ± 0.14	0.75 ± 0.09	1.04 ± 0.11	1.30 ± 0.16	1.16 ± 0.12
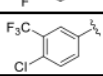	**27L**	>2	1.60 ± 0.24	1.03 ± 0.07	0.71 ± 0.09	0.59 ± 0.39	0.58 ± 0.12	0.88 ± 0.12	1.14 ± 0.12	1.05 ± 0.12
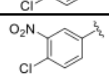	**28L**	>2	1.65 ± 0.10	0.28 ± 0.28	0.18 ± 0.16	0.29 ± 0.30	0.66 ± 0.05	0.97 ± 0.23	0.95 ± 0.07	0.93 ± 0.08
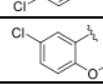	**29L**	>2	>1.8	1.38 ± 0.22	1.15 ± 0.27	1.19 ± 0.31	0.81 ± 0.09	1.01 ± 0.21	0.96 ± 0.07	1.04 ± 0.08
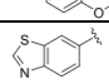	**30L**	>2	1.76 ± 0.06	0.79 ± 0.23	0.36 ± 0.37	0.99 ± 0.25	0.56 ± 0.18	1.07 ± 0.20	0.97 ± 0.07	1.05 ± 0.10
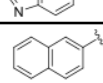	**31L**	>2	>1.8	1.28 ± 0.30	1.04 ± 0.16	1.37 ± 0.24	0.73 ± 0.08	0.90 ± 0.24	0.87 ± 0.09	0.89 ± 0.08
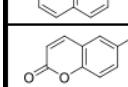	**32L**	>2	>1.8	1.24 ± 0.21	1.16 ± 0.23	1.33 ± 0.28	0.62 ± 0.09	1.10 ± 0.16	0.97 ± 0.05	1.05 ± 0.08
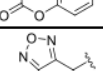	**33L**	>2	1.77 ± 0.05	1.38 ± 0.10	1.09 ± 0.17	1.11 ± 0.013	0.94 ± 0.10	1.22 ± 0.21	1.40 ± 0.08	1.27 ± 0.04
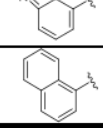	**34L**	>2	>1.8	1.23 ± 0.17	1.11 ± 0.19	1.26 ± 0.28	0.34 ± 0.21	0.81 ± 0.22	0.87 ± 0.13	0.71 ± 0.08

Table 12A – EC_{50} and CC_{50} cell viability results for analogs **15** and **16L-34L**.

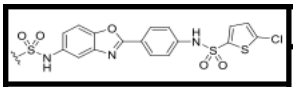 Compounds & Substituents		Cell Viability EC_{50} or CC_{50} (μM) or % Inhibition at 200 μM				
		M. smegmatis	*M. tuberculosis*		THLE3 (Liver)	HEK 293 (Kidney)
			% Inhibition	EC_{50}		
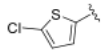	**15**	>100	41		48	37
	**16L**	>100	85	104	84	91
	**17L**	>100	52	36	44	44
	**18L**	>100	72	40	32	37
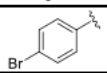	**19L**	>100	28		24	24
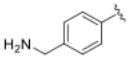	**20L**	71	91	59	36	50
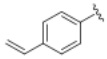	**21L**	>100	10		20	25
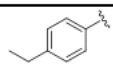	**22L**	>100	0		20	23
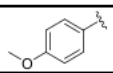	**23L**	>100	41		33	35
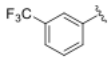	**24L**	>100	0		36	44
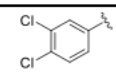	**25L**	>100	0		25	30
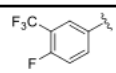	**26L**	85	0		55	52
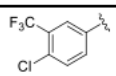	**27L**	>100	0		28	30
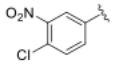	**28L**	>100	1		11	34
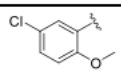	**29L**	>100	39		22	25
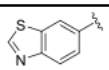	**30L**	>100	50		56	52
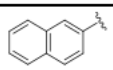	**31L**	>100	0		26	39
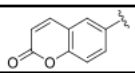	**32L**	>100	18		62	35
	**33L**	>100	14		73	79
	**34L**	>100	12		29	38

Table 12B – Log(EC_{50} and CC_{50}) cell viability results ± SD for analogs **15** and **16L**-**34L**.

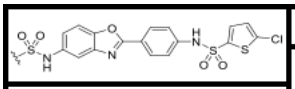 Compounds & Substituents		Cell Viability EC_{50} or CC_{50} (μM) or % Inhibition at 200 μM				
		M. smegmatis	*M. tuberculosis*		THLE3 (Liver)	HEK 293 (Kidney)
			% Inhibition	EC_{50}		
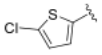	**15**	>2	41		1.68 ± 0.29	1.61 ± 0.23
	**16L**	>2	85	2.02 ± 0.03	1.90 ± 0.12	1.96 ± 0.08
	**17L**	>2	52	1.56 ± 0.06	1.63 ± 0.12	1.70 ± 0.20
	**18L**	>2	72	1.61 ± 0.10	1.49 ± 0.15	1.57 ± 0.11
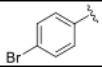	**19L**	>2	28		1.38 ± 0.16	1.46 ± 0.31
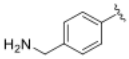	**20L**	1.85 ± 0.20	91	1.77 ± 0.02	1.54 ± 0.17	2.00 ± 0.01
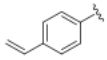	**21L**	>2	10		1.28 ± 0.18	1.48 ± 0.27
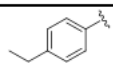	**22L**	>2	0		1.28 ± 0.18	1.44 ± 0.33
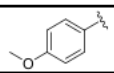	**23L**	>2	41		1.49 ± 0.15	1.60 ± 0.25
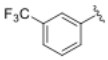	**24L**	>2	0		1.51 ± 0.20	1.68 ± 0.16
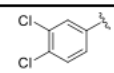	**25L**	>2	0		1.38 ± 0.13	1.54 ± 0.31
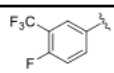	**26L**	1.93 ± 0.09	0		1.67 ± 0.24	1.77 ± 0.17
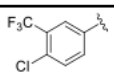	**27L**	>2	0		1.43 ± 0.18	1.54 ± 0.33
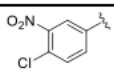	**28L**	>2	1		1.06 ± 0.15	1.69 ± 0.33
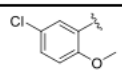	**29L**	>2	39		1.34 ± 0.16	1.53 ± 0.24
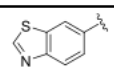	**30L**	>2	50		1.72 ± 0.15	1.80 ± 0.23
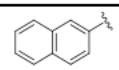	**31L**	>2	0		1.40 ± 0.14	1.66 ± 0.17
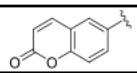	**32L**	>2	18		1.73 ± 0.23	1.83 ± 0.24
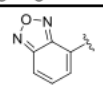	**33L**	>2	14		1.83 ± 0.11	1.94 ± 0.09
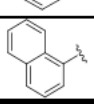	**34L**	>2	12		1.46 ± 0.09	1.71 ± 0.24

Table 13A – IC_{50} and EC_{50} biochemical assay results for analogs **R35**-**R51**. Compounds that were tested in the *Mtb* PtpB phosphatase assay for which their dose-response curves first showed an activation, followed by inhibition of enzymatic activity at increasing compound concentrations are labeled with a superscript "AI". A superscript "A" indicates only activation was observed with increasing compound concentrations.

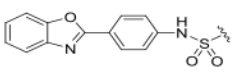			Biochemical Assay IC_{50} (μM)								
			Reporter Counter-Screens:		GroEL/ES refolding of:		HSP60/10-dMDH refolding	*Mtb* PtpB	Human PTPN1 (PTP1B)	Human PTPN2 (TCPTP)	Human PTPN5 (STEP)
Compounds & Substituents			nRho	nMDH	dRho	dMDH					
	**R35**		>100	>63	>250	>100	>100	>100^{A}	>100	>100	>100
	**R36**		>100	>63	239	>100	63	48^{AI}	>100	>100	93
	**R37**		>100	>63	217	94	>100	80^{AI}	65	66	51
		***- o***	>100	>63	180	>100	>100	85^{AI}	55	80	70
	R38	***- m***	>100	>63	225	92	71	91^{AI}	62	80	54
		- p	>100	>63	224	93	73	64^{AI}	68	76	59
		***- o***	>100	>63	171	86	>100	47^{AI}	59	64	51
	R39	***- m***	>100	>63	168	79	54	43^{AI}	37	67	54
		- p	>100	>63	151	>100	61	46^{AI}	43	42	36
	**R40**		>100	>63	156	53	31	32^{AI}	63	72	64
		***- o***	>100	>63	166	75	74	58^{AI}	44	61	53
	R41	***- m***	>100	>63	170	53	57	49^{AI}	44	48	40
		- p	>100	>63	159	77	50	52^{AI}	35	38	39
	**R42**		>100	>63	104	43	25	25^{AI}	29	33	30
	**R43**		>100	>63	112	34	28	36^{AI}	40	36	43
	**R44**		>100	>63	67	23	12	29^{AI}	28	28	34
	**R45**		>100	>63	44	20	17	35^{AI}	38	62	46
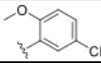	**R46**		>100	>63	83	59	>100	29^{AI}	21	28	37
		***- o***	>100	>63	111	76	85	38^{AI}	52	50	32
	R47	***- m***	>100	>63	165	92	>100	40^{AI}	37	40	28
		- p	>100	>63	157	>100	>100	52^{AI}	42	49	45
	**R48**		>100	>63	172	91	>100	46^{AI}	37	36	31
	**R49**		>100	>63	165	91	>100	52^{AI}	47	33	31
		***- o***	>100	>63	113	90	>100	59^{AI}	54	53	44
	R50	***- m***	>100	>63	174	76	80	67^{AI}	51	67	48
		- p	>100	>63	140	63	>100	61^{AI}	42	53	45
		***- o***	>100	>63	126	83	>100	31^{AI}	33	57	36
	R51	***- m***	>100	>63	132	72	62	79^{AI}	>100	>100	84
		- p	>100	>63	138	54	78	93^{AI}	70	>100	81

Table 13B – Log(IC_{50} and EC_{50}) biochemical assay results ± SD for analogs **R35**-**R51**.

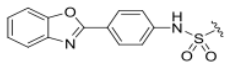			Biochemical Assay IC_{50} (μM)								
			Reporter Counter-Screens:		GroEL/ES refolding of:		HSP60/10-dMDH refolding	*Mtb* PtpB	Human PTPN1 (PTP1B)	Human PTPN2 (TCPTP)	Human PTPN5 (STEP)
Compounds & Substituents			nRho	nMDH	dRho	dMDH					
	R35		>2	>1.8	>2.4	>2	>2	>2	>2	>2	>2
	R36		>2	>1.8	2.38 ± 0.02	>2	1.80 ± 0.09	1.68 ± 0.30	>2	>2	1.97 ± 0.05
	R37		>2	>1.8	2.34 ± 0.04	1.97 ± 0.08	>2	1.91 ± 0.11	1.81 ± 0.09	1.82 ± 0.18	1.71 ± 0.05
		- *o*	>2	>1.8	2.25 ± 0.20	>2	>2	1.93 ± 0.09	1.74 ± 0.16	1.90 ± 0.16	1.85 ± 0.10
	R38	- *m*	>2	>1.8	2.35 ± 0.06	1.96 ± 0.12	1.85 ± 0.18	1.96 ± 0.05	1.79 ± 0.12	1.91 ± 0.16	1.74 ± 0.05
		- *p*	>2	>1.8	2.35 ± 0.07	1.97 ± 0.09	1.86 ± 0.19	1.80 ± 0.17	1.83 ± 0.09	1.88 ± 0.16	1.77 ± 0.13
		- *o*	>2	>1.8	2.23 ± 0.06	1.94 ± 0.07	>2	1.67 ± 0.18	1.77 ± 0.11	1.81 ± 0.14	1.71 ± 0.04
	R39	- *m*	>2	>1.8	2.23 ± 0.07	1.90 ± 0.13	1.73 ± 0.30	1.64 ± 0.19	1.57 ± 0.05	1.83 ± 0.11	1.74 ± 0.06
		- *p*	>2	>1.8	2.18 ± 0.07	>2	1.79 ± 0.24	1.66 ± 0.18	1.64 ± 0.13	1.63 ± 0.26	1.55 ± 0.08
	R40		>2	>1.8	2.19 ± 0.02	1.73 ± 0.16	1.49 ± 0.10	1.50 ± 0.15	1.80 ± 0.20	1.86 ± 0.11	1.81 ± 0.11
		- *o*	>2	>1.8	2.22 ± 0.13	1.88 ± 0.17	1.87 ± 0.16	1.76 ± 0.22	1.64 ± 0.06	1.79 ± 0.14	1.72 ± 0.06
	R41	- *m*	>2	>1.8	2.23 ± 0.07	1.73 ± 0.25	1.76 ± 0.23	1.69 ± 0.19	1.65 ± 0.07	1.69 ± 0.17	1.60 ± 0.07
		- *p*	>2	>1.8	2.20 ± 0.06	1.89 ± 0.11	1.70 ± 0.28	1.72 ± 0.21	1.55 ± 0.05	1.58 ± 0.28	1.59 ± 0.11
	R42		>2	>1.8	2.02 ± 0.21	1.64 ± 0.15	1.41 ± 0.22	1.41 ± 0.09	1.46 ± 0.07	1.52 ± 0.06	1.47 ± 0.06
	R43		>2	>1.8	2.05 ± 0.04	1.54 ± 0.07	1.45 ± 0.08	1.55 ± 0.08	1.60 ± 0.14	1.55 ± 0.06	1.63 ± 0.12
	R44		>2	>1.8	1.82 ± 0.12	1.36 ± 0.05	1.08 ± 0.17	1.47 ± 0.07	1.44 ± 0.10	1.45 ± 0.10	1.54 ± 0.01
	R45		>2	>1.8	1.65 ± 0.05	1.30 ± 0.04	1.22 ± 0.20	1.55 ± 0.04	1.58 ± 0.03	1.79 ± 0.12	1.67 ± 0.04
	R46		>2	>1.8	1.92 ± 0.16	1.77 ± 0.13	>2	1.46 ± 0.09	1.33 ± 0.05	1.45 ± 0.09	1.57 ± 0.04
		- *o*	>2	>1.8	2.05 ± 0.15	1.88 ± 0.12	1.93 ± 0.16	1.59 ± 0.09	1.71 ± 0.08	1.70 ± 0.20	1.51 ± 0.11
	R47	- *m*	>2	>1.8	2.22 ± 0.09	1.97 ± 0.09	>2	1.61 ± 0.10	1.56 ± 0.10	1.60 ± 0.23	1.45 ± 0.09
		- *p*	>2	>1.8	2.20 ± 0.07	>2	>2	1.72 ± 0.19	1.62 ± 0.09	1.70 ± 0.16	1.65 ± 0.08
	R48		>2	>1.8	2.24 ± 0.11	1.97 ± 0.17	>2	1.66 ± 0.19	1.57 ± 0.11	1.56 ± 0.11	1.49 ± 0.11
	R49		>2	>1.8	2.22 ± 0.18	1.96 ± 0.18	>2	1.72 ± 0.23	1.67 ± 0.12	1.52 ± 0.11	1.50 ± 0.06
		- *o*	>2	>1.8	2.06 ± 0.05	1.96 ± 0.08	>2	1.77 ± 0.19	1.73 ± 0.07	1.72 ± 0.12	1.65 ± 0.06
	R50	- *m*	>2	>1.8	2.24 ± 0.04	1.88 ± 0.15	1.90 ± 0.14	1.83 ± 0.17	1.71 ± 0.05	1.83 ± 0.14	1.68 ± 0.13
		- *p*	>2	>1.8	2.15 ± 0.09	1.80 ± 0.21	>2	1.79 ± 0.18	1.62 ± 0.10	1.72 ± 0.16	1.65 ± 0.10
		- *o*	>2	>1.8	2.10 ± 0.10	1.92 ± 0.19	>2	1.49 ± 0.07	1.52 ± 0.09	1.76 ± 0.05	1.55 ± 0.05
	R51	- *m*	>2	>1.8	2.12 ± 0.02	1.86 ± 0.13	1.79 ± 0.13	1.90 ± 0.10	>2	>2	1.92 ± 0.10
		- *p*	>2	>1.8	2.14 ± 0.10	1.74 ± 0.18	1.89 ± 0.09	1.97 ± 0.05	1.84 ± 0.10	>2	1.91 ± 0.08

Table 14A – EC_{50} and CC_{50} cell viability results for analogs **R35**-**R51**.

Compounds & Substituents			Cell Viability EC_{50} or CC_{50} (μM) or % Inhibition at 200 μM				
			M. smegmatis	*M. tuberculosis*		THLE3 (Liver)	HEK 293 (Kidney)
				% Inhibition	EC_{50}		
	**R35**		>100	23		>100	>100
	R36		>100	68	>200	98	>100
	**R37**		>100	71	179	96	>100
		***- o***	>100	8		>100	>100
	R38	***- m***	>100	80	185	>100	>100
		- p	>100	83	144	77	>100
		***- o***	>100	11		>100	>100
	R39	***- m***	>100	33		83	>100
		- p	>100	7		81	>100
	**R40**		>100	70	185	85	>100
		***- o***	>100	58	>200	91	>100
	R41	***- m***	>100	50	>200	82	>100
		- p	>100	78	161	71	94
	**R42**		>100	37		84	>100
	**R43**		>100	77	>200	72	82
	**R44**		>100	18		81	69
	**R45**		>100	52	193	24	85
	**R46**		>100	0		42	75
		***- o***	>100	58	176	86	>100
	R47	***- m***	>100	13		81	>100
		- p	>100	28		82	88
	**R48**		>100	82	153	77	82
	**R49**		>100	73	>200	82	>100
		***- o***	>100	0		>100	>100
	R50	***- m***	>100	74	156	84	>100
		- p	>100	72	179	86	>100
		***- o***	>100	0		81	>100
	R51	***- m***	>100	61	189	97	>100
		- p	>100	77	>200	>100	>100

Table 14B – Log(EC_{50} and CC_{50}) cell viability results ± SD for analogs **R35**-**R51**.

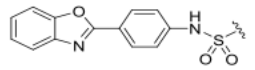 Compounds & Substituents			Cell Viability EC_{50} or CC_{50} (μM) or % Inhibition at 200 μM				
			M. smegmatis	*M. tuberculosis*		THLE3 (Liver)	HEK 293 (Kidney)
				% Inhibition	EC_{50}		
	R35		>2	23		>2	>2
	R36		>2	68	>2.3	1.99 ± 0.02	>2
	R37		>2	71	2.25 ± 0.02	1.98 ± 0.01	>2
		- *o*	>2	8		>2	>2
	R38	- *m*	>2	80	2.27 ± 0.07	>2	>2
		- *p*	>2	83	2.16 ± 0.01	1.89 ± 0.06	>2
		- *o*	>2	11		>2	>2
	R39	- *m*	>2	33		1.92 ± 0.02	>2
		- *p*	>2	7		1.91 ± 0.01	>2
	R40		>2	70	2.27 ± 0.05	1.93 ± 0.02	>2
		- *o*	>2	58	>2.3	1.96 ± 0.04	>2
	R41	- *m*	>2	50	>2.3	1.92 ± 0.02	>2
		- *p*	>2	78	2.21 ± 0.01	1.85 ± 0.08	1.97 ± 0.03
	R42		>2	37		1.92 ± 0.01	>2
	R43		>2	77	>2.3	1.86 ± 0.09	1.92 ± 0.12
	R44		>2	18		1.91 ± 0.01	1.84 ± 0.16
	R45		>2	52	2.29 ± 0.06	1.38 ± 0.06	1.93 ± 0.13
	R46		>2	0		1.62 ± 0.08	1.88 ± 0.11
		- *o*	>2	58	2.25 ± 0.01	1.94 ± 0.01	>2
	R47	- *m*	>2	13		1.91 ± 0.01	>2
		- *p*	>2	28		1.91 ± 0.01	1.94 ± 0.09
	R48		>2	82	2.19 ± 0.01	1.89 ± 0.04	1.92 ± 0.07
	R49		>2	73	>2.3	1.91 ± 0.01	>2
		- *o*	>2	0		>2	>2
	R50	- *m*	>2	74	2.19 ± 0.01	1.93 ± 0.01	>2
		- *p*	>2	72	2.25 ± 0.02	1.94 ± 0.01	>2
		- *o*	>2	0		1.91 ± 0.15	>2
	R51	- *m*	>2	61	2.28 ± 0.03	1.99 ± 0.02	>2
		- *p*	>2	77	>2.3	>2	>2

Table 15A – IC_{50} and EC_{50} biochemical assay results for analogs **L35**-**L51**. Compounds that were tested in the *Mtb* PtpB phosphatase assay for which their dose-response curves first showed an activation, followed by inhibition of enzymatic activity at increasing compound concentrations are labeled with a superscript "AI".

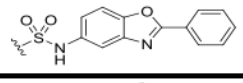			Biochemical Assay IC_{50} (μM)								
			Reporter Counter-Screens:		GroEL/ES refolding of:		HSP60/10-dMDH refolding	*Mtb* PtpB	Human PTPN1 (PTP1B)	Human PTPN2 (TCPTP)	Human PTPN5 (STEP)
Compounds & Substituents			nRho	nMDH	dRho	dMDH					
	**L35**		>100	>63	193	>100	>100	>100	>100	>100	>100
	**L36**		>100	>63	214	>100	90	81^{AI}	>100	88	85
	**L37**		>100	>63	190	>100	>100	87^{AI}	77	64	42
		***- o***	>100	>63	171	>100	>100	80^{AI}	59	69	44
	L38	***- m***	>100	>63	146	>100	>100	93^{AI}	71	>100	42
		- p	>100	>63	195	>100	>100	85^{AI}	78	61	41
		***- o***	>100	>63	103	90	>100	50^{AI}	40	42	35
	L39	***- m***	>100	>63	124	78	>100	>100^{AI}	88	51	>100
		- p	>100	>63	149	>100	>100	56^{AI}	44	35	26
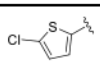	**L40**		>100	>63	234	>100	70	54^{AI}	76	72	44
		***- o***	>100	>63	162	92	>100	58^{AI}	44	55	37
	L41	***- m***	>100	>63	180	95	>100	77^{AI}	83	76	45
		- p	>100	>63	159	64	>100	26^{AI}	36	44	27
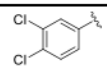	**L42**		>100	>63	152	79	>100	33^{AI}	35	33	25
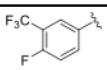	**L43**		>100	>63	122	48	69	46^{AI}	76	39	26
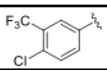	**L44**		>100	>63	132	92	>100	40^{AI}	40	34	28
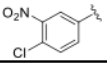	**L45**		>100	>63	18	16	17	33^{AI}	35	40	32
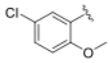	**L46**		>100	>63	105	81	>100	31^{AI}	27	25	37
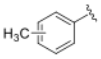		***- o***	>100	>63	127	>100	>100	59^{AI}	41	29	30
	L47	***- m***	>100	>63	200	>100	>100	63^{AI}	53	57	39
		- p	>100	>63	157	>100	>100	68^{AI}	48	49	39
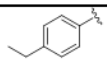	**L48**		>100	>63	237	>100	>100	67^{AI}	57	55	42
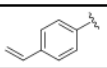	**L49**		>100	>63	175	>100	>100	51^{AI}	45	46	35
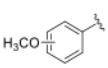		***- o***	>100	>63	89	85	>100	67^{AI}	37	34	38
	L50	***- m***	>100	>63	220	>100	>100	>100^{AI}	86	87	44
		- p	>100	>63	175	95	>100	73^{AI}	46	50	37
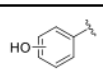		***- o***	>100	>63	194	70	85	98^{AI}	76	>100	68
	L51	***- m***	>100	>63	103	58	76	98^{AI}	>100	>100	72
		- p	>100	>63	111	64	88	97^{AI}	92	>100	84

Table 15B – Log(IC_{50} and EC_{50}) biochemical assay results ± SD for analogs **L35**-**L51**.

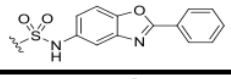			Biochemical Assay IC_{50} (μM)								
			Reporter Counter-Screens:		GroEL/ES refolding of:		HSP60/10-dMDH refolding	*Mtb* PtpB	Human PTPN1 (PTP1B)	Human PTPN2 (TCPTP)	Human PTPN5 (STEP)
Compounds & Substituents			nRho	nMDH	dRho	dMDH					
	**L35**		>2	>1.8	2.29 ± 0.05	>2	>2	>2	>2	>2	>2
	**L36**		>2	>1.8	2.33 ± 0.07	>2	1.95 ± 0.10	1.91 ± 0.10	>2	1.95 ± 0.09	1.93 ± 0.07
	**L37**		>2	>1.8	2.28 ± 0.11	>2	>2	1.94 ± 0.10	1.89 ± 0.10	1.81 ± 0.13	1.63 ± 0.07
		***- o***	>2	>1.8	2.23 ± 0.11	>2	>2	1.90 ± 0.15	1.77 ± 0.12	1.84 ± 0.08	1.65 ± 0.09
	L38	***- m***	>2	>1.8	2.17 ± 0.02	>2	>2	1.97 ± 0.05	1.85 ± 0.12	>2	1.63 ± 0.10
		- p	>2	>1.8	2.29 ± 0.15	>2	>2	1.93 ± 0.17	1.89 ± 0.07	1.79 ± 0.20	1.61 ± 0.12
		***- o***	>2	>1.8	2.01 ± 0.08	1.96 ± 0.08	>2	1.70 ± 0.19	1.60 ± 0.04	1.63 ± 0.09	1.55 ± 0.06
	L39	***- m***	>2	>1.8	2.09 ± 0.05	1.90 ± 0.10	>2	>2	1.94 ± 0.20	1.71 ± 0.19	>2
		- p	>2	>1.8	2.17 ± 0.09	>2	>2	1.75 ± 0.18	1.64 ± 0.06	1.54 ± 0.19	1.41 ± 0.05
	**L40**		>2	>1.8	2.37 ± 0.05	>2	1.85 ± 0.18	1.73 ± 0.15	1.88 ± 0.11	1.86 ± 0.13	1.65 ± 0.06
		***- o***	>2	>1.8	2.21 ± 0.09	1.96 ± 0.08	>2	1.77 ± 0.22	1.65 ± 0.06	1.74 ± 0.17	1.57 ± 0.04
	L41	***- m***	>2	>1.8	2.26 ± 0.09	1.98 ± 0.16	>2	1.89 ± 0.21	1.92 ± 0.08	1.88 ± 0.16	1.65 ± 0.17
		- p	>2	>1.8	2.20 ± 0.14	1.81 ± 0.14	>2	1.41 ± 0.16	1.56 ± 0.11	1.64 ± 0.07	1.43 ± 0.10
	**L42**		>2	>1.8	2.18 ± 0.33	1.90 ± 0.14	>2	1.53 ± 0.14	1.55 ± 0.12	1.51 ± 0.08	1.41 ± 0.08
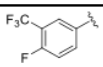	**L43**		>2	>1.8	2.09 ± 0.42	1.68 ± 0.07	1.84 ± 0.32	1.66 ± 0.16	1.88 ± 0.12	1.59 ± 0.14	1.41 ± 0.12
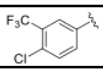	**L44**		>2	>1.8	2.12 ± 0.23	1.97 ± 0.20	>2	1.60 ± 0.20	1.61 ± 0.18	1.54 ± 0.07	1.45 ± 0.09
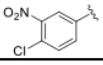	**L45**		>2	>1.8	1.26 ± 0.18	1.20 ± 0.22	1.22 ± 0.28	1.51 ± 0.09	1.55 ± 0.10	1.60 ± 0.05	1.50 ± 0.08
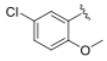	**L46**		>2	>1.8	2.02 ± 0.35	1.91 ± 0.18	>2	1.50 ± 0.10	1.43 ± 0.15	1.40 ± 0.12	1.56 ± 0.03
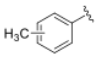		***- o***	>2	>1.8	2.11 ± 0.17	>2	>2	1.77 ± 0.23	1.61 ± 0.14	1.47 ± 0.28	1.47 ± 0.05
	L47	***- m***	>2	>1.8	2.30 ± 0.11	>2	>2	1.80 ± 0.24	1.72 ± 0.09	1.76 ± 0.15	1.59 ± 0.09
		- p	>2	>1.8	2.20 ± 0.11	>2	>2	1.83 ± 0.21	1.69 ± 0.07	1.69 ± 0.15	1.60 ± 0.07
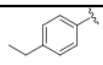	**L48**		>2	>1.8	2.37 ± 0.08	>2	>2	1.83 ± 0.22	1.76 ± 0.12	1.74 ± 0.10	1.63 ± 0.07
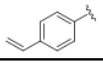	**L49**		>2	>1.8	2.24 ± 0.24	>2	>2	1.71 ± 0.20	1.66 ± 0.12	1.66 ± 0.09	1.55 ± 0.10
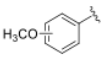		***- o***	>2	>1.8	1.95 ± 0.05	1.93 ± 0.09	>2	1.83 ± 0.19	1.57 ± 0.08	1.53 ± 0.20	1.58 ± 0.06
	L50	***- m***	>2	>1.8	2.34 ± 0.12	>2	>2	>2	1.94 ± 0.11	1.94 ± 0.13	1.65 ± 0.10
		- p	>2	>1.8	2.24 ± 0.18	1.98 ± 0.08	>2	1.86 ± 0.21	1.66 ± 0.07	1.70 ± 0.12	1.56 ± 0.09
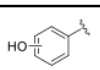		***- o***	>2	>1.8	2.29 ± 0.15	1.84 ± 0.15	1.93 ± 0.07	1.99 ± 0.21	1.88 ± 0.19	>2	1.83 ± 0.10
	L51	***- m***	>2	>1.8	2.01 ± 0.01	1.77 ± 0.10	1.88 ± 0.03	1.99 ± 0.01	>2	>2	1.86 ± 0.08
		- p	>2	>1.8	2.05 ± 0.10	1.81 ± 0.12	1.95 ± 0.02	1.99 ± 0.02	1.96 ± 0.07	>2	1.93 ± 0.12

Table 16A – EC_{50} and CC_{50} cell viability results for analogs **L35**-**L51**.

Compounds & Substituents			Cell Viability EC_{50} or CC_{50} (μM) or % Inhibition at 200 μM				
			M. smegmatis	*M. tuberculosis*		THLE3 (Liver)	HEK 293 (Kidney)
				% Inhibition	EC_{50}		
	**L35**		>100	6		>100	>100
	**L36**		38	68	>200	35	97
	**L37**		>100	76	105	33	46
	**L38**	***- o***	63	12		53	72
		- m	>100	56	>200	41	68
		- p	>100	47		38	68
	**L39**	***- o***	93	13		43	73
		- m	>100	45		45	70
		- p	88	0		40	65
	**L40**		>100	71	>200	43	>100
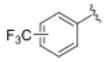	**L41**	***- o***	>100	45		59	80
		- m	>100	41		58	>100
		- p	>100	0		49	74
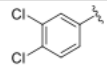	**L42**		>100	22		55	71
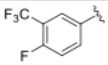	**L43**		>100	23		55	>100
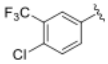	**L44**		>100	0		47	66
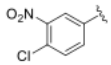	**L45**		>100	1		25	90
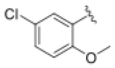	**L46**		>100	0		31	74
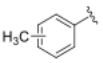	**L47**	***- o***	>100	61	197	35	57
		- m	>100	82	161	38	69
		- p	>100	87	172	53	75
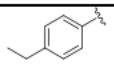	**L48**		>100	87	148	63	81
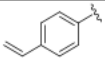	**L49**		>100	86	151	50	53
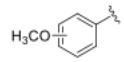	**L50**	***- o***	>100	3		29	41
		- m	>100	83	162	37	63
		- p	>100	75	167	53	91
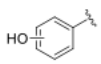	**L51**	***- o***	>100	18		32	33
		- m	>100	3		79	>100
		- p	>100	9		>100	>100

Table 16B – Log(EC_{50} and CC_{50}) cell viability results ± SD for analogs **L35**-**L51**.

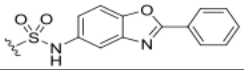 Compounds & Substituents			Cell Viability EC_{50} or CC_{50} (μM) or % Inhibition at 200 μM				
			M. smegmatis	*M. tuberculosis*		THLE3 (Liver)	HEK 293 (Kidney)
				% Inhibition	EC_{50}		
	**L35**		>2	6		>2	>2
	**L36**		1.58 ± 0.27	68	>2.3	1.55 ± 0.01	1.99 ± 0.16
	**L37**		>2	76	2.02 ± 0.01	1.52 ± 0.04	1.66 ± 0.33
		***- o***	1.80 ± 0.23	12		1.72 ± 0.03	1.86 ± 0.28
	L38	***- m***	>2	56	>2.3	1.62 ± 0.07	1.83 ± 0.22
		- p	>2	47		1.58 ± 0.02	1.84 ± 0.21
		***- o***	1.97 ± 0.04	13		1.64 ± 0.08	1.86 ± 0.26
	L39	***- m***	>2	45		1.66 ± 0.06	1.84 ± 0.22
		- p	1.95 ± 0.10	0		1.60 ± 0.02	1.81 ± 0.18
	**L40**		>2	71	>2.3	1.63 ± 0.05	>2
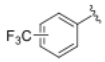		***- o***	>2	45		1.77 ± 0.16	1.90 ± 0.15
	L41	***- m***	>2	41		1.76 ± 0.14	>2
		- p	>2	0		1.69 ± 0.06	1.87 ± 0.19
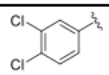	**L42**		>2	22		1.74 ± 0.18	1.85 ± 0.19
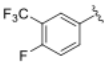	**L43**		>2	23		1.74 ± 0.18	>2
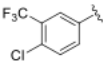	**L44**		>2	0		1.67 ± 0.14	1.82 ± 0.14
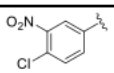	**L45**		>2	1		1.39 ± 0.10	1.96 ± 0.04
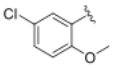	**L46**		>2	0		1.49 ± 0.13	1.87 ± 0.11
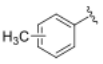		***- o***	>2	61	2.29 ± 0.02	1.55 ± 0.01	1.75 ± 0.22
	L47	***- m***	>2	82	2.21 ± 0.01	1.58 ± 0.01	1.84 ± 0.16
		- p	>2	87	2.23 ± 0.05	1.73 ± 0.05	1.88 ± 0.16
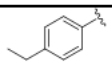	**L48**		>2	87	2.17 ± 0.04	1.80 ± 0.12	1.91 ± 0.09
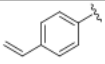	**L49**		>2	86	2.18 ± 0.02	1.70 ± 0.16	1.80 ± 0.14
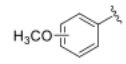		***- o***	>2	3		1.46 ± 0.15	1.62 ± 0.34
	L50	***- m***	>2	83	2.21 ± 0.03	1.57 ± 0.01	1.80 ± 0.17
		- p	>2	75	2.22 ± 0.01	1.73 ± 0.04	1.96 ± 0.06
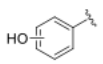		***- o***	>2	18		1.50 ± 0.03	1.51 ± 0.27
	L51	***- m***	>2	3		1.90 ± 0.11	>2
		- p	>2	9		>2	>2

REFERENCES

Abdeen, S., Salim, N., Mammadova, N., Summers, C. M., Frankson, R., Ambrose, A. J., Anderson, G. G., Schultz, P. G., Horwich, A. L., Chapman, E., and Johnson, S. M. (2016) GroEL/ES inhibitors as potential antibiotics. *Bioorg Med Chem Lett* **26(13),** 3127-3134

Abdeen, S., Salim, N., Mammadova, N., Summers, C. M., Goldsmith-Pestana, K., McMahon-Pratt, D., Schultz, P. G., Horwich, A. L., Chapman, E., and Johnson, S. M. (2016) Targeting the HSP60/10 chaperonin systems of Trypanosoma brucei as a strategy for treating African sleeping sickness. *Bioorg Med Chem Lett* **26(21),** 5247-5253

Abdeen, S., Kunkle, T., Salim, N., Ray, A., Mammadova, N., Summers, C., Stevens, M., Ambrose, A., Park, Y., Schultz, P. G., Horwich, A. L., Hoang, Q. Q., Chapman, E., and Johnson, S. M. (2018) Sulfonamidio-2-arylbenzoxazole GroEL/ES Inhibitors as Potent Antibacterials against Methicillin-Resistnant *Staphylococcus aureus* (MRSA). *Journal of Medicinal Chemistry* **61(16),** 7345-7357

Altaf, M., Miller, C. H., Bellows, D. S., and O'Toole, R. (2010) Evaluation of the Mycobacterium smegmatis and BCG models for the discovery of Mycobacterium tuberculosis inhibitors. *Tuberculosis* **90(6),** 333-337, doi: 10.1016/j.tube.2010.09.002

Barberis, I., Bragazzi, N. L., Galluzzo, L., and Martini, M. (2017) The history of tuberculosis: from the first historical records to the isolation of Koch's bacillus. *Journal of preventive medicine and hygiene* **58(1),** E9-E12

Butler, R., and Carr., J. (2016) First-Line Treatment of TB for Drug-Sensitive TB. *NIH-NIAID* **OMB#:** 0925-0668

CDC Features: Tuberculosis Disease and Prevention. (2018, January 31). Retrieved from http://www.cdc.gov/features/tbsymptoms/index.html

Chapman, E., Farr, G. W., Usaite, R., Furtak, K., Fenton, W. A., Chaudhuri, T. K., Hondorp, E. R., Matthews, R. G., Wolf, S. G., Yates, J. R., Pypaert, M., and Horwich, A. L. (2006) Global aggregation of newly translated proteins in an Escherichia coli strain deficient of the chaperonin GroEL. *Proceedings of the National Academy of Sciences* **103(43),** 15800-15805, doi:10.1073/pnas.0607534103

Chaudhry, C., Horwich, A. L., Brunger, A. T., and Adams, P. D. (2004) Exploring the Structural Dynamics of the *E. coli* Chaperonin GroEL Using Translation-libration-screw Crystallographic Refinement of Intermediate States. *Journal of Molecular Biology* **342(1),** 229-245

Cheng, M. Y., Hartl, F. U., Martin, J., Pollock, R. A., Kalousek, F., Neupert, W., Hallberg, E. M., Hallberg, R. L., and Horwich, A. L. (1989) Mitochondrial heat-shock protein hsp60 is essential for assembly of proteins imported into yeast mitochondria. *Nature* **337,** 620-625

D'Ambrosio, L., Centis, R., Tiberi, S., Tadolini, M., Dalcolmo, M., Rendon, A., Esposito, S., and Migliori, G. B. (2017) Delamanid and bedaquiline to treat multidrug-resistant and extensively drug-resistant tuberculosis in children: a systematic review. *Journal of Thoracic Disease* **9(7),** 2093-2102, doi:10.21037/jtd.2017.06.16

Daniel, T. M. (2006) The History of Tuberculosis. *Respiratory Medicine* **100,** 1862-1870
Etienne, G., Laval, F., Villeneuve, C., Dinadayala, P., Abouwarda, A., Zerbib, D., Galamba, A., and Daffé, M. (2005) The cell envelope structure and properties of *Mycobacterium smegmatis* mc^2155: is there a clue for the unique transformability of the strain? *Microbiology* **151,** 2075-2086, doi: 10.1099/mic.0.27869-0

Flynn, J. L. and Chan, J. (2001) Tuberculosis: Latency and Reactivation. *Infection and Immunity* **69,** 4195-4201, doi:10.1128/IAI.69.7.4195-4201.2001

Gill, W. P., Harik, N. S., Whiddon, M. R., Liao, R. P., Mittler, J. E., and Sherman, D. R. (2009) A replication clock for Mycobacterium tuberculosis. *Nature Medicine* **15(2),** 211-214

Grundner, C., Ng, H., and Alber, T. (2005) Mycobacterium tuberculosis Protein Tyrosine Phosphatase PtpB Structure Reveals a Diverged Fold and a Buried Active Site. *Structure* **13(11),** 1625-1634, doi:10.1016/j.str.2005.07.017

Grundner, C., Perrin, D., Huijsduijnen, R. H., Swinnen, D., Gonzalez, J., Gee, C. L., Wells, T. N., and Alber, T. (2007). Structural Basis for Selective Inhibition of *Mycobacterium tuberculosis* Protein Tyrosine Phosphatase PtpB. *Structure* **15(4),** 499-509, doi:10.1016/j.str.2007.03.003

He, Z. and Buck, J. D. (2010) Cell wall proteome analysis of *Mycobacterium smegmatis* strain MC2 155. *BMC Microbiology* **10(121),** doi:10.1186/1471-2180-10-121

Horwich, A. L., Farr, G. W., and Fenton, W. A. (2006) GroEL−GroES-Mediated Protein Folding. *Chemical Reviews* **106(5),** 1917-1930, doi:10.1021/cr040435v

Houston, S., Long, R., and Hoeppner, V. (2002) Latent tuberculosis treatment. *CMAJ* **167(5),** 452-453

Hu, Y., Henderson, B., Lund, P. A., Tormay, P., Ahmed, M. T., Gurcha, S. S., Besra, G. S., and Coates, A. R. (2008) A Mycobacterium tuberculosis Mutant Lacking the groEL Homologue cpn60.1 Is Viable but Fails To Induce an Inflammatory Response in Animal Models of Infection. *Infection and Immunity* **76(4),** 1535-1546, doi:10.1128/iai.01078-07

Jackson, Carey, and David Roesel. (2016) Epidemiology of TB: Primary Care Tools for the Management of TB. *Somali Cultural Profile - EthnoMed*, ethnomed.org/clinical/tuberculosis/firland/epidemiology-of-tb

Johnson, S. M., Sharif, O., Mak, P. A., Wang, H. T., Engels, I. H., Brinker, A., Schultz, P. G., Horwich, A. L., and Chapman, E. (2014) A biochemical screen for GroEL/GroES inhibitors. *Bioorganic & Medicinal Chemistry Letters* **24(3),** 786-789

Kunkle, T., Abdeen, S., Salim, N., Ray, A., Stevens, M., Ambrose, A., Victorino, J., Park, Y., Hoang, Q. Q., Chapman, E., and Johnson, S. M. (2018) Hydroxybiphenylamide GroEL/ES Inhibitors Are Potent Antibacterials against Planktonic and Biofilm Forms of *Staphylococcus aureus*. *Journal of Medicinal Chemistry* **Article ASAP,** doi:10.1021/acs.jmedchem.8b01293

Leininger, K. R. and Westley J. (1968) The Mechanism of the Rhodanese-catalyzed Thiosulfate-Cyanide Reaction. *The Journal of Biological Chemistry* **243(8),** 1892-1899
Luca, S. and Mihaescu, T. (2013) History of BCG Vaccine. *MAEDICA – a Journal of Clinical Medicine* **8(1),** 53-58

Lupoli, T. J., Vaubourgeix, J., Burns-Huang, K., and Gold, B. (2018) Targeting the Proteostasis Network for Mycobacterial Drug Discovery. *ACS Infectious Diseases* **4(4),** 478-498, doi:10.1021/acsinfecdis.7b00231

Ollinger, J., Bailey, M. A., Moraski, G. C., Casey, A., Florio, S., Alling, T., Miller, M. J., Parish, T. (2013) A Dual Read-Out Assay to Evaluate the Potency of Compounds Active against *Mycobacterium tuberculosis. PLoS ONE* **8(4),** e60531, doi:10.1371/journal.pone.0060531

Pai, M., Behr, M. A., Dowdy, D., Dheda, K., Divangahi, M., Boehme, C. C., Ginsberg, A., Swaminathan, S., Spigelman, M., Getahun, H., Menzies, D., and Raviglione, M. (2016) Tuberculosis. *Nature Review Disease Primers* **2,** 1-23

Smith, I. (2003) Mycobacterium tuberculosis Pathogenesis and Molecular Determinants of Virulence. *Clinical Microbiology Reviews* **16(3),** 463-496, doi:10.1128/cmr.16.3.463-496.2003

Treatment of Tuberculosis: Guidelines. 4th edition., Essential first-line antituberculosis drugs, (2010) *Geneva: World Health Organization,* Available from: https://www.ncbi.nlm.nih.gov/books/NBK138747/

"Tuberculosis." Mayo Clinic, Mayo Foundation for Medical Education and Research. (2018, January 4). Retrieved from www.mayoclinic.org/diseases-conditions/tuberculosis/symptoms-causes/syc-20351250

Vaudry, W. (2003) "To BCG or not to BCG, that is the question!". The challenge of BCG vaccination: Why can't we get it right? *Paediatr Child Health* **8(3),** 141-144

Xu, Z., and Sigler, P. B. (1998) GroEL/GroES: Structure and Function of a Two-Stroke Folding Machine. *Journal of Structural Biology* **124(2-3),** 129-141, doi:10.1006/jsbi.1998.4060

Zhou, B., He, Y., Zhang, X., Xu, J., Luo, Y., Wang, Y., Franzblau, S. G., Yang, Z., Chan, R. J., Liu, Y., Zheng, J., and Zhang, Z. Y. (2010) Targeting mycobacterium protein tyrosine phosphatase B for antituberculosis agents. *Proceedings of the National Academy of Sciences* **107(10),** 4573-4578, doi:10.1073/pnas.0909133107

CURRICULUM VITAE

J. Alex Washburn

Education:

Indiana University, Indianapolis, Indiana:

2017-2019:

- Completed MS degree in the Department of Biochemistry and Molecular Biology.
- Thesis title: *Exploring Dual-Targeting GroEL/ES & PtpB Inhibitors as a New Antibiotic Strategy for Tuberculosis.*

Indiana University, Bloomington, Indiana:

2012-2016:

- Completed BS degree in Biology. Also acquired a chemistry and animal behavior minor.

Hauser Jr/Sr High School, Hope, Indiana:

2008-2012:

- Completed academic honors diploma, graduating with distinction.

Employment:

Adidas, Edinburgh, Indiana:

2012 (February) -2016 (May): Sales Associate.

- Worked on the floor, cash register, and shipments in the back.

Volunteer Work:

Area 10 Agency, Bloomington, Indiana:

2015 (January) -2016 (May): Driver and visitor.

- Delivered food and also visited people on a route around Bloomington Indiana.

Field Experiences:

Major Hospital, Shelbyville, Indiana:

2013 (June) & 2015 (June)

- I shadowed Dr. George Wairiuko in the OR and watched the removal of cancerous glands. During these shadows I gained an interest in oncology.

Forensic Chemistry Center (FDA), Cincinnati, Ohio:

2016 (May)

- I shadowed a forensic chemistry lab led by Adam Lanzarotta where he showed me around the labs and I was able to see a wide array of biochemical and inorganic chemistry techniques.

Wayne State University, Detroit, Michigan:

2016 (July) -2017 (July): Biochemistry & Molecular Biology

- I worked at viral genomics lab and others in the biochemistry department learning an array of biochemistry and molecular biology techniques, namely qPCR.

Publications:

- Chitre, S.; Ray, A.M.; Stevens M.; Salim, N.; Abdeen, S.; **Washburn, A.**; Sivinski, J.; Park, Y.; Hoang, Q.Q.; Chapman, E.; Johnson, S.M. Tentative title: Investigating Chalcones and Their Ability to Inhibit HSP60 and Colorectal Cancer. *In preparation.*
- **Washburn, A.**; Abdeen, S.; Ovechkina, Y.; Ray, A.M.; Stevens M.; Chitre, S.; Sivinski, J.; Park, Y.; Horwich, A.L; Hoang, Q.Q.; Chapman, E.; Parish, T.; Johnson, S.M. GroEL/ES chaperonin system inhibitors can also target *Mycobacterium tuberculosis* Protein Tyrosine Phosphatase B (PtpB): A potential dual-targeting therapeutic strategy? Submitted to *Bioorg. Med. Chem. Lett.* **2019.**
- Stevens, M.; Abdeen, S.; Salim, N.; Ray, A.M.; **Washburn, A.**; Chitre, S.; Sivinski, J.; Park, Y.; Hoang, Q.Q.; Chapman, E.; Johnson, S.M. HSP60/10 chaperonin systems are inhibited by a variety of approved drugs, natural products, and known bioactive molecules. Submitted to *Bioorg. Med. Chem. Lett.* **2018.**

Technical Skills:

- Protein expression & purification techniques
- Performing a variety of biochemical *in vitro* assays with multiple proteins
- Evaluating compounds in cell viability assays using several human cell lines
- Recombinant DNA technology
- qPCR
- Genotyping
- Agarose Gel Electrophoresis/ SDA-PAGE/ Western Blotting

Software Knowledge:

- Auto-Dock Molecular Docking
- ChemDraw chemical drawing and visualization program
- SciFinder scientific searching database
- Discovery Studio Visualizer crystal structure viewing program
- GraphPad Prism
- Adobe Photoshop & Illustrator
- Endnote
- BLAST
- SoftMaxPro
- MS Office: Word, Excel, PowerPoint

IUSM Biochemistry & Molecular Biology MSc Courses:

Fall 2017:

- G715 Biochemical Basis of Metabolic Disease: B
- G716 Molecular Biology: B^+
- B890 Biochemistry Seminar: B^+
- G505 Responsible Conduct of Research: A
- G828 Concepts in Biotechnology: A^-
- B854 Introduction to Research: A

Spring 2018:

- B890 Seminar in Biochemistry: B^+
- G807 Structural and Chemical Biology: B^+
- G848 Bioinformatics: B^+
- G828: Concepts in Biotechnology: A
- B855 Research in Biochemistry: A

Summer 2018:

- B855 Research in Biochemistry: A

Current cGPA: 3.68/4.00